

Proceedings of the 24th Annual Meeting

CONTRIBUTED PAPERS

MONDAY, JUNE 20, 1977

MONDAY, 10:45 a.m.-12:15 p.m.

CHICAGO ROOM

CARDIOVASCULAR 1

Chairman: B. Leonard Holman
Co-Chairman: Glen W. Hamilton

DUAL RADIONUCLIDE IMAGING OF MYOCARDIAL INFARCTION IN MAN: DISCORDANT SIZE OF DECREASED Tl-201 ACTIVITY AND INCREASED Tc-99m PYROPHOSPHATE UPTAKE. Harvey J. Berger, Alexander Gottschalk, Barry L. Zaret. Yale Univ., New Haven, Ct.

Superimposition of thallium-201 (Tl) and technetium-99m pyrophosphate (PYP) images may help define regions of myocardial infarction (MI), ischemia, or scar that are not evident from either image alone. Therefore, 80 patients (pts) with acute MI (55 transmural (T) and 25 nontransmural (NT)) were imaged with both tracers within 1 week of MI. Studies were performed in the coronary care unit using a stationary computerized multicrystal scintillation camera.

Sensitivity of dual imaging was 100%, with all pts having at least a positive (+) Tl or +PYP. Sixty-nine pts (86%) had both +Tl and +PYP (29/29 anterior (ant) TMI, 19/26 inferior (inf) TMI, and 21/25 NTMI). There were 4 pts with +Tl and negative (-) PYP (3 inf TMI and 1 NTMI) and 7 with -Tl and +PYP (4 inf TMI and 3 NTMI). Sixteen Tl images were diagnostic for MI only when computer-smoothed and displayed as 16-color isocount images (2 ant TMI, 6 inf TMI, and 8 NTMI). In pts with TMI, 90% of +Tl and 89% of +PYP images correctly identified the electrocardiographic site of acute MI. However, assessment of areas of decreased Tl activity and localized PYP uptake revealed major size discordance in 50% of 49 TMI pts in whom both images were +. The size of the MI zone on the PYP image was larger than that on the Tl image in 21/49 pts, even in 5 pts with previous MI and corresponding Tl defects. The size of the MI zone on Tl was larger than that on PYP only in 4 pts with previous MI.

While dual radionuclide imaging is a sensitive technique for detecting and localizing acute MI, superimposition of Tl and PYP images often reflects a discordance in MI zone size. This discordance must be considered in quantification of MI with dual imaging.

QUANTITATIVE THALLIUM SCINTIGRAPHY IN THE ASSESSMENT AND FOLLOW UP OF CORONARY ARTERY BYPASS GRAFTS. Ray J. Wainwright, Michael N. Maisey, Edgar Sowton. Guy's Hospital, London, England.

Stress myocardial scintigraphy using thallium-201 (Tl-201 SMS) has been performed on 20 patients with angiographically normal coronary arteries without angina and compared quantitatively to 16 patients who had Tl-201 SMS before and after CABG.

Digitized thallium images were segmented and a normal count profile constructed. Before surgery all patients had at least one significant scintigraphic abnormality. Following surgery, Tl-201 SMS was repeated in all patients exercised to an equivalent pre-operative work load.

Paired t test analysis showed a significant increase in Tl-201 uptake in the ventricular septum ($p < 0.001$) with a further significant increase in tracer uptake in the whole myocardium ($p < 0.05$). Individual patients showed improvement, no change or deterioration of tracer uptake.

Graft patency predicted by Tl-201 SMS has been confirmed at follow-up coronary arteriography in 5 out of 16 patients, and premature graft closure detected in 2 out

of 16 patients, confirmed angiographically. A further 2 patients had graft closure undetected by Tl-201 SMS.

It is concluded that:

- Tl-201 SMS is a sensitive indicator of altered myocardial perfusion following CABG
- the sensitivity to detect graft closure is directly related to the importance of the graft with respect to the severity of native coronary disease.

THALLIUM-201 SCINTIGRAPHY IN UNSTABLE ANGINA. Frans J.Th. Wackers, K.I.Lie, Koen L.Liem, Ellinor Busemann Sokole, G. Samson, Jan van der Schoot, Hein J.J.Wellens and Dirk Durrer. Departments of Cardiology and Nuclear Medicine, Wilhelmina Gasthuis, Amsterdam, The Netherlands.

To determine the value of Thallium-201 scintigraphy in patients (pts) with unstable angina (UA) 108 pts with crescendo angina of recent onset or acute progression of stable angina were studied. Pts with previous infarction were excluded. Scintigraphy was performed in absence of chest pain but within 7 hours of last anginal attack. Analogue unprocessed scans were judged as + (defect), ± (questionable) or as - (normal). In 51 pts the ECG remained normal. In 57 pts the ECG was transiently abnormal (development of negative T, ST depression or ST elevation during pain). Enzyme determinations were normal at the time of scintigraphy in all 108 pts. In six pts subsequently within 24 hours of scintigraphy acute myocardial infarction (AMI) developed. Ten pts were resistant to treatment with B-blocking drugs and underwent coronary bypass surgery (CBS). None of the 108 pts died within three weeks after scintigraphy. Results: 29 (27%) of all pts with UA had in absence of chest pain + scintiscans. The scans were + in 25 (43%) of 57 pts with abnormal ECG and in four of 51 pts with normal ECG ($P < 0.01$). The six pts who developed AMI all had abnormal scans. Seven of 10 pts who underwent CBS had + scans, but three had normal scans. Conclusions: 1) Pts without AMI may have + Thallium-201 scans in the setting of UA. 2) In pts with UA, in absence of chest pain, scintiscans have no prospective value in identifying candidates for CBS or those who will develop AMI.

MONDAY 10:45 a.m.-12:15 p.m.

JANE ADDAMS ROOM

RENAL/ELECTROLYTES

Chairman: David L. Lilien
Co-Chairman: George A. Wilson

DIFFERENTIAL Tc-99m DIMERCAPTOSUCCINIC ACID (DMSA) RENAL LOCALIZATION: CORRELATION WITH RENAL FUNCTION. Michael J. Daly, William A. Jones, Thomas G. Rudd, and James A. Tremann. University of Washington, Seattle, Washington

The relationship between differential Tc-99m DMSA renal uptake and differential renal function was examined in normal and abnormal dogs by correlating Tc-99m DMSA localization with relative renal blood flow and creatinine clearance.

9 mongrel dogs (13-20 kg) were studied as follows: Controls (3), unilateral renal stenosis (4), ureteral

obstruction (2). Under general anesthesia, bilateral ureteral catheters were placed and quantitative injection of Tc-99m DMSA was given. Over the next 2-4 hours, serial (3) differential creatinine clearances were made. An arterial (left ventricle or aorta) injection of Sr-85 microspheres (15µ) was then given to estimate relative renal blood flow, and the animal sacrificed and the kidneys removed. Fractional distribution of Tc-99m and Sr-85 in each kidney was quantitated and expressed as L/L+R. Absolute renal uptake (% dose), cortex/medulla ratios, and urinary excretion of Tc-99m DMSA were also determined.

The fractional Tc-99m DMSA localization correlated well with both relative blood flow ($r=.87$), and creatinine clearance ($r=.95$) over a range of 0.35-0.71 (L/L+R). Absolute total renal uptake of Tc-99m DMSA ranged from 22-49% (2-4 hrs.). The cortex/medullary ratio averaged 30/1 and maximal urinary excretion was 33% in 4 hours. In the 3 normal dogs, Tc-99m DMSA distribution correlated closely with renal mass.

These preliminary data indicate Tc-99m DMSA renal localization correlates well with differential renal function in both normal and diseased kidneys.

ASSESSMENT OF RECOVERABLE RENAL FUNCTION: A COMPARISON OF TWO RADIOPHARMACEUTICALS. J. R. Perry, W. H. McCartney, W. B. Bateman, W. D. Mattern, and E. V. Staab. University of North Carolina, Chapel Hill, N. C.

Tc-99m Dimercaptosuccinic acid (DMSA) and I-131 Orthoiodohippurate (OIH) were compared in patients with renal failure to assess potential for recoverable renal function. Renal scans were performed with both radiopharmaceuticals in close temporal sequence on 98 patients. Interpretations were made without reference to clinical data. Visualization of the kidneys was considered evidence for recoverable or stable function, while non-visualization indicated end-stage renal disease.

Forty-four patients studied with both Tc-99m DMSA and I-131 OIH were ultimately shown to have recoverable or stable renal function. All of these patients had visualization of the kidneys with both radiopharmaceuticals. Six patients died of non-renal problems less than one month following scanning and before their renal outcome was determined. Forty-eight patients' renal function deteriorated to end-stage renal disease. Tc-99m DMSA results for this group were renal visualization in 37 cases and non-visualization in 11 instances. I-131 OIH showed renal visualization in 28 cases and non-visualization in 20 instances.

Both radiopharmaceuticals were helpful in determining which patients had recoverable renal function. However, I-131 OIH was significantly more reliable in predicting which patients lacked recoverable function (end-stage renal disease) and required chronic dialysis to sustain life. There was no instance of renal non-visualization in which the patient recovered renal function.

QUANTITATIVE ASSESSMENT OF RENAL TRANSPLANTS WITH Tc-99m-DTPA(Sn): EXPERIENCE WITH 955 CASES. Andrew J.W. Hilson, Michael N. Maisey, Chisholm S. Ogg, Colin B. Brown and Michael Bewick. Guy's Hospital, London, England.

A method of studying renal transplants suitable for routine use has been developed. Following bolus injection of 12-15 mCi Tc-99m-DTPA(Sn), serial images are recorded over a period of 30 minutes. Simultaneously the data is recorded on a computer (GAMMA-11, DEC) at 1 frame/second for 30 seconds, then 1 frame/minute for 29 minutes.

Curves are generated from regions of interest over the iliac artery, the transplant and a background area. From the areas under the curves up to the time of the peak in the arterial curve due to the first passage of the bolus, a perfusion index is generated as

$$\frac{\text{counts per unit area of iliac ROI}}{\text{counts per unit area of renal ROI}} \times 100$$

Data is based on 955 studies with this method, 779 with the computer. By comparison of the images and the computer data it is possible to define clearly the status of the kidney. The normal kidney shows good perfusion, with a perfusion index of less than 150, good selective accumula-

tion of chelate, and rapid transit into the collecting system. In ATN the kidney may show slight impairment of perfusion, which improves with repeated studies. There is variable retention of chelate in the kidney, depending on the degree of functional impairment. In rejection there is always impairment of perfusion, reflected in a rise in the perfusion index. This may occur several days before clinical evidence of rejection, and can be detected even in the anuric patient. The method is rapid, taking about 40 minutes, and has proved capable of resolving many of the problems which occur in the postoperative period, and especially of distinguishing between ATN and rejection.

RENAL LOCALIZATION OF RADIOGALLIUM--A RETROSPECTIVE STUDY. Rashid A. Fawwaz and Philip M. Johnson. College of Physicians and Surgeons, Columbia University, New York City.

Review of 287 consecutive Ga-67 citrate scans revealed renal localization at 24 or 48 hrs. in 30 patients belonging to 3 groups. (1) Patients with renal transplants: of 8 patients studied, seven exhibited localization of Ga-67 in the transplanted kidney. All had normal renal function at the time of scan and 1 month later, despite the fact that in 3 patients renal biopsies close to the time of scan demonstrated varying degrees of monocytic infiltrate. (2) Patients with urinary tract infections: all 7 patients who had positive urine cultures at the time of the scan showed renal localization of Ga-67. However, renal uptake was also observed in 11 asymptomatic patients with a history of pyelonephritis and in whom sterile pyuria was present at the time of the scan. (3) Miscellaneous: this group comprised 2 patients with nephrotic syndrome, one with acute tubular necrosis, and 2 with leukemia or lymphoma with no signs or symptoms referable to the kidney. Biopsy of one of the nephrotic kidneys was normal on light microscopy.

It has been shown that the intensity of the cellular reaction in a transplanted kidney does not correlate with its functional integrity. Our results with renal transplants likewise indicate that renal uptake of Ga-67 is of no value in assessing kidney function and/or clinical rejection. The Ga-67 uptake in the kidneys of patients exhibiting sterile pyuria raises the possibility that it may be related to an autoimmune cellular reaction within the kidney. The mechanism of renal localization in the miscellaneous group is not clear.

Therefore, renal localization of gallium is nonspecific and not necessarily indicative of clinical renal disease.

ACCURACY OF THE KIDNEY/AORTIC BLOOD FLOW INDEX (K/A RATIO) FOR ASSESSING RENAL TRANSPLANT FUNCTION. P.T. Kirchner, M. Goldman, S. Leapman, R.F. Kiepfer. NIMC, Bethesda, Md.

The K/A ratio, representing the slopes of the upstrokes of gamma camera derived first transit blood flow curves, was assessed for accuracy in reflecting transplant function. 20 patients (26 transplants) were studied serially with a total of 148 Tc-99m DTPA or sulfur colloid studies. Reliable K/A ratios were available in 105 studies. Clinical course, transplant flow sheets, biopsy and autopsy data were the basis for retrospective diagnoses of normal, improving or deteriorating function and acute tubular necrosis (ATN), rejection and surgical complications; these were established without knowledge of scan results.

The K/A ratio clearly separated normally functioning transplants (mean .86) from stable abnormal (.55), but normal transplants fell below normal patients (1.04). All 5 oliguric ATN's had very low values (.25) initially; three improved (mean rise .22) but none became normal. 7 of 8 kidneys removed for failure had even lower terminal ratios (.16). 10 of 13 acute rejections were correctly identified (mean fall .15 or 31%) as were all 8 improvements (mean rise .28 or 118%). One urine leak and one episode of sepsis showed a fall in K/A ratio; two urine leaks and one obstruction did not. The K/A ratio is most accurate when used serially with the patient serving as his own control. Rejections are identified as a fall from a baseline, while ATN's tend to hold stable or improve. Accuracy in employing the K/A ratio requires good bolus injections and careful duplication of regions of interest for aorta and kidney.

Used properly, the K/A blood flow ratio is a reliable index of renal transplant function. It has particular value in post-transplantation anuria when other parameters of renal function are not applicable.

SEGMENTAL ATN IN LIVING RELATED DONOR TRANSPLANTED KIDNEYS WITH MULTIPLE RENAL ARTERIES. Robert Shimshak, Robert Hattner, Carol Tucker and Oscar Salvaterra. University of California, San Francisco, Ca.

A retrospective analysis of 131-iodo-orthohippuran renograms and sequential images done 24 hours post operatively on all patients who received living related donor transplanted kidneys over three years was performed.

Ten of 47 kidneys had two renal arteries. 3/10 had simultaneous revascularization of both renal arteries while 7/10 had sequential revascularized with the lower pole artery revascularized last causing a differential ischemia time between poles. Kidneys with simultaneous revascularization showed no differential function between upper and lower poles. All kidneys with delayed revascularization of the lower pole artery demonstrated significant late cortical retention of isotope in the lower pole with normal upper pole excretion suggesting segmental ATN involving the lower pole. Followup examinations demonstrated resolution of the late cortical retention with subsequent symmetrical function of both poles in all cases.

The group of patients with segmental ATN had no significantly different morbidity compared to the group without this finding. However, recognition of the characteristic appearance of segmental ATN prevents confusion with other abnormalities such as urine extravasation due to ureteral necrosis. Microscopic analysis of biopsy specimens obtained at the time of transplant from both renal poles in patients who are likely to develop segmental ATN may help clarify the early pathogenesis of ATN in man.

MONDAY, 4:00 p.m.-5:30 p.m.

LINDHEIMER ROOM

PEDIATRICS

Chairman: Eugene L. Saenger

Co-Chairman: David L. Gilday

ASSESSMENT OF CEREBRAL PERFUSION IN CHILDHOOD STROKES.
Gary F. Gates, Lawrence S. Fishman and Hervey D. Segall.
Childrens Hospital of Los Angeles, Los Angeles, Calif.

24 children with strokes had cerebral scintiangiograms using Tc-99m DTPA and a gamma camera interfaced with a digital computer. Cerebral perfusion was evaluated by serial scintiphotos plus hemispheric time-activity histogram curves. Initial interhemispheric nuclide distribution was estimated by: (1) integrating each curve from the upswing to the time at which the first of the pair reached its peak and expressing each side as a percent of the total integral counts, and (2) plotting the left-to-right hemispheric count ratio during each ½ second of the 30 second study. Four stroke patterns resulted: (1) early, persistent hypervascularity in the affected hemisphere, (2) prompt collateral flow into the initially ischemic hemisphere from the opposite side, (3) hemispheric ischemia with late collateral flow, (4) hemispheric ischemia with poor collateral flow. Collateralization in category #3 was identified by close approximation of the terminal portions of the hemisphere curves whereas wide divergence occurred with poor collateralization (i.e., #4 when abnormal curve tail was below the normal one) or with early collateralization (i.e., #1 and #2 when abnormal tail was above the normal one). Estimation of early interhemispheric nuclide distribution correlated with the clinical magnitude of the stroke. Identification of collateral flow into the diseased hemisphere was a favorable prognostic sign often heralding prompt recovery. All scinti-

graphic and cerebral angiographic studies were in agreement and correlated with the clinical status, whereas 30% of computerized tomographic scans were normal.

SCINTIGRAPHIC DETECTION OF CONGENITAL HYPERVASCULAR CEREBRAL ABNORMALITIES. Gary F. Gates, Lawrence S. Fishman and Hervey D. Segall. Childrens Hospital of Los Angeles, Los Angeles, Ca.

Accurate detection of congenital cerebral arteriovenous malformations (AVM's) and aneurysms is crucial since the prognosis has improved following advances in microsurgery. Cerebral angiography is necessary prior to surgery but is not suitable as a widespread screening test. Six children with AVM's and a seventh with a cerebral aneurysm were studied with radionuclide scintigraphy and computerized tomography (CT) (including scans following iodinated contrast administration) to determine which was the most effectual screening test. Cerebral scintiangiography was performed using Tc-99m DTPA and a scintillation camera interfaced with a digital computer, the latter used for image processing and histogram curve generation. In all cases scintiangiography demonstrated the vascular abnormality but 2 of the AVM's were barely (if at all) identifiable on CT scans. Histogram curves generated from the hemispheres and components of AVM's estimated maldistribution of hemispheric perfusion and identified the route of venous drainage from the malformation. Unilateral hemispheric hypoperfusion could occur when an AVM was in the contralateral hemisphere, whereas bilateral hemispheric hypoperfusion occurred with deep, midline AVM's. Hemispheric perfusion was neither diminished nor maldistributed with the cerebral aneurysm. The most hemodynamically significant AVM in a child with multiple lesions was apparently only by scintiangiography. Compared to CT scanning scintigraphy was the most effectual screening test for these patients due to its accuracy, lower cost and lack of required anesthesia/heavy sedation.

SCINTIGRAPHIC ABNORMALITIES IN GLYCOGEN STORAGE DISEASE.
John H. Miller, Gary F. Gates, Benjamin A. Landing, Maurice Kogut and Thomas F. Roe. Childrens Hospital of Los Angeles Los Angeles, Calif.

Glycogen storage disease, type I (GSD I or von Gierke's disease), often results in hepatomegaly and liver failure. Fourteen patients with glycogen storage disorders (average age 12 years, 10 male and 4 female) were studied with Tc-99m sulfur colloid liver-spleen scintigraphy. Follow-up studies covering up to three years were serially performed in eight patients with a total of 31 examinations for the group. Hepatomegaly occurred in all cases, whereas splenomegaly was seen in only 5. However, splenic uptake of radionuclide was increased in all cases. Abnormal bone marrow accumulation occurred in 7 patients. While many of these abnormalities were nonspecific and commonly found in patients with diffuse hepatic dysfunction, focal hepatic defects were of special interest. Seven individuals demonstrated focal defects at scintigraphy varying in size from small to large of which 3 were multiple or diffuse. Serial scintigraphy aided in differentiation between the potential presence of regenerating nodules and malignant neoplasia. Tissue specimens in these patients have revealed a histologic spectrum ranging from adenomatous hyperplasia to malignant hepatoma. Benign changes occurred in patients with small or stable scintigraphic defects while malignant changes occurred in those with either growing or large lesions. The potential malignant endpoint for hepatic changes in GSD I is not widely appreciated and warrants careful, serial liver scintigraphy so that palliative surgical resection may be considered.

NON-OPERATIVE TREATMENT OF CHILDREN WITH SPLENIC RUPTURE-- EXTENDED FOLLOW-UP WITH SCINTIGRAPHIC ASSESSMENT OF HEALING. Keith C. Fischer, Pedro Rossello, Angelo Eraklis, and

S. Treves. Children's Hospital Medical Center and Harvard Medical School, Boston, Mass.

Because of the increased risk of overwhelming and even lethal infections in splenectomized children, conservative, non-operative management of splenic trauma is becoming more commonplace. In our hospital, patients suspected of splenic trauma undergo scintigraphy in multiple projections utilizing 60 $\mu\text{Ci}/\text{kg}$ of Tc-99m sulfur colloid. If "rupture" is demonstrated, the patients are placed at bed rest, closely monitored, and if stable, surgery is not performed. Since December, 1975, 17 patients with blunt abdominal trauma have had scintigraphic evidence of "splenic rupture" and have been followed without surgery. Fifteen of these patients had at least one follow-up study and 7 patients had scans two months or later after trauma. Two patients went on to complete "scintigraphic healing" of their splenic trauma by 3 months. The other 5 had a decrease in size of the areas of decreased activity in the spleen but residual defects persisted. One patient showed a residual complete separation of the spleen at 3 months. Our small number of cases suggests that the areas of decreased activity within the damaged spleen tend to fill in and that complete resolution of splenic defects can be obtained as early as 3 months. The meaning of residual defects for management of patients is uncertain at this time, but all patients in our study are free of pain and have resumed normal activity. No post-traumatic cysts have been demonstrated scintigraphically. We feel that splenic scintigraphy is a sensitive method for diagnosing splenic damage and a safe and effective method to assess healing.

METAPHYSEAL DOSE FOR $^{99\text{m}}\text{Tc}$ -EHDP BONE IMAGING IN CHILDREN. Stephen R. Thomas, Michael J. Gelfand, James G. Kereiakes, Frank A. Ascoli, Harry R. Maxon, and Eugene L. Saenger, Radioisotope Laboratory, General Hospital, Cincinnati, Ohio; Paul A. Feller, Nuclear Medicine Laboratory, Bureau of Radiological Health, FDA, Cincinnati, Ohio.

In children, the spatial and temporal distribution of radiopharmaceuticals may differ greatly from accepted adult data. A specific illustration is the localization of bone-seeking agents (as $^{99\text{m}}\text{Tc}$ -EHDP) in the ends of long bones. Radioactivity in the metaphyseal growth complexes of the distal femur and proximal tibia was quantitated with a gamma camera-computer system, providing exact definition of areas of interest and precise conjugate view (anterior and posterior) count rate information for these areas. The effective attenuation coefficient across this patient thickness was obtained from transmission measurements using a point source. Repeated measurements provided the effective half-life. From above measurements, the cumulated activity, \bar{A} , was calculated. The mean dose per cumulated activity, S , was obtained using $\Delta_1 \cdot \phi_1 / M$. Δ_1 , the equilibrium dose constant, was calculated from the decay characteristics of $^{99\text{m}}\text{Tc}$. ϕ_1 , the fraction of the energy emitted which is absorbed in the metaphysis, and M , the mass of the complex, were determined based on the assumption that the complex simulated a disc having dimensions: 2-6 mm height, 1-4 cm radius, and a density of 1.3 g/cm^3 . The product of $\bar{A} \cdot S$ provided doses ranging from 1.5 rad to 4.4 rad to the metaphysis of children of several age groups, when adjusted to an administered activity of 220 $\mu\text{Ci}/\text{kg}$. *supported in part-Nuclear Medicine Support Services Contract No. 233-73-6203, Bureau of Radiological Health, FDA.

COMPARISON OF SCINTIGRAPHIC AND ECHOCARDIOGRAPHIC METHODS FOR ESTIMATION OF LEFT-TO-RIGHT SHUNTS. Michael J. Gelfand, James Breitwieser, Terrence Dillon, Richard A. Meyer, Wesley Covitz, Edward B. Silberstein, and Samuel Kaplan. Radioisotope Laboratory, University of Cincinnati, and Division of Pediatric Cardiology, Children's Hospital Medical Center, Cincinnati, Ohio.

Radionuclide angiography (RnAngio) has been used to estimate the magnitude of left-to-right shunts in children. Echocardiography (Echo), using measurements of left atrial diameter (LA) and aortic root diameter (Ao), has been proposed as an alternate non-invasive technique. This study

compares both techniques, in two overlapping groups of patients, with determinations of Qp:Qs by the Fick method using measured O_2 consumption. In 4 patients without clinical evidence of shunts, Fick Qp:Qs was assumed to be 1.0.

21 patients had RnAngio, 14 with ventricular septal defect (VSD), 3 with patent ductus arteriosus and 4 without shunts. Area-ratio analysis of the pulmonary dilution curve correlated well with Fick Qp:Qs ($r=0.92$).

26 patients with VSD had Echo. Correlation was shown between Fick Qp:Qs and calculated ratios of LA/Ao, LA/(body surface area) and LA/(body length) ($r=0.54$, $r=0.59$ and $r=0.63$, respectively). A test statistic based on the Fisher z-transformation indicated that the correlation coefficient with Fick Qp:Qs was higher for the 21 RnAngio patients than for the 26 Echo patients ($p<0.01$).

12 patients with VSD were common to both of the above groups. Area-ratio analysis by RnAngio correlated well with Fick Qp:Qs ($r=0.91$). Correlation coefficients for Fick Qp:Qs and Echo were $r=0.75$ for LA/Ao, $r=0.64$ for LA/(body surface area) and $r=0.73$ for LA/(body length).

In this study, RnAngio appeared superior to Echo for non-invasive estimation of left-to-right shunts.

MONDAY, 4:00 p.m.-5:30 p.m.

CHICAGO ROOM

CARDIOVASCULAR 2

Chairman: William L. Ashburn
Co-Chairman: Robert O. Smith

CORRELATION OF PROTEIN BINDING AND THE LOCALIZATION OF Tc-99m PYROPHOSPHATE AND OTHER AGENTS IN INFARCTED MYOCARDIUM. Mrinal K. Dewanjee, Mayo Clinic and Mayo Foundation, Rochester, MN.

Although Tc-99m pyrophosphate (Tc-PP) has been used for imaging infarcted myocardium, its mechanism of localization is poorly understood. We have performed double labeling, gel filtration, dialysis and separation of serum and muscle protein by modified Katz method in normal and infarcted myocardium in rabbits, obtained by coronary artery ligation. Rabbits were then injected with Tc-PP, Tc-99m glucoheptonate (Tc-GH), Tc-DTPA, I-131 HSA and P-32 pyrophosphate. Tc-PP, a strong serum protein binder gives a ratio of 50:1, for IM/NM (infarcted vs normal myocardium) in contrast to the ratio of 2:1 for Tc-DTPA a poor protein binder. The intermediate serum protein binders e.g. Tc-GH show ratios of (10-15:1). The gel filtration of serum containing Tc-PP show that Tc-PP is always in equilibrium with Tc-PP protein complex. This Tc-PP in equilibrium with Tc-PP protein complex reaches necrotic cells and binds with the denatured soluble protein of cytoplasm of the infarcted myocardium. The subcellular studies of infarcted myocardium indicate that 65-75% of the Tc-pyrophosphate is protein bound. Analysis of this supernate after separation of subcellular organelles, by gel filtration, dialysis and sucrose gradient analysis confirms this concept of protein binding. Myosin of infarcted myocardium contains only (2-4)% of Tc-PP activity in contrast to (50-60)% in the cytoplasmic protein. In the infarcted area, with I-131 HSA a ratio of (2:1) for (IM/NM) is obtained. Blood flow study with Sr-85 microsphere and plasma transport with labeled HSA, show that Tc-PP enters infarct zone not via blood flow but by other mechanisms of transport probably by lymph flow.

KINETICS AND DISTRIBUTIONAL DYNAMICS OF MYOCARDIAL INFARCT GROWTH IN DOGS. Patrick T. Cahill, Shean-Lan Ho, Jerome G. Jacobstein, Daniel R. Alonso, Martin R. Post and Susan A. Kline, Cornell Medical College, New York, and Polytechnique Institute of New York

Recent evidence strongly supports the hypothesis that myocardial infarct (MI) is a dynamic and evolving process. In order to develop imaging techniques to evaluate the

effects of therapeutic modalities on this process, it is important to learn some of the dynamics of interaction of appropriate radiopharmaceuticals with the acutely evolving MI. We have studied the kinetics of uptake of Tc-99m glucoheptonate since it is the only "hot spot" imaging agent capable of demonstrating this process within the first few hours of MI when salvageable myocardium still remains. In 5 dogs with MI produced by occlusion of the LAD coronary artery we have determined the characteristics of MI growth in terms of activity corrected for background. The area of scintigraphic "MI" increased until between 6 and 9 hr after occlusion when it reached a plateau; however, MI activity continued to increase up to 12 to 14 hr in a linear monotonic fashion. We separated the outer and middle regions of the MI utilizing our newly developed edge detection and deconvolution procedures and studied the kinetics of accumulation of TcGH in each. We found a relatively constant level of uptake in the central, presumably necrotic, region compared to a rapid and continuing accumulation of activity in the outer, presumably salvageable, region. A 5 compartment kinetic model has been developed to describe these findings. The ability to define and identify a potentially salvageable portion of ischemic myocardium offers the potential of evaluating the efficacy of interventions designed to protect ischemic myocardium, one of the principle goals of cardiological research today.

USE OF CORONARY VASODILATORS IN MYOCARDIAL SCANNING--A NEW METHOD FOR VISUALIZATION OF CORONARY INSUFFICIENCY. Angel K. Markov, Robert O. Smith, Patrick H. Lehan, and Harper K. Hellemis. University of Mississippi Medical Center, Jackson, Miss.

As an alternative procedure to the exercise stress test used in myocardial scanning, vasoactive drugs were employed to elicit deficits in blood flow to myocardial regions supplied by stenotic arteries or collateral circulation. The data was collected from: (1) 10 dogs had partial occlusion by a silver clamp of either the circumflex (CFX) or anterior descending artery (LAD) reducing the lumen by 70%. (2) In 10 dogs Ameroid constrictors were implanted and studied from a fortnight post-operatively up to two years. (3) In 4 dogs complete ligation of the LAD or CFX. Coronary hemodynamics and myocardial K-43 dispersion were evaluated in 6 acute experiments with ~70% stenosis. After four rapid serial rectilinear control scans from K-43 (750 μ Ci) were recorded; dipyridamole, nitroglycerin or lidoflazine were administered iv. When the selected drug reached a peak vasodilator effect, a second equal bolus of K-43 was given and four additional scans were recorded. The last scan of the first set was subtracted from the corresponding regional count rates of all serial scans from the second set and the resulting images were interpreted to be myocardial perfusion patterns produced by the drug intervention. Control scans from dogs with partial stenosis or an Ameroid constrictor showed homogeneous distribution of the K-43. When drugs were used, regions supplied by compromised circulation became apparent because of lower counts. With total ligation, the contrast between normal and infarcted myocardium was enhanced. Coronary vasodilators as opposed to exercise in myocardial imaging have a lesser effect on cardiac dynamics and peripheral hemodynamics, increase twofold K-43 uptake in normally perfused myocardium, and elicit true coronary reserve.

RAPID SERIAL SCANS (K-43) DETECT TRANSIENT MYOCARDIAL ISCHEMIA WITHOUT STRESS. Robert O. Smith, Angel K. Markov, Patrick H. Lehan, William M. Flowers, Jr., and Harper K. Hellemis. University of Mississippi Medical Center, Jackson, Miss.

In order to determine whether regions of scar could be distinguished from ischemic myocardium by scanning without exercise stress, 32 patients received one mCi K-43 iv both at rest (bolus and scanning simultaneously begun) and at peak exercise (ex). Multiple serial anterior and oblique 5.5 min scans were obtained without pause. The images were correlated with ventriculography and coronary arteriograms. Zones of diminished uptake were seen in all series when angiography confirmed coronary artery disease

(CAD) was present. When blood flow was by stenosed (~50% or more) or collateral arteries, the first serial resting scan demonstrated lower uptake in corresponding regions followed by a short period (5-10 min) of homogeneous counts. Areas of delayed uptake also usually evidenced rapid K-43 washout. When no collaterals were shown and the artery was totally occluded, the scarred myocardium had persistent low counts in both rest and ex scans. There was >80% agreement with arteriograms of both rest and ex scans. These studies show that rapid serial imaging with a single bolus of K-43 without exercise can locate areas of ischemia that appear reversible if reserve blood flow were returned. Regions of scar and ischemia were separately identified and rapid washout appears to be another indicator of ischemic myocardium. (Supported by NIH Grant 1 RO1 HL19289.)

FACTORS INFLUENCING THE MYOCARDIAL UPTAKE OF THALLIUM-201. Heinz Schelbert, Joanne Ingwall, Robyn Watson, William Ashburn. University of California, San Diego, California

Uptake and distribution of Tl-201 in myocardium is related to regional flow and cell viability. To eliminate the effects of flow, myocardial uptake of Tl-201 was studied in intact, beating fetal mouse hearts (FMH) in organ culture. Thirty-one litters were randomly divided into a control (C) and an intervention group (I) and exposed to Tl-201 contained in the medium at a concentration of 5×10^{-8} mg/ml for 20, 40 and 60 min. Uptake of Tl-201 and the rate of uptake (RU) in each I were compared to the litter mate hearts in C. To ascertain reproducibility each experiment was duplicated. After equilibration, the RU (2×10^{-8} mg Tl-201/mg heart/min) was linear between 20 and 60 min. Raising the temperature from 20° to 37° increased the RU by 71.8% (P < .005) and the myocardial Tl-201 concentrations at 60 min (MC) by 58.6% (P < .001). Quabain (10^{-4} M) reduced the RU by 31.1% (P < .001) and lowered MC by 27% as compared to C (P < .001). Propranolol (10^{-3} M) similarly depressed the RU by 35.5% (P < .002) and MC by 23.1% (P < .001). Procainamide (10^{-4} M) had no significant effect on RU and MC. However, isoproterenol (10^{-5} M) considerably increased the RU by 46.5% (P < .002) and the MC by 51.1% (P < .003). Tl-201 uptake remained constant over a wide range of pH, but significantly increased at pH > 8.0. We conclude, that commonly used drugs, changes in temperature and pH can alter the RU and myocardial concentrations of Tl-201. These effects should be considered if quantitation of regional myocardial Tl-201 content or its rate of change by external imaging are to be used as an index of regional myocardial perfusion or cell viability.

TIME COURSE OF REDISTRIBUTION OF Tl-201 AFTER TRANSIENT ISCHEMIA. Heinz Schelbert, Gerhard Schuler, William Ashburn, James Covell. University of California, San Diego, CA.

"Redistribution" (RD) of Tl-201 (Tl) injected during stress and monitored by repeat imaging may permit differentiation of transient from permanent ischemia. To study the time course of RD, 16 closed chest dogs with indwelling left atrial (LA) catheters and occlusive cuffs at the proximal left circumflex coronary artery (LCA) were used. In 12 dogs, the LCA was occluded, and—as an index of regional myocardial (M) perfusion at the time of occlusion—cardiac output and Sr-85 microspheres (15 μ) were injected into the LA and Tl administered. Four dogs were sacrificed immediately (t_0), 4 dogs after 30 min. (t_{30}) of reperfusion (RP) and 4 after 4 hrs. (t_{310}) of RP. Four dogs with 1 week old myocardial infarctions (MI) were studied 4 hrs. after injection of Tl and microspheres. Compared to normal myocardium (NM) Tl in regions with transient flow reductions >95% (IM) was decreased by 94.6 ± 0.9 (SEM)% (P < .01) at t_0 , by $53.8 \pm 7\%$ (P < .025) at t_{30} and by only $16.1 \pm 1.6\%$ (P < .025) at t_{310} . During the first 30 min. of RP, the change in Tl distribution between NM and IM was due to a $340.9 \pm 40.1\%$ (P < .01) increase of Tl in IM and a $29.9 \pm 1.7\%$ (P < .05) fall in NM. During the next 3.5 hrs. of RP Tl fell only in NM by $31.9 \pm 3.4\%$ without changing significantly in

IM. In dogs with MI, Tl in regions with flow reductions > 95% were still reduced by 86% relative to NM. Thus, early RD reflects primarily active Tl-201 uptake by IM while late RD primarily represents loss of Tl-201 from NM. We conclude that transient ischemia is visualized best early after stress and that repeat imaging begun 30 min. after stress may not permit differentiation between transient and permanent ischemia.

THALLIUM-201 REDISTRIBUTION IN CORONARY HEART DISEASE (CHD). EARLY AND DELAYED MYOCARDIAL SCANS

Gustav Hör, Helmut Sebening, Eckart Sauer, Jochen Dressler, Carola Wagner-Manslau, Ioannes Bofilias, Leopoldo Lutitsky, and Hans W. Pabst. Nuklearmedizinische Klinik and I. Medizinische Klinik, Technische Universität München, Munich, FRG.

Exercise Tl-201 myocardial scans in significant CHD show decreased Tl-uptake in the region of stress-induced ischemia immediately after ex (ex) with redistribution on delayed scans. 8 healthy subjects (HS) and 25 with CHD proven by angiography and ventriculography including 6 with previous myocardial infarction (PMI) were scanned at rest, ex, 1 and 2 hrs after ex. Data was collected by ON 100 gamma camera interfaced to ON 150 data system. In HS Tl distribution was homogeneous at rest after ex, in 19 patients with CHD only at rest. 6 with PMI presented a locally diminished Tl uptake even at rest. In scans 1 and 2 hrs after ex significant increase of count rate ratio (ROI min/ROI max) was measured ($p < 0.001$) in CHD without PMI interpretable as Tl redistribution. Scans beyond 2 hrs were equal to those at rest. 6 patients with CHD and PMI had Tl-defects larger under ex than at rest, 1 and 2 hrs after ex defects persisted without redistribution being observed in ROI min. Rapid (lack of) redistribution in delayed scans within areas underperfused in early ex scans is a sign of (ir-)reversible ischemia in CHD. Scans at rest may be omitted in CHD, because transient ischemia is undetectable.

tions were within 16% in all cases, but varied up to 43% if a single depth was assumed for both adrenals.

NP-59 adrenal images show greater detail than prior agents, providing the opportunity for greater accuracy in adrenal disease detection. However, such results will be obtained only if normal scintigram patterns are appreciated. A major factor impairing interpretation is the depth variation between the left and right adrenal gland. Accurate interpretation requires correlation of information derived from anterior and lateral as well as posterior views.

RESULTS OF AN ADRENAL IMAGING STUDY BY EIGHT (8) INVESTIGATORS USING ADRENOSCAN (I-131-19-iodocholesterol). Irvin Strathman and Mary Ann Leeper. Searle Laboratories, Skokie, Ill.

Eight (8) investigators following a uniform protocol used Searle Laboratories' Adrenoscan (I-131-19-iodocholesterol) to investigate 73 patients with suspected adrenal disease including primary aldosteronism (34 patients), Cushing's disease (22 patients) and other less common adrenal disease states (17 patients). Of the 83 scans performed, 64 (77.1%) accurately diagnosed unilateral lesions, bilateral pathology or normal adrenals. Only one false positive scan (1.2%) incorrectly suggested adenoma; a repeat scan confirmed by surgery correctly identified bilateral hyperplasia. There were no false negatives. Eleven scans are not yet confirmed; in seven cases, the adrenals failed to take up the radioactive materials for unknown reasons although possible mechanisms are discussed. Only three of the patients experienced mild and transient discomfort after injection. Radiation absorbed dosages and optimum imaging times differed somewhat from those reported in previous clinical studies. Such differences may well be attributable to improved quality control associated with current preparative techniques. Other factors contributing to optimum imaging and interpretation of imaging information are discussed. Adrenoscan is a safe and effective adrenal-imaging agent. The conclusion is that adrenal imaging using Adrenoscan should be used early in the investigation of suspected adrenal disease states.

MONDAY, 4:00 p.m.-5:30

JANE ADDAMS ROOM

ENDOCRINE/METABOLISM 1: ADRENAL

*Chairman: Martin L. Nusynowitz
Co-Chairman: Thomas P. Haynie*

NORMAL ADRENAL IMAGING. John E. Freitas, James H. Thrall, Dennis P. Swanson, Ayman N. Rifai, and William H. Beierwaltes. University of Michigan Medical Center, Ann Arbor, MI.

Previously unrecognized scintigraphic differences between normal right and left adrenal glands can now be appreciated using I-131-6 β -iodomethyl-19-norcholesterol (NP-59). Adrenal scintigrams in 21 patients without evidence of adrenal disease were reviewed. Posterior, left lateral, and occasional anterior views were obtained 2-8 days post-injection of 1-2 mCi of NP-59 with a gamma camera-computer system. Adrenal depth was determined from the lateral view and percent uptake calculated for each gland.

On posterior views, the following differences between the left and right adrenal were noted: 1) more cephalad location of the right adrenal (81%); 2) round or truncated shape of the right adrenal as compared to the oval or elongated left adrenal (62%); and 3) apparent greater activity of right versus left adrenal (66%). On the lateral view, the left adrenal was more anterior than the right adrenal (81%). Asymmetric activity on the posterior view was reversed on the anterior view in all cases studied (4), indicating that the asymmetry was a function of adrenal depth variation. Percent uptake using individual depth correc-

ADRENAL SCINTIGRAPHY IN LOW RENIN "ESSENTIAL" HYPERTENSION. Ayman Rifai, William H. Beierwaltes, John E. Freitas. University of Michigan Medical Center, Ann Arbor, MI.

We have reported three types of adrenal cortical abnormalities in primary hyperaldosteronism (i.e. aldosteronoma, macronodular and micronodular hyperplasia) with dexamethasone suppression and I-131-19-iodocholesterol adrenal imaging. Twenty-three patients with low renin "essential" hypertension were imaged using identical technique because Gunnels showed the same histopathology in 32 adrenalectomized patients with this syndrome.

Standard adrenal scintiscans were performed in 17 patients but were of little help.

Suppression scintiscans (13 patients) revealed four patterns of adrenal uptake. Four patients had symmetrical bilateral visualization before and after the fifth day of tracer injection (macronodular hyperplasia), five had symmetrical visualization on the fifth day or thereafter (micronodular), one patient had asymmetrical uptake (adenoma - proved by venography), and three had no visualization of the adrenals (normal). Three control patients had a normal pattern (2 = normal renin hypertension, 1 = eutensive, hirsutism).

Good blood pressure response to spironolactone was found in all patients with the macronodular pattern and in three of five with micronodular pattern. Poor response was found in all patients with a normal pattern.

The demonstration of abnormal adrenal cortical suppression in patients with low renin "essential" hypertension who had a good response to spironolactone, and normal suppression with no response to spironolactone is additional evidence of adrenal cortex abnormality in most patients with low renin "essential" hypertension and the utility of radionuclide adrenal imaging in this syndrome.

VISUALIZATION OF NONFUNCTIONING ADRENAL ADENOMAS WITH IODOCHOLESTEROL: POSSIBLE RELATIONSHIP TO SUBCELLULAR DISTRIBUTION OF TRACER. Robert A. Rizza, Heinz W. Wahner, Thomas C. Spelsberg, Robert C. Northcutt, and Harold L. Moses. Mayo Clinic and Mayo Foundation, Rochester, Minn.

Intense uptake of I-131-19-iodocholesterol (I-131 C) was observed in five cases of nonfunctioning adrenocortical adenoma. Adrenocortical steroids were normal. Four of the five tumors showed significant accumulation of lipid histologically. I-131 C was taken up avidly without steroid hypersecretion. To clarify this discordance, the subcellular localization of I-131 C was studied. Rats were injected intravenously with I-131 C or H-3 cholesterol (H-3 C) and killed after 3 days. The distribution of I-131 C vs. H-3 C in various cell fractions after differential centrifugation was: lipid ($90 \pm 2.3\%$ vs. $86 \pm 2.5\%$, $P < 0.005$); microsomal-soluble protein ($1.2 \pm 0.52\%$ vs. $3.4 \pm 0.48\%$, $P < 0.001$); and mitochondrial and crude nuclear fractions (no difference). Treatment of rats with aminoglutethimide (AG) increased both the amount and the percent contained in the lipid fraction of both I-131 C and H-3 C:

Tracer	dpm/ mg	Untreated	AG	Untreated	AG
I-131 C		655±167	1976±417*	90±2.3	93±1.5†
H-3 C	adren	13156±5995	41665±11374*	86±2.5	93±1.3*

(* $P < 0.001$, † $P < 0.05$). ACTH treatment did not change I-131 C content in the lipid layer but it decreased H-3 C content. Thus, adrenal tumor scanning with I-131 C does not require excess steroid production for imaging. Adrenal imaging of nonfunctioning tumors may be explained by I-131 C uptake into the nonsteroid lipid fraction. I-131 C scanning is therefore an appropriate technique in evaluating adrenal lesions regardless of their secretory state.

DEVELOPMENT AND INITIAL EVALUATION OF 123-IODINE LABELED 68-IODOMETHYL-19-NORCHOLEST-5(10)-EN-38-OL(NP59) FOR ADRENAL SCINTIMAGING. Susanne von Schuching and Henry N. Wellman. Indiana University School of Medicine, Division of Nuclear Medicine, Indianapolis, Indiana.

Two reports have been published on the enhanced adrenal uptake of 68-131-iodomethyl-9-iodocholesterol (1,2). In order to extend the scintimaging quality of I-131-NP59 molecule, a rapid exchange procedure was developed for the introduction of 123-iodine into the NP59 molecule. Only 45 minutes are needed for an 85% exchange. The relative distribution of I-123 from I-123-NP59 was studied in 24 rabbits following intravenous injection of 0.5mCi I-123-NP59. The thyroids were not blocked and 6 animals were sacrificed at 1, 2, 3 and 4 days after the dose. The data obtained

from the distribution of radioactivity in 13 tissues and body fluids was used for the calculation of the radiation dose. The 2 kg dose/gm in the adrenals was 4.54% at 2 days and 5.65% at 3 days; the ratio per gm of adrenal:kidney was 28:1 at 2 days and 37:1 at 3 days. Previous studies with I-131-19-iodocholesterol had given a ratio per gm of adrenal:kidney of 10:1 at 2 days and 15:1 at 3 days. Dogs were given 2mCi I-123 intravenously and scintimages were obtained 2 and 3 days later, satisfactorily demonstrating the adrenals. The studies in animals indicate that scintimaging of adrenals in the human is possible employing I-123-NP59, resulting in a reduced radiation dose to the patient.

1. Kojima M, Maeada M, Ogawa H, Nitta K, Ito T, J Nucl Med 16:666, 1975.
2. Sarkar S, Beierwaltes W, Ice R, Basradjian G, Hetzel K, Kennedy W, Mason M, J Nucl Med 16:1038, 1975.

Supported by NIH Grant GM-FD 233692-01

TELLURIUM-123m LABELED 24-NOR-23-(ISOPROPYL TELLURA)-5α-CHOLAN-38-OL: A NEW POTENTIAL ADRENAL IMAGING AGENT.* F. F. Knapp, Jr. and Kathleen R. Ambrose, Radioisotope Dept., Oak Ridge National Laboratory, Oak Ridge, Tenn.

This study was initiated to determine the efficacy of Te-123m labeled 24-nor-23-(isopropyl tellura)-5α-cholan-38-ol as an adrenal imaging agent. Male rats were injected intravenously with 6 μCi (25 mCi/mole) of the labeled steroid and the tissue distribution of radioactivity was determined at periods from one hour to seven days after injection. The results (% dose/gm) indicated an adrenal/liver ratio of 25/1 after one day which increased to 60/1 after seven days. The adrenal cortex/medulla ratio was approximately 2/1. Approximately 50% of the administered dose was excreted after five days, primarily in the feces. The adrenal glands of rats injected with 60-100 μCi of the labeled steroid were clearly imaged with a rectilinear scanner one day after injection. Lipids extracted from the adrenals and liver were subjected to absorption column chromatographic analyses. The adrenal extract contained non-polar radioactive material with the expected mobility of steryl esters in addition to more polar components. The liver extract contained predominantly very polar components. These combined results indicate that radioactivity from Te-123m labeled 24-nor-23-(isopropyl tellura)-5α-cholan-38-ol accumulates in rat adrenals following intravenous administration. More importantly, rat adrenal glands can be clearly imaged using this new agent.

*Research sponsored by U. S. Energy Research and Development Administration under contract with Union Carbide Corporation.

TUESDAY, JUNE 21, 1977

TUESDAY, 8:30 a.m.-10:00 a.m.

CHICAGO ROOM

CARDIOVASCULAR 3: VENTRICULAR FUNCTION

Chairman: Barry L. Zaret
Co-Chairman: Michael L. Goris

FIRST-PASS AND BLOOD POOL RADIOISOTOPE ANGIOGRAPHY AS METHODS OF DETERMINING LEFT VENTRICULAR EJECTION FRACTION. Edward D. Folland, James L. Ritchie, Glen W. Hamilton, and J. Ward Kennedy. VA Hospital, Seattle, Wa.

Left ventricular ejection fraction (LVEF) can be measured by radioisotope angiography (RA) using first-pass or

blood pool (equilibrium) imaging. This study compared LVEF measured by these two techniques with LVEF measured by RAO x-ray contrast angiography in 27 consecutive patients (pts). Twenty-five mCi ^{99m}Tc labelled autologous red blood cells (3.5 cc) were delivered into the superior vena cava via a percutaneous catheter. First-pass imaging data was collected in serial mode in the 40° left posterior oblique position during the first 60 seconds after injection. After 5 min, the cardiac blood pool was imaged in the 45° LAO position. ECG R wave signals were simultaneously recorded for gating. LVEF was calculated from the ECG synchronized, background corrected, time-activity curve obtained by summing 5-6 consecutive cycles on the first-transit study and 200-400 cycles on the equilibrium study.

The 3 methods of determining LVEF were compared by linear regression analysis and construction of 65% and 95% confidence limits for the mean and individual measurements. The relationship of RA LVEF using either first-transit

or equilibrium to the contrast LVEF was virtually identical with r values of 0.85 and 0.80, respectively. The relationship of the RA LVEF by first-transit and equilibrium was similar with an r value of 0.87. Both RA methods tended to overestimate low and underestimate high LVEF as determined by contrast angiography.

We conclude that both the first-transit and equilibrium radioisotope methods can be used to determine the LVEF with equal accuracy.

QUANTITATIVE REGIONAL WALL MOTION: VALIDATION OF RADIOCARDIOGRAPHIC STUDIES BY CONTRAST ANGIOGRAPHY. Richard N. Pierson, Jr., Marvin I. Friedman, Samir E. Alam, Arun V. Prabhu, Seichi Shimomura, and Harvey G. Kemp, St. Luke's Hospital Center, Columbia University, New York City, N.Y. 10025.

Quantitative wall motion (WM) has been well correlated with myocardial injury, and may relate to infarct size. Radionuclide Angiocardiography (RAC) and Contrast Ventriculography (CVG) were performed in 14 patients (7 with normal and 7 with abnormal patterns of systolic contraction) during cardiac catheterization using TcHSA-99m, Anger camera, and computer. In 67 normal and 47 abnormal segments, RAC WM, both by first pass (1⁰P) and equilibrium (EQ) gating, was analyzed quantitatively from a 32 x 32 digital matrix, and compared with calibrated CVG studies. WM ranged from -.5 to 2.7 cm by RAC, vs -.8 to 2.7 cm by CVG. Slopes, intercepts, and correlation coefficients varied by segment; the Table lists slopes and (r) values:

Segment	1 ⁰ P Normal	Abnormal	EQ Normal	Abnormal
Ant Basal (AB)	.9x (.89)	.8x (.80)	---	---
Lateral	.8x (.85)	.8x (.80)	.1x (.13)	.6x (.41)
Apical	.2x (.38)	.7x (.82)	.3x (.44)	-.1x (.08)
Inferior	.3x (.19)	.4x (.86)	.3x (.72)	0x (.04)
Post Basal(PB)	1.0x (.88)	1.1x (.91)	---	---

For normal segments, overall 1⁰P RAC WM was .81x (CVG) + .2 cm, (r=.78), for the RAO position; in abnormal segments, correlation was .54x(CVG) + .4 cm, (R=.56). EQ RAC is invalid for the hidden AB and PB, and less well correlated for other segments. Both 1⁰P and EQ were reliable for the 4 segments seen in LAO.

Quantitative RAC is more accurate for normally contracting (>1 cm) than for abnormal segments. 1⁰P RAC showed much greater quantitative agreement with CVG, but EQ showed useful qualitative correlation for direction of WM in 71 of 93 segments.

NONINVASIVE RADIONUCLIDE ASSESSMENT OF RIGHT VENTRICULAR EJECTION FRACTION IN CHRONIC OBSTRUCTIVE PULMONARY DISEASE. Harvey J. Berger, Richard A. Matthay, Alexander Gottschalk, Barry L. Zaret, Yale University, New Haven, Ct.

Right ventricular ejection fraction (RVEF) was evaluated noninvasively in 34 patients (pts) with chronic obstructive pulmonary disease (COPD) and in 30 normal (nl) control pts without COPD. Quantitative radionuclide angiocardiograms were obtained in the anterior position with a computerized multicrystal scintillation camera following peripheral venous injection of Tc-99m pertechnetate. A high count rate time-activity curve (TAC) from the RV region of interest was used to identify 1-5 cardiac beats. A reproducible right atrial (RA) background was selected at the RA-RV interface and subtracted from the RV TAC. RVEF was calculated using end-diastolic and end-systolic counts from the background-corrected RV TAC. In the control pts, RVEF averaged (+SD) 55±5%, with a nl range of 45 to 65%.

RVEF was abnormal (abnl) in 17 pts with COPD (38±2%, mean±SEM) and nl in 17 (57±2%). Cor pulmonale, with RV hypertrophy on electrocardiogram, was present only in pts (8/17) with abnl RVEF; in these 8 pts, RVEF (35±2%) was significantly less than in the remaining pts with abnl RVEF (p<.05). Arterial oxygen tension was 53±2 mm Hg in pts with abnl RVEF and 64±3mm Hg in those with nl RVEF (p<.05). While forced expiratory volume in one-second (FEV₁) was 37±4% of predicted in pts with abnl RVEF, FEV₁ was significantly greater in those with nl RVEF (54±5% of predicted, p<.001). RVEF averaged 43±3% in the 18 pts with FEV₁<liter and 53±2% in the 16 with FEV₁>1 liter (p<.01).

Thus, radionuclide RVEF correlates with the presence of cor pulmonale and the severity of pulmonary impairment. RVEF distinguishes abnl from nl RV function and appears to be a useful noninvasive index for hemodynamic evaluation of COPD.

GATED CARDIAC POOL AND MYOCARDIAL PERFUSION STUDIES.

Masahiro Iio, Hinako Toyama, Hajime Murata, Kazuo Chiba, Shinichiro Kawaguchi, Hideo Yamada, and Kengo Matsui, Tokyo Metropolitan Geriatric Hospital, Tokyo, Japan.

High temporal resolution EKG gated analysis was performed either 5mCi of Technetium-99m Albumin or 4mCi of Thallium-201 Chloride to visualize cardiac pool or myocardium. Using 32 KW computer system and LIST mode data acquisition, sequential events during 10 to 50 msec. intervals are continuously recorded for 1500 to 2000 cardiac cycles. Besides high temporal resolution sequential images of cardiac pool and myocardial mass during a cardiac cycle, such parameters were obtained as relative volume curve(V(t)/V_{ED}) (RV), ejection fraction(EF), relative volume velocity(dV(t)/dt)/V_{ED}(RVV), maximum systolic volume velocity(MSVV), maximum diastolic volume velocity(MDVV), contraction pattern of left ventricle and relative myocardial volume curve(RMVC). Normal control at rest and under physical stress, cases with ischemic heart disease, primary myocardial disease(PMD), hyperthyroidism were evaluated by this method. Mean EF were 70 % for control, 71 % for hyperthyroidism, 47 % for old myocardial infarction(OMI), 21 % for OMI with decompensation, 40 % for PMD. Mean MSVV and MDVV were 3.8 and 3.6 for control, 4.5 and 5.5 for hyperthyroidism, 2.7 and 2.4 for OMI, 1.6 and 1.7 for OMI with decompensation and 2.4 and 1.9 for PMD. MSVV and MDVV were proved to be of special value to elucidate the left cardiac function. Gated myocardial perfusion image produced the sequential high temporal change of myocardial muscle volume during each cardiac cycle. Cyclic change of muscle volume was found to occur in different grade at apex, free wall and septal wall of control. Asynchronous change of muscle contraction was noted in such cases as OMI and PMD.

CHARACTERISTICS OF LEFT VENTRICULAR TIME-ACTIVITY CURVES IN PATIENTS WITH HEART DISEASE. Saeeda Qureshi, Henry N. Wagner, Jr., Philip O. Alderson, Mattheus G. Lotter, Kenneth H. Douglass, Lloyd G. Knowles, The Johns Hopkins Medical Institutions, Baltimore, Md.

Left ventricular time-activity curves were obtained in 112 patients with various types of heart disease using a scintillation camera-computer system. After intravenous injection of Tc-99m albumin scintillation camera images synchronized with the patients' ECG's were acquired at 64 intervals during the cardiac cycle and left ventricular time-activity curves were generated. The following indices were measured from these curves: Pre-ejection period (PEP); R-R interval (R-R); PEP/R-R; left ventricular emptying time (LVET); LVET/R-R; left ventricular fast filling time (LVDT1); LVDT1/R-R; left ventricular slow filling time (LVDT2); LVDT2/R-R; PEP/LVET; ejection fraction (EF) and EF/LVET. The mean values in 8 normal controls were: PEP/R-R 0.085, LVET/R-R 0.351, LVDT1/R-R 0.345, LVDT2/R-R 0.202, PEP/LVET 0.239, EF 0.55, EF/LVET 1.91. There was shortening of LVET/R-R and prolongation of LVDT1/R-R in patients with essential hypertension. Patients with congestive heart failure had shortening of LVET/R-R but an increased PEP/LVET ratio. EF remained normal in hypertensive patients but was slightly decreased in myocardial infarction and markedly reduced in congestive heart failure and cardiomyopathy. These initial results suggest that display and analysis of synchronized left ventricular time-activity curves may be of value in the detection and differential diagnosis of patients with certain types of heart disease.

RELATION BETWEEN THE EXTENT OF ACUTE MYOCARDIAL INFARCTION AND LEFT VENTRICULAR PERFORMANCE ASSESSED BY SCINTIGRAPHIC AND ENZYMATIC METHODS. Hartmut Henning, Heinrich Schelbert, William Ashburn, and Joel Karlner, University of California, San Diego.

A relation between abnormalities in left ventricular (LV) performance and the extent of muscle damage in patients (pts) with acute myocardial infarction (AMI) has not previously been well-documented by noninvasive means. In 38 pts with AMI, ejection fraction (EF) was calculated from the LV time-activity curve obtained during the

initial passage of a bolus of Tc-99m pyrophosphate (PYP). The extent of AMI was calculated both by integrating the area under the completed creatinine phosphokinase (CPK) curve and by planimetry the largest area of PYP uptake. In 21 pts with anterior AMI, the CPK curve area correlated well with PYP area ($r = 0.92$). By contrast, in 17 pts with inferior AMI the correlation was poor ($r = 0.45$). In 21 pts with transmural AMI, but no evidence of prior MI or LV hypertrophy (LVH), EF ranged from 39 to 72% and correlated inversely with CPK curve area ($r = -0.76$). In 10 pts with a first transmural anterior AMI there was a good correlation between EF and PYP area ($r = -0.88$). In 7 pts with LVH and a first anterior AMI, EF was with 54 ± 6 significantly higher ($p < 0.05$) than in 10 pts with AMI, and no LVH (41 ± 5), although PYP area did not differ significantly for both groups. We conclude that in pts with transmural AMI alterations in EF correlate well with the extent of infarction measured by the CPK curve area. Furthermore, in pts with anterior AMI, a single procedure, radionuclide scintigraphy, can be used to estimate the extent of infarction and also to assess LV performance.

PROGNOSTICATION AFTER ACUTE MYOCARDIAL INFARCTION WITH A PORTABLE PROBE RADIONUCLIDE LEFT VENTRICULAR FUNCTION STUDY. Michael Kelly, Michael Quinlan, and Peter Thompson. Perth Medical Centre, Perth, Western Australia.

This study's aim was to determine the prognostic value of bedside measurements of left ventricular function after acute myocardial infarction (AMI). Over a 12 month period, measurements of left ventricular ejection fraction (EF) and pulmonary transit time (PTT) were made in 171 patients with AMI, at a median time of 24 hours after onset of pain. A probe method described by Steele et al. was used. The results were correlated with clinical outcome.

In 14 controls without heart disease EF (mean \pm SD) was 0.61 ± 0.06 , and PTT was 6.4 ± 1.1 seconds. In the 171 patients with AMI EF was 0.36 ± 0.10 , and PTT was 8.8 ± 3.7 ; in only 18 (11%) was EF > 0.50 .

In the 90 patients with EF > 0.34 there were no episodes of ventricular fibrillation (VF), pump failure deaths (PFD), or post-hospital deaths (PHD) (mean follow-up time 6 months). EF (mean \pm SD) was 0.26 ± 0.06 in 8 with "primary" VF (all hospital survivors), 0.20 ± 0.07 in 12 with PFD, and 0.23 ± 0.07 in 5 with PHD, which was sudden in each case. PTT was > 14 in 11/12 with PFD (mean 17.6, SD 3.4), but in only 3/159 without PFD. In 6 patients who died of other causes (2 of cardiac rupture, 3 of ruptured septum, and 1 of sudden "electromechanical dissociation") EF (mean \pm SD) was 0.44 ± 0.12 and PTT was 7.2 ± 2.2 .

It is concluded that bedside measurements of left ventricular function after AMI with a simple, inexpensive radionuclide method are of high prognostic value. EF < 0.35 indicates a high risk of VF, PFD, and PHD. A PTT > 14 indicates the subgroup with the highest risk of PFD. However, mechanical ventricular defects are not associated with a particularly low EF or a long PTT.

ated fibrinogen is cleared from the blood more rapidly than fibrinogen iodinated at 2 atoms of iodine per molecule of fibrinogen. In order to determine whether fibrinogen modified in this manner retained its oncophilic properties, the distribution and clearance of *I-fibrinogen (2,5,25,45,65 iodine atoms per molecule of fibrinogen) labeled by the IC1 or electrolytic methods was measured at 1-24 hours in the KHJJ tumor model. Heavily iodinated fibrinogen concentration localized in the tumor at least as well as 2 atoms of iodine per molecule of fibrinogen, although heavily iodinated fibrinogen by electrolytic method cleared more rapidly after 4 hours. Blood clearance of heavily iodinated fibrinogen labeled by IC1 at 45 and by electrolytic method at 42 atoms per molecule was 2 and 5-10 times faster than that of fibrinogen (2 iodine atoms per molecule) during the initial 4 and 8 hours, respectively. Subsequent clearances were similar. Highly iodinated fibrinogen did not concentrate excessively in any organs, e.g. liver, indicating the absence of aggregated or grossly denatured fibrinogen. Tumor:blood of heavily iodinated fibrinogen was greater than that of normal fibrinogen (almost 7-fold at 4 hours). If this data can be extrapolated to cancer in patients, heavily iodinated fibrinogen labeled with ^{123}I has exciting potential as an oncophilic radiopharmaceutical.

Ga-67 TUMOR UPTAKE IN ANIMALS AFTER WHOLE BODY IRRADIATION. William P. Bradley, Philip O. Alderson, William C. Eckelman and Joseph F. Weiss. Armed Forces Radiobiology Research Institute, Bethesda, Md. and the George Washington University, Washington, D.C.

The mechanism of decreased Ga-67 retention after whole-body irradiation is unknown. To investigate this mechanism, and determine the effects of prior irradiation on Ga-67 tumor uptake, Sprague-Dawley rats bearing a subcutaneous Walker-256 carcinosarcoma were exposed to Co-60. Each animal received 10 μCi of Ga-67 citrate intravenously 24 hours after exposure to whole-body doses of 250, 500, 750 or 1000 rads. Control animals received Ga-67, but were not irradiated. Urine was collected for 48 hrs after exposure to determine the % injected dose (ID) excreted. Animals were sacrificed at 48 hrs and the % ID/gm in tumor and other tissues was determined. A blood sample was also obtained to determine the serum iron, unbound iron-binding capacity (UIBC) and transferrin level. Tumor uptake and serum UIBC were decreased in irradiated animals, while serum iron levels and Ga-67 urinary excretion were increased. There was a significant correlation between the UIBC and the Ga-67 tumor uptake ($r = +0.74$, $n = 22$). Transferrin levels in the irradiated population were not different from control values. Local irradiation of the tumor without whole-body exposure had no effect on Ga-67 tumor uptake or urinary excretion. When the experiments were repeated with a 15 mg/animal dose of transferrin preceding Ga-67 injection, urinary excretion and tumor uptake returned toward normal. The results indicate that the decreased Ga-67 retention and tumor uptake seen after whole-body irradiation is related, at least in part, to saturation of transferrin by increased levels of circulating iron.

TUESDAY, 8:30 a.m.-10:00 a.m.

LINDHEIMER ROOM

ONCOLOGY 1

Chairman: William D. Kaplan
Co-Chairman: Alan D. Waxman

MOUSE TUMOR LOCALIZATION AND BLOOD CLEARANCE OF HEAVILY IODINATED FIBRINOGEN. Gerald L. DeNardo, Kenneth A. Krohn, Sally J. DeNardo, David W. Wheeler. Department of Nuclear Medicine, University of California, Davis, Sacramento Medical Center. (Supported by ACS Grant #DT-45)

Our earlier work demonstrated that the tumor concentration at 4 hours of fibrinogen labeled with 2 atoms of iodine per molecule of fibrinogen was equal to the maximum tumor concentration of ^{67}Ga -citrate in KHJJ tumor-bearing mice. Other investigators have found that heavily iodinated

MOSSBAUER SPECTROSCOPIC STUDY OF THE CHEMICAL BONDING OF Co-57-BLEOMYCIN IN TUMORS. M. R. Zalutsky, A. M. Friedman, J. C. Sullivan, S. L. Ruby, and G. V. S. Rayudu. Argonne National Laboratory, Argonne, Illinois and Rush University Medical Center, Chicago, Illinois.

Several radiolabeled bleomycin complexes have been proposed as possible tumor scanning agents; however, only Co-57-bleomycin has been shown to possess biological properties suitable for clinical use. In this work, we have investigated the chemical bonding in the Co-57-bleomycin complex using Mössbauer Spectroscopy. Measurements were taken using standard Mössbauer techniques using a $\text{Fe}(\text{CN})_6$ absorber with both the source and absorber at 80°K. Co-57-bleomycin was prepared by addition of Co-57-Cl₂ to a solution of bleomycin in 0.9% NaCl. The reaction mixture was passed through a Sephadex G-25 column to remove any unbound Co-57. The Co-57 bleomycin was injected into the lateral tail vein of Sarcoma-180 bearing, ICR strain mice. Forty-eight hours later, the mice were sacrificed, the

tumors were removed and cooled to 80°K, and the Mössbauer spectrum of the Co-57 activity in the tumor was measured. This spectrum was compared to those measured for several compounds with known chemical bonding as well as to a spectrum for the Co-57-bleomycin taken prior to injection. The results show that 1) the Cobalt in the Co-57-bleomycin complex is rapidly air oxidized to a mixture of Co(II) and Co(III) and 2) only the Co(III) complex concentrates in the tumors. We conclude that the Cobalt-57-bleomycin complex should be oxidized prior to its administration in order to increase its accumulation in tumors.

Cross-sectional images with tissue density discrimination of 1% at the spatial resolution of the scintillation camera are acquired in several minutes. The radiation dose is 0.5 rads. Several economical long-lived radionuclides are currently under investigation as alternatives to Tc-99m. Following Compton scatter tomographic (CST) studies, the irradiating beam is shut off with the patient still in position and a conventional vertex radionuclide cerebral perfusion study is performed with 20 mCi of Tc-99m DTPA. The anatomical structures demonstrated by CST images and the functional information of the radionuclide images are uniquely correlated in this system by superimposing the two studies.

TUESDAY, 8:30 a.m.-10:00 a.m.

JANE ADDAMS ROOM

INSTRUMENTATION 1: TOMOGRAPHY

Chairman: Gordon L. Brownell

Co-Chairman: David A. Weber

A NEW EMISSION COMPUTED AXIAL TOMOGRAPH FOR POSITRON EMITTERS. Michael E. Phelps, Edward J. Hoffman, Robert Highfill and David E. Kuhl, Center for Health Sciences, University of California, Los Angeles, Los Angeles, Ca. and Oak Ridge Associated Universities, Oak Ridge, Tenn.

This Emission Computed Axial Tomograph (ECAT) is designed to image positron-emitting radioisotopes in any body part. A hexagonal array of 66 NaI detectors is employed with an annihilation coincidence detection scheme which gives the system a "fan beam" geometry. This design produces high sensitivity while maintaining high resolution and high image contrast. Sensitivity at 1.9cm FWHM resolution is 29,000 cps/ μ ci/ml for 20cm diameter uniform cylinder, which is approximately 3 times the sensitivity of PETT III. Resolution is user selectable and will typically be 1.0 to 1.9cm FWHM. The high contrast of this system is demonstrated by its ability to detect .75cm cold spots in 20cm diameter phantoms while employing shadow shields with 1.6cm FWHM resolution. Intrinsic field uniformity and resolution uniformity within a 20cm diameter phantom are better than $\pm 2\%$ and $\pm 5\%$, respectively.

The redundant sampling scheme employed in ECAT protects against patient movement and detector instability. In studies with uniform phantoms in which as many as 3 detectors were disconnected only minimal distortion was observed.

Indexing of the patient bed is under computer (PDP-11)/45 control which allows accurate repositioning of patient for multiple scans, accurately spaced scans and minimal time loss between scans. This effectively increases sensitivity of system by minimizing data loss from decay of short lived isotopes. This indexing capability also allows the ECAT to do high contrast, quantitative rectilinear whole body scans producing AP and 60° left and right oblique views.

COMPTON SCATTER TOMOGRAPHY OF THE BRAIN. S. G. Mirell and W. H. Bland, Veterans Administration Wadsworth Hospital Center, Los Angeles; and School of Medicine, University of California, Los Angeles.

A new technique of tomographic brain imaging is presented. A specially designed gamma irradiator accessory, an unmodified Searle LFOV scintillation camera, and a mini-computer have been integrated into a system capable of acquiring images of tissue density from 1 cm-thick cross-sections of the head. The images are analogous to those obtained by CT scanners. The gamma irradiator consists of a planar-collimated ring that contains 5 Ci of Tc-99m which surrounds the head at the cross-sectional level to be imaged. Compton scattered gamma rays are detected by the camera in a vertex position. The acquired image is a representation of local electron densities or the nearly proportional mass densities in the cross-section of tissue. Computer algorithms correct for attenuation artifacts from overlying sections of tissue. The images are displayed on a 128 x 128 matrix at a selected tissue density range.

TRANSVERSE SECTIONS IN CONE BEAM GEOMETRY. Gerd Muehlllehner, Joseph H. Dudek, Frank Atkins, Paul V. Harper, Searle Radiographics, Des Plaines, Ill and University of Chicago, Ill.

By rotating a positron camera consisting of two opposed uncollimated Anger cameras around the patient, data are collected which represent projections through a three-dimensional volume which are not restricted to lie in a plane. Algorithms developed in the field of computed tomography are not readily applicable, since they deal with single planes. The problem is two-fold: 1) incoming data must be organized for processing and 2) the appropriate filter function must be found. Since during a rotation the number of possible independent coincidence channels exceeds 10^7 , data are not summed into coincidence channels but are backprojected directly through a 64 X 64 X 16 element volume. The backprojected volume is then filtered to obtain the original distribution.

Programs to perform this operation have been implemented on a minicomputer (Interdata 8/32) which is currently being connected on-line to the positron camera. Both phantom and clinical results show high contrast typical of computed tomography transverse sections.

COMPARISON OF THE ANGER TOMOGRAPHIC SCANNER AND THE 15" SCINTILLATION CAMERA IN GALLIUM IMAGING. Mary F. Hauser and Alexander Gottschalk, Yale University, New Haven, Ct.

A clinical evaluation of 29 patients was made to determine the relative merit of the Anger Tomographic Scanner (Pho/Con) for gallium scanning by comparing it to the 15" detector Gamma Cameras.

After IV administration of 6 - 10mCi of gallium citrate (Ga-67) the patients were examined by both the Pho/Con and a 15" Gamma Camera, (either a Searle LFOV with a medium energy parallel hole collimator and 20% windows at the 3 principal peaks or a Picker 4/15 with a high energy parallel hole collimator with 20% windows at the 184 and 296 keV peaks). The time interval between injection and imaging varied according to the nature of the suspected pathology, i.e. 48 hours or more for malignant disease and frequently 24 hours or less for inflammatory disease. Both posterior and anterior views of all areas of interest were obtained on the camera.

On the basis of a simultaneous "side-by-side" scrutiny of the read-out from both imaging modalities, each case was classified I - V. The results were: Category I (lesion(s) seen only with Pho/Con) - 1; II (better visualization with the Pho/Con) - 6; III (equivalent with either instrument) - 22; IV (better visualization with the camera) - 0; and V (lesion(s) seen only with the camera) - 0. In 7 of 29 cases (24%) we found that the tomographic effect was helpful in either distinguishing normal structures such as colon from pathologic collections of activity or increasing the contrast of lesions.

Although virtually all lesions were detected with the cameras, we show a clear preference for the tomographic read-out. We believe the tomographic scanner to be the current instrument of choice for Gallium-67 scintigraphy.

CORRECTION OF POSITRON SCINTIGRAMS FOR DEGRADATION DUE TO RANDOM COINCIDENCES: Charles A. Burnham, Nathaniel M. Alpert, Bernard Hoop, Jr., and Gordon L. Brownell. Massachusetts General Hospital, Boston, Massachusetts

A premature limit on the amount of activity which can be imaged with a positron camera is imposed by random coincidences which are detected along with true coincidence events. Detection of random coincidences invariably increases with activity, degrading image contrast. Unlike the background in conventional scintigrams due to Compton scattering, detection of random coincidences adds a background which may be measured and subtracted. The distribution of random coincidences within the image depends strongly on the geometry of the source distribution, usually following that of true coincidences but with greatly reduced resolution. Because the random coincidences are smoothly distributed, their amplitude can be estimated with relatively few events.

Logic permitting accumulation of delayed (i.e. random) as well as prompt (i.e. true + random) coincidences has been incorporated in the MGH positron camera. Delayed coincidence images are accumulated for 1/7 the total imaging time smoothed and subsequently subtracted from the prompt coincidence image. Using the MGH camera without random subtraction, image degradation can become observable with less than 1 mCi in the field of view. Measurements with phantoms and in routine imaging studies have shown that random subtraction can restore image contrast with activities in excess of 5 mCi in the field of view. The correction is limited only by its statistical nature and may be adapted to any coincidence counting device. (This work was supported in part under ERDA EY-76-S-02-3333.*000, USPHS "An Interdepartmental Stroke Program," 5 P5ONS10828-03, and USPHS 1-P17HL17665, "Ischemia SCOR Imaging.")

TUESDAY, 10:45 a.m.-12:15 p.m.

JANE ADDAMS ROOM

BONE/JOINT 1

Chairman: Robert E. O'Mara

Co-Chairman: Larry L. Heck

AN IMAGING, AUTORADIOGRAPHIC, RADIOGRAPHIC, ISOTOPIC, AND HISTOPATHOLOGIC STUDY OF IRRADIATED BONE. Michael A. King, George W. Casarett, David A. Weber and Francis A. Burgener. University of Rochester Medical Center, Rochester, N.Y.

A study was conducted to correlate the post-irradiation changes in Tc-99m pyrophosphate (PPI) deposition with pathological and radiological changes in bone. A 1,000 kVp x-ray machine was used to deliver 1,750 rads to the left hind legs of 40 rabbits. Serial quantitative images of both the irradiated and control legs were recorded before irradiation and at numerous times over the first 12 months following irradiation. Six rabbits (5 irradiated and 1 sham irradiated) were included at each imaging time. Both cortical bone (tibial shaft) and trabecular bone (tibial and femoral epiphyses) were evaluated in these serial studies.

Radiographs were taken before irradiation and at 3, 6, 7½, 9, 10½, and 12 months post-irradiation and were compared to the camera images. At 1 day, 1, 3, 6 and 12 months post-irradiation, 3 rabbits were sacrificed for study of Tc-99m PPI, Sr-85, Cr-51 RBC and Rb-86 (blood flow) activity levels in skin, muscle, marrow and bone. Also at these times, 3 additional animals were sacrificed for Tc-99m PPI autoradiographic and histopathologic studies.

The changes in Tc-99m PPI uptake observed on the images showed a bimodal response with maxima occurring in the irradiated leg at 1 day and 3-4 months post-irradiation. The early response was found to be a vascular effect;

whereas, the later maximum correlated with a large increase in bone remodeling as observed histologically and autoradiographically. With the exception of a single lytic lesion, radiographic changes consistently lagged behind changes in radiopharmaceutical deposition. Bone imaging with Tc-99m PPI was found to provide a sensitive indicator for radiation damage to bone.

HETEROTOPIC BONE, A POTENTIAL SOURCE OF ERROR IN EVALUATING HIP PROSTHESIS BY RADIONUCLIDE TECHNIQUES. Jay Mall, Paul Hoffer, William Murray, Juan Rodrigo, Hal Anger, Audrey Samuel. University of California, San Francisco, CA.

While investigating patterns of radionuclide uptake following installation of hip prostheses, we observed a serious potential problem in distinguishing radionuclide uptake in heterotopic bone from increased uptake due to loosening and/or infection in the femoral component.

Eight patients who had a hip prosthesis installed 4 months to 6 years previously were evaluated by technetium-99m MDP joint scan prior to surgery. A total of 10 hips with prostheses were evaluated, 5 with clinical evidence of loosening and 5 asymptomatic hips scanned incidental to installation of a prosthesis in the opposite hip. All but one patient had scans performed with a conventional gamma camera, tomoscanner and multi-angle imaging device.

Eight hips had radiographically demonstrable heterotopic bone in the region of the proximal femur. Six of these 8 hips demonstrated increased radionuclide uptake in the region of the heterotopic bone which was easily confused with the patterns of uptake described in the literature in loose or infected prostheses. Two of these confusing patterns of heterotopic bone uptake of radionuclide were seen in hips with no evidence of prosthetic dysfunction.

The tomographic and multiangle view systems provided excellent images of the hip but were only slightly superior to the conventional camera in helping to distinguish heterotopic bone uptake from prosthetic loosening.

Increased uptake of radionuclide at the distal end of the femoral prosthesis was the only finding seen in all 5 hips with prosthetic loosening and none of the 5 asymptomatic hip prostheses. It was the only sign of prosthetic loosening not easily confused with heterotopic bone.

JAW IMAGING IN CLINICAL DENTAL DIAGNOSES. Daniel A. Garcia, Donald E. Tow, Dace Jansons, Thomas M. Sullivan and Richard Niederman. VA Hospital, West Roxbury, MA

Bone imaging of the jaws was evaluated as an adjunct dental diagnostic method to determine potential usefulness in presurgical screening for infectious dental lesions.

Comparisons were made between the findings of dental examinations and jaw images of 31 males prescribed for bone imaging with Tc-99m diphosphonate, for reasons other than oral disease. The positive findings from clinical and radiographic dental examinations were divided into 4 categories: Healing of recent extractions and 3 ranked categories of disease. The jaws were each divided into 4 quadrants and the regions scored for the type of finding present. Anterior and right and left lateral jaw images were made with a scintillation camera, and areas of positive uptake were assigned to specific jaw quadrants.

Of the 248 total quadrants, 12 of 13 scored for bone healing were image positive as expected. Quadrants in which both radiographic and clinical findings of disease were present were generally image positive (15 of 18, positive), while those in which radiographic evidence of disease was not accompanied by clinical symptoms were largely image negative due to arrested disease, as evidenced by treatment findings in one of the quadrants. 20 of the 207 quadrants scored as normal or minimally diseased were image positive, indicating incipient disease, one of which was subsequently found to contain a focal lesion of infectious osteitis.

It was concluded that bone imaging is potentially useful for detecting incipient dental disease not readily identified in dental examinations. More importantly, imaging could be a valuable adjunct to dental radiography to distinguish active from arrested or inactive disease.

FACIAL BONE SCANNING BY EMISSION TOMOGRAPHY. M.L. Brown, J.W. Keyes, Jr., P.F. Leonard, and J.H. Thrall. University of Michigan Medical Center, Ann Arbor, Michigan.

Facial bone anatomy is complex and localized areas of increased or decreased activity may become lost among overlapping structures even when multiple views are obtained. This study was undertaken to evaluate the use of emission computed tomography to overcome these difficulties.

Using a single photon emission tomographic system, the Humongotron, we have studied normal facial anatomy and a number of patients having abnormalities of the facial bones. Three to four hours following the injection of 15 mCi of Tc-99m pyrophosphate routine bone scans were obtained. Emission tomography of the face and head was then performed. Total time for tomographic projection data collection was thirty minutes. From this data, serial tomographic reconstruction of all levels of the head and face from below the mandible to the vertex were made. These reconstructions were compared with the conventional bone images and x-rays.

The resulting images demonstrated resolution comparable to the standard gamma camera images but the tomographic presentation was superior in defining the anatomy of the facial region and in the characterization and localization of various forms of pathology including osteomyelitis, cancer, osteoradionecrosis and post-surgical changes.

Emission computed tomography is a useful technique. It offers particular advantages in problem areas such as bone scanning of the face and skull where the complex structure of the mandible and facial bones is easily studied and well defined.

CONTRIBUTION OF THE BONE SCAN, SERUM ACID AND ALKALINE PHOSPHATASE, AND THE RADIOGRAPHIC BONE SURVEY TO THE MANAGEMENT OF NEWLY-DIAGNOSED CARCINOMA OF THE PROSTATE. Rex B. Shafer and Donovan B. Reinke. Nuclear Medicine and Radiology Svcs., V.A. Hospital, Minneapolis, MN.

Cancer of the prostate is the most common neoplasm metastatic to bone. Early detection of skeletal involvement is important in staging and selection of therapy. This study was undertaken to determine the accuracy of nonoperative techniques for detecting bony metastases from carcinoma of the prostate.

One hundred ten unselected patients with biopsy-proven carcinoma were examined by Tc-99m PYP bone scan and radiographic bone survey. Bone scans and radiographic surveys were obtained within one month of the initial diagnosis and prior to the introduction of therapy. Heat-labile serum alkaline phosphatases and prostatic fractionated serum acid phosphatases were obtained at the time of bone scan.

Results show that 37 of 110 patients had evidence of bony metastases on bone scan. In 25 of these patients, there were abnormal radiographic surveys. Twenty of these patients had abnormal alkaline phosphatases and 18 patients had abnormal acid phosphatases. In 77 patients with normal bone scans, 18 had elevated alkaline phosphatases and 12 had elevated acid phosphatases.

These findings suggest that bone scanning is of considerable importance in the management of newly-diagnosed carcinoma of the prostate. As a screening procedure, bone scanning is superior to radiographic bone survey. Surprisingly, elevated serum acid phosphatase was not as useful as bone scanning in the diagnosis of bony metastases from carcinoma of the prostate.

TRANSCAPILLARY EXTRACTION BY THE CANINE TIBIA OF Tc-99m PYROPHOSPHATE AND ETHANE-1-HYDROXY-1,1-DIPHOSPHONATE. Sean P. F. Hughes, Heinz W. Wahner, Patrick J. Kelly, James B. Basingthwaight, and David R. Davies. Mayo Clinic and Mayo Foundation, Rochester, Minn.

Uptake by bone of Tc-99m-labeled pyrophosphate (PP) and ethane-1-hydroxy-1,1-diphosphonate (HEDP) involves passage through capillaries in the haversian system, extracellular fluid space, and membrane of osteoblasts before adsorption onto available apatite surfaces. Passage through capillaries was studied by the outflow dilution technique in a canine tibia model (Coffield et al. *J Appl Physiol* 39:596,

1975) in 14 mongrel dogs. Cr-51 albumin (nondiffusible reference tracer), sucrose (diffusible reference tracer), PP, and HEDP were injected into the isolated tibial artery. Blood was collected from the ipsilateral tibial vein every 5 s for 2 min. Emax, the apparent extraction at the time of the peaks of the dilution curves, is influenced little by back diffusion; for PP, Emax (mean \pm S.D.) = 0.42 ± 0.08 (N = 4); for HEDP, Emax = 0.27 ± 0.05 (N = 10). Net extraction (apparent fractional retention by bone at 2 min) was 0.36 ± 0.1 and 0.27 ± 0.05 . Emax for Sr-85 chloride and F-18 sodium in our laboratory is 0.65 ± 0.14 (N = 24) and 0.64 ± 0.14 (N = 26). Permeabilities (P) were calculated by $PS = -Fs \log e(1 - E_{max})$, where Fs = plasma flow and S = capillary surface area; the ratio of P for HEDP to P for sucrose was 0.71, which is close to the ratio of diffusion coefficients, 0.76. The data suggest that HEDP and probably also PP pass through the capillaries by passive diffusion. As expected, the extraction through capillary walls for HEDP and PP was lower than for Sr-85 and F-18 because of their larger molecular size. (Supported in part by NIH grant AM-15980.)

BONE SCINTIGRAPHY IN RENAL OSTEODYSTROPHY. Pieter de Graaf, Ieke M. Schicht, Ernest K.J. Pauwels, and Jaap de Graeff. University Hospital, Leiden, The Netherlands.

The value of bone scintigraphy in renal osteodystrophy was studied in 30 patients on maintenance hemodialysis, using Tc-99m EHDP. In order to reduce background activity to levels found in normal controls, all patients were dialyzed for 5 hours, starting 15 min. after radionuclide administration. After 6 hours qualitative and quantitative scintigraphic skeletal examination took place. The results were compared with a normal control group.

All patients had histological proof of renal osteodystrophy. Only 48% showed roentgenological abnormalities. In contrast 80% had pathological scintigrams. Increased activity was noted mainly in the pelvis (46%), hips (60%), knees (70%), ankles (53%), chest (42%), spine (42%) and skull (46%). In addition metastatic visceral calcifications were detected in some patients. Quantitative analysis revealed increased skeletal activity accumulation in all patients compared to controls even when scintigrams appeared normal.

These findings suggest that bone scintigraphy is superior to conventional roentgenological techniques. Quantitative assessment of skeletal activity appears to be an even more sensitive technique to detect renal osteodystrophy.

TUESDAY, 2:00 p.m.-3:30 p.m.

CHICAGO ROOM

PULMONARY 1

Chairman: Naomi P. Alazraki
Co-Chairman: Philip O. Alderson

VENTILATION-PERFUSION LUNG IMAGING AND SELECTIVE PULMONARY ANGIOGRAPHY IN ANIMALS WITH EXPERIMENTAL PULMONARY EMBOLISM. P.O. Alderson, J.L. Doppman, S.S. Diamond, K.G. Mendenhall. Armed Forces Radiobiology Research Institute and National Institutes of Health, Bethesda, MD.

To determine the accuracy and limitations of Xenon-133 ventilation and Tc-99m perfusion (V-P) lung images in detecting pulmonary emboli (PE), these studies were per-

formed in 23 dogs after experimental production of PE. Each dog had a baseline V-P study. Several days later venous thromboemboli were formed using a modified Wessler technique and released to the lungs. Each dog then had a repeat V-P study, and 14 also had bilateral selective pulmonary angiography. Each dog had both a 20-ml intravenous injection of India ink prior to sacrifice to outline perfused segments of the lung and a post-mortem lung dissection. Two of 23 animals (8.7%) with normal baseline Xe-133 studies had Xe-133 abnormalities when studied immediately after embolization. These abnormalities were in regions where emboli completely obstructed large (>6mm diameter) vessels. Perfusion images revealed the location of 84% of emboli which completely obstructed pulmonary vessels, but only 26% of those which partially obstructed flow. Perfusion defects were seen with 97% of emboli which completely obstructed vessels greater than 2.0 mm in diameter, but in only 65% of those which lodged in smaller vessels. Small (<2x2 cm) perfusion defects revealed by India ink were detected much less frequently (16%) than larger ones (93%). V-P imaging is an accurate technique for detecting perfusion defects due to PE, but has a limited ability to detect very small or incompletely obstructing emboli. PE-induced Xe-133 abnormalities should not significantly interfere with interpretation, as they occur infrequently.

RELATION BETWEEN PULMONARY DEPOSITION OF RADIOAEROSOL AND VENTILATION. Norman D. Poe. University of California, Los Angeles, California.

The use of radioaerosols to study regional pulmonary ventilation has been criticized because a direct correlation between peripheral lung deposition of inhaled aerosols and ventilation has not been proven. The relationship between aerosol deposition and ventilation measured by the single breath Xe-133 and Xe washout rates in dogs was determined after production of unilateral hypoventilation. Using a controlled respiration device and a gamma camera with computer, single breath Xe, Xe washout and Tc-99m sulfur colloid aerosol studies were performed in sequence. Hypoventilation was produced by ligation of the left main pulmonary artery, partial external occlusion of the left main bronchus, or intraluminal bronchial obstruction with a removable perforated silastic ball.

The Xe washout rate was used as reference. In PA occlusion and external obstruction animals (n=6), measurements were made 48 hours post surgery then weekly for 1 month. Both procedures produced uniform reduction in Xe uptakes and aerosol deposition. The best correlation was found with the single breath method; in contrast, there was a tendency for relatively greater reductions in aerosol deposition as hypoventilation increased. With intraluminal obstruction (n=5), a "hot spot" was usually evident at the site of the obstruction. Surprisingly, ventilation was only slightly reduced in this group while aerosol deposition was usually markedly reduced.

Qualitatively, the results with Xe and radioaerosols are similar although the latter tend to quantitatively overestimate the degree of hypoventilation.

IMAGING SITES OF OBSTRUCTION AND MEASURING FUNCTION RESPONSE TO THERAPY IN ASTHMA. Sawtantra K. Chopra, George V. Taplin, Donald P. Tashkin, Everett Trevor and Dennis Elam. University of California, Los Angeles, California.

The sites of airway dilatation following terbutaline inhalation and systemic injection were compared in 9 asthmatic subjects. Baseline studies included functional tests of large and small airway obstruction and 2 inhalation radio-nuclide lung imaging procedures (Xenon-133 gas - single breath and washout examination followed by Tc-99m sodium pertechnetate aerosol imaging). On each of 3 study days, subjects were treated in a random, double-blind fashion with either 1) aerosolized terbutaline + subcutaneous (SC) saline; 2) aerosolized saline + SC terbutaline or 3) aerosolized saline + SC saline (placebo). Ten to 30 minutes after each treatment regime, functional tests and lung imaging were repeated. The placebo regime was followed by little or no improvement. Injected terbutaline gave less central deposition and more peripheral penetration of in-

haled radioaerosol (indicating large airway dilatation) in 8 and faster washout of Xenon-133 (indicating small airway dilatation) in all 9 patients. Lung imaging results correlated well with physiologic indicators of large and small airway function. Inhaled terbutaline gave evidence of large airway dilatation both on function tests and lung images in 7 of 9 subjects and of small airway dilatation in only 4. In asthma, inhaled radioaerosols are deposited in highest concentration in large airways and presumably inhaled terbutaline aerosol has a similar distribution, thereby giving its maximum bronchodilator response in the large airways. In conclusion, xenon lung imaging failed to detect evidence of the sites of large airway obstruction or dilatation in this study, whereas this important supplementary information is clearly revealed in aerosol images.

LUNG SCAN PATTERNS IN FIFTY CASES OF PROVEN PULMONARY AIR EMBOLISM. Robert G. Carroll, Maurice Albin, Peter Waterman and Lewis W. Gumerman. Presbyterian-University Hospital, Pittsburgh, Penna.

Fifty neurosurgical patients in whom air embolism was proven by Doppler detection and subsequent aspiration of air via central venous catheter were scanned in the immediate post operative period. Most patients had been operated in the semi-sitting position. Follow up lung scans were obtained. Scan lesions of a segmental nature were seen in nineteen of the fifty patients studied. A pathognomonic pattern of peripheral decortication crossing segmental lines and distributing in accord with the effects of gravity on air bubbles were found in seven patients. Gross lesions of the lung apices of a non segmental pattern were found in sixteen patients, and lesions involving the posterior and superior portions of both upper lungs were found in six patients. When segmental lesions were present, they most commonly involve the anterior segment of the right upper lobe. Patients with segmental lesions commonly had other subsegmental lesions as well. All lesions resolved partially or completely without the use of anticoagulant therapy as demonstrated by the follow up lung scans. Our clinical impression is that when air enters rapidly in moderate amounts, there is a tendency to the production of segmental lesions which mimic pulmonary thromboemboli. When air enters slowly, but in large quantities over a protracted period of time, the pathognomonic peripheral decoration pattern is seen. When air enters in moderate quantities over a moderate period of time, lesions involving the apex and posterior portions of both lung fields are commonly encountered. Air embolism and subsequent perfusion defects can occur in many operative settings.

OBSERVATIONS ON REGIONAL VENTILATION AND PERFUSION IN KYPHOSCOLIOSIS. R.H. Secker-Walker and J.E. Ho. St. Louis University School of Medicine, St. Louis, Mo.

Little has been written on regional lung function in kyphoscoliosis. This study reviews our observations on ten patients with kyphoscoliosis.

Regional ventilation was studied in the upright position, during the washin and washout of 133Xe. Regional perfusion was studied in the same position after the injection of (Tc-99)HAM. Images of ventilation and blood flow were obtained with a gamma camera. The results of the ventilation-perfusion studies have been compared to the degree and position of the kyphoscoliosis and the results of pulmonary function tests (PFTs).

The PFTs showed the expected pattern of restrictive lung disease and diminished air flow rates, mild hypoxia, mean PaO2 74mmHg, but normal overall alveolar ventilation, mean PaCO2 37.5mmHg. Clearance of 133Xe was more severely impaired from the zone with the greatest curvature, than from other parts of the lung in 7 patients, and averaged 4.5 min. longer than the opposite zone. No difference was seen in 2 patients with Harrington rods in place, and in 1 patient with a minor kyphoscoliosis. The normal vertical gradient of blood flow was seen in 5 patients, an even gradient in 3 and a reversal of the gradient in 2 others. Additional defects in blood flow were seen in each patient.

The hypoxia was most likely due to the failure to match

blood flow with the reduced ventilation that occurred chiefly in those regions of the lung most disturbed by the kyphoscoliosis. These findings differ from those of Dollery et al, (Thorax 20,175,1965) in that the effect of the major curvature on impaired clearance was not appreciated, and the blood flow was more even in their study.

TUESDAY, 2:00 p.m.-3:30 p.m.

JANE ADDAMS ROOM

DATA ANALYSIS 1

Chairman: A. Bertrand Brill

Co-Chairman: Stephen M. Pizer

OPERATOR INDEPENDENT EDGE DETECTION ALGORITHMS IN NUCLEAR MEDICINE. P. Cahill, L. Ho, E. Ornstein, D.V. Becker. The New York Hospital-Cornell Medical Center, New York, N.Y. and Polytechnic Institute of New York, Brooklyn, N.Y.

For the computer analysis of radionuclide images, maximum effectiveness depends largely upon reproducible operator independent edge detection methods for the precise delineation of borders. We have evaluated the suitability of six state-of-the-art edge detection methods using two and three dimensional phantoms, I-131 Hippuran renograms and Tc-99m Glucoheptonate (TcGH) images of myocardial infarcts (MI) in dogs. A new method, the nearest neighbor algorithm (NNA) was developed which selects an edge on the basis of relative derivative changes at the observed point and its eight nearest neighbors. It proved to be the only operator independent method which could detect both inner and outer edges at stochastic noise levels.

The NNA has permitted the accurate determination of the outside border of the kidney using I-131 Hippuran. By this method, the hippuran distribution can be obtained in the outside and middle regions of the kidney by deconvolution analysis. Because this NNA functions for overlapping and inner edges, it is the optimal edge detection method for the quantification of the size of MI's in the presence of overlapping liver activity and variable background. The NNA gave $r = 0.94$ when scintigraphic area of TcGH was compared to infarct weight determined by pathology in 20 dogs contrasted to $r = 0.84$ using visual measurements. Equally important, the average deviation decreased from a visual of ± 2.3 grams to ± 1.1 grams by the NNA.

A COMPARISON OF SOFTWARE AND HARDWARE GATED CARDIAC STUDIES F.A. Leger and A.E. Todd-Pokropek, La Pitié Paris France, University College Hospital London U.K.

Whereas 'gated' cardiac studies have been performed almost exclusively using an external trigger to synchronise images, an alternative software technique exists with much greater power and flexibility. Here, either during the data collection, or, in our hands, using the stored list mode data including the ECG trace, the counts may be sorted into corresponding frames using the time delay from the previous 'R' wave peak, the preceding 'R-R' interval, the succeeding 'R-R' interval, or some information based on 'T'. Synchronisation was performed by creating frames of fixed duration (time slicing) or variable duration (phase slicing) triggered by 'R' with a variable offset, and 'windowed' dependant on the 'R-R' interval. In order to compare the two techniques the hardware system was simulated by software. The first passage and equilibrium studies were recorded in LAO projection, and a LV region of interest and a background area defined.

The two techniques were compared by determining the ejection fraction in normal, regular and irregular patients.

In normal regular cases, no difference was observed. In abnormal regular patients, the EF was found to be significantly raised ($p < .001$) by 4% on average. In irregular patients, the hardware technique was found unsatisfactory and 'windowing' valuable. Phase slicing was found to be inferior to time slicing. An additional benefit from the post processing technique was the possibility of performing low temporal resolution slicing for images, followed by high temporal resolution slicing for the time activity curves, with a considerable economy in time and storage required.

NEW COMPARTMENTAL MODEL FOR TRANSPLANTED KIDNEY RENOGRAMS. P. Cahill, E. Ornstein, J. Hurley, The New York Hospital-Cornell Medical Center, New York, N.Y. and Polytechnic Institute of New York, Brooklyn, N.Y.

An 8 compartmental model for the analysis of dynamic I-131 Hippuran renal studies in transplanted kidneys was developed with separate compartments for the proximal cells and for the glomeruli. Three compartments represent the delay for the transit of hippuran through the medulla of the kidney. The glomeruli and proximal cell pools are considered to have return paths to the plasma which are dictated by the typical plateau shaped or rapidly increasing radioactivity curves observed in renograms of acute tubular necrosis. The rate equations and steady state masses for this model are interactively solved on a minicomputer using a Runge-Kutta integration method to fit the observed time activity curves for the total kidney, bladder, and outside and middle regions of the kidney. The outside region is related to the effective cortex and the middle to the effective medulla. To substantiate the glomerulus compartment, the clearance, ml/min, for Tc-99m DTPA was determined and compared to the patients creatinine clearance (CrCl) where an $r = 0.99$ with a 4% deviation in the slope was observed. In this method, the Tc-99m DTPA clearance was calculated using the slope of the % dose of DTPA in the bladder and % dose/cc in the serum. A comparable filtration rate was obtained for I-131 Hippuran by our model, thus supporting the validity of our new compartmental model. The steady state masses and rate constants provide a new quantitative mode for reporting renogram results which is directly related to kidney physiology and function.

A COMPREHENSIVE SOFTWARE SYSTEM FOR PRODUCING FUNCTIONAL MAPS. Renee G. Dunham, Bruce R. Line, and Gerald S. Johnston. National Institutes of Health, Bethesda, Md.

A comprehensive set of functional mapping procedures for clinical use has been developed in FORTRAN II for the HP 5407 minicomputer. The processing techniques used in generating many types of functional images were analyzed, resulting in the definition of a set of nineteen operations which may be used as building blocks. These elemental operations fall into several categories: those which 1) produce minimum or maximum count maps from sequenced images, 2) produce images of the time to some event (such as time to maximum count), 3) select out of a region those values which are greater than, equal to, or less than values in a comparative region, 4) transform images using a table driven substitution technique, and 5) full image arithmetic operations, such as addition, subtraction, multiplication, division inversion, negation, thresholding, and computing logarithmic and absolute values.

All functions are part of a comprehensive computer system which enables a clinician to write functional mapping procedures in a high level language. Procedures may be developed interactively and executed automatically. One such automated procedure for producing maps of left ventricular peak ejection and time to peak ejection has proved useful in cardiac analysis.

This software system has significantly reduced time spent in program development and has been routinely used to produce functional maps for lung, heart, and renal studies in over 300 patients.

A SEMI-AUTOMATIC EDGE DETECTION PROGRAM FOR THE ANALYSIS OF MULTIPLE GATED ACQUISITION CARDIAC BLOOD POOL IMAGES. Robert Burow, Malcolm Pond, Terry Rehn, H. William Strauss, and Bertram Pitt. Johns Hopkins Hospital, Baltimore, Md.

Time activity curves (TAC) obtained from the left ventricle (LV) of multiple gated cardiac blood pool images (MUGA) can be used to calculate left ventricular ejection fraction (LVEF). A semi-automatic technique for analyzing MUGA - TAC's was developed. Data was collected in 28 frames of 64 x 64 word images triggered by the R wave of the ECG over approximately 1000 cardiac cycles. A remote area of the end diastolic frame which yielded a flat TAC over the 28 frames was selected as background activity. Background activity/cell was subtracted from each cell of the 28 frames. A rectangle was then circumscribed about the LV to isolate it from the remainder of the image. Threshold values as a percentage of peak activity were selected for each quadrant within the rectangle about the centroid in order to define the LV edge. The LV edge was automatically determined in each of the 28 frames and a TAC from the area described by the edge displayed.

In 17 patients evaluated by single plane contrast angiography (CA) for coronary artery disease % LVEF calculated from the CA was $55.5\% \pm 3.1$ and $54.7\% \pm 3.1$ by TAC, $r = 0.93$. A point by point correlation of the TAC and the CA - LV volume curve was $r = 0.96$. The reproducibility of 4 individual observers was less than 2% for calculating LVEF by TAC.

The semi-automatic edge program for MUGA provides accurate and reproducible TAC's for evaluation of left ventricular function.

AN IMAGE PROCESSING COMPUTER SYSTEM FOR NUCLEAR MEDICINE. John Verba, Martin Sperling, Naomi Alazraki, and Andrew Taylor, Jr. VA Hospital, San Diego, California

A computer system for image-oriented processing of nuclear medicine data has been designed based on recent "state of the art" advances developed for military, industrial and medical applications. The system is currently being implemented at the Veterans Administration Hospital, San Diego.

The system is organized around a 16-bit minicomputer and includes processors for high-speed algebraic manipulation and display control. The algebraic processor is programmed in microcode with a 200 nanosecond cycle and 400 nanosecond multiply. Low noise levels and expanded look-up table for pseudocolor displays permit long tone scales with subtle gradations. Analog to digital interfaces accept data from scintillation cameras and/or other analog output devices in a variety of computer selected formats and resolutions at rates to 200,000 events per second with good linearity.

The configuration and operating system allow simultaneous acquisition of clinical data, development of data reduction programs and/or execution of such programs on previously stored data by four or more concurrent users. Images are displayed in static and dynamic modes with operator intervention via touch-sensitive display screens. Dynamic display of the beating heart in real time is possible with excellent display resolution without seriously slowing concurrent computations. Functions of the system include image filtration and other perception enhancing manipulations as well as three-dimensional reconstructions.

A NEW COMPUTER LANGUAGE FOR RIA. Robert D. Grant, Steven J. Spencer, Sue Weiss, David E. Lieberman. The Children's Memorial Hospital, Chicago, Ill.

A useful application of dedicated nuclear medicine computer systems is the on-line computation of radioimmunoassay (RIA). In the past, only high level computer languages such as FORTRAN and BASIC have been available for this purpose. The inexperience programmer may have difficulty writing or executing radioimmunoassay programs in these languages. A special programming language for computing radioimmunoassays has been developed on a

16K dedicated minicomputer utilizing a 1.2 megabit disk as the primary source of storage. The language is an interpreter, oriented towards the inexperienced computer operators. Features of the program include correction for broken tubes, quality control, several methods of curve fitting including logit, piecewise linear, and power equations, a sophisticated curve display package, long term storage of data, and easily formatted outputs. The language has been successfully applied to B-12, Digoxin, T-3-RIA, TSH, FSH, and other assays with results comparing favorably with previous computer analysis or hand calculation. The design of the language enables simultaneous acquisition of normal clinical studies during on-line radioassay processing. Input to the program is accepted by terminal, storage disk or paper tape.

THALLIUM-201 COMPUTER EVALUATION OF MYOCARDIAL BLOOD FLOW. Robert Meade, V. Bamrah, J. Porgan, P. Chayapraks, C. Kronenwetter, En-Lin Veh. Veterans Administration Center, Milwaukee, WI.

This study was undertaken to develop a method to quantitatively evaluate the myocardial distribution of the isotope following stress and after 4-5 hours rest to better distinguish ischemia vs infarction. In ischemia there is redistribution of flow at rest to the area poorly perfused during stress.

Th-201 was injected at time of maximum stress, angina or EKG changes, and stress continued for one minute. Multiple views were taken from 10-30 minutes after injection and repeated 4-5 hours later. A HP IV Searle camera was interfaced to a PDP 12/40 Digital Computer. All results were compared to coronary angiography.

The data matrix was filtered using a fast Fourier transform technique (J.N.M. 17:647, 1976). An operator locates the center position of a computer generated circle which approximates the center of the left ventricular wall. A straight line plot of the activity along a circular profile is generated as a function of the angle from 0 to 360°. A plot comparing the distribution of myocardial activity following stress and rest is obtained following normalization. An automatic method in which the computer selects the optimum value along the radius is being run simultaneously.

Patients with myocardial infarction show little recovery compared to those with ischemia. In a study of 22 patients there appears to be good correlation between the radionuclide and the cardiac angiography results. Atrial pacing vs the treadmill is also being compared but is not completed.

The method developed allows quantitation of the myocardial blood flow with direct comparison of stress vs. rest.

AUTOMATED SYSTEM FOR RECORDING REPORTS IN NUCLEAR MEDICINE. Kikuo Machida and Junichi Nishikawa. Department of Radiology, University of Tokyo.

With nuclear medicine rapidly expanding as a diagnostic tool, we have developed a system to automatically record the clinical report using a Tosbac 40 time sharing system electronic computer and keymat-editor (DTZ 0008A). The system is composed of three modules: reader, editor and writer. The reader module is used to register sentences and terms which can be easily added to and changed. The editor module is used for the intermediate file of the reports. With the aid of the keymat-editor, the physician inserts the necessary sentences and terms usually in the following order: procedure, interpretation, diagnosis, recommendation and the physicians code. In this procedure, message errors, if any, may be printed out on the terminal typewriter. Finally, the writer module is used to edit the intermediate file. After storing several clinical reports, the computer produces the written reports in as many copies as desired. In the rapidly progressing field of nuclear medicine, it is very important that the physician has the capability of updating the system by changing and adding terms and sentences. This capability is a characteristic advantage of the system.

TUESDAY, 2:00 p.m.-3:30 p.m.

LINDHEIMER ROOM

**RADIOPHARMACEUTICAL 2:
NOVEL RADIONUCLIDES**

Chairman: Joanna S. Fowler
Co-Chairman: Dennis R. Hoogland

A XENON-122-IODINE-122 GENERATOR. Powell Richards and Thomas H. Ku. Brookhaven National Laboratory, Upton, New York.

A generator system has been developed to produce the ultrashort-lived positron-emitter iodine-122 (3.62 m, 154% 511 keV γ ray) from its parent, xenon-122 (20.1 h). The parent, xenon-122, can be produced as a by-product in the production of xenon-123 from proton irradiation of sodium-iodide target. The generator consists of a xenon reservoir chamber and an ingrowth or milking chamber. The sequence of operation involves transferring xenon using liquid nitrogen from the reservoir to the milking vessel, allowing fresh iodine-122 to grow in for a few minutes, transferring the xenon back to the storage reservoir, and then rapidly rinsing the iodine out of the milking vessel. The radionuclidic purity of the carrier-free iodine-122 is high, containing less than 0.1% radioxenons and other radioiodines. The potential applications of iodine-122 include cardiac and large-vessel angiography and the study of heart dynamics. Rapid iodination techniques are being developed for the preparation of iodine-122-labelled radiopharmaceuticals for positron emission tomography.

GENERATOR PRODUCTION OF RUBIDIUM-82 FOR CLINICAL USE. H. Krizek, P.V. Harper, University of Chicago, Chicago, IL., and P.M. Grant, J.W. Barnes, H.A. O'Brien, Jr., Los Alamos Scientific Laboratory, Los Alamos, New Mexico.

The reported methods for elution of the 75-second positron-emitting rubidium-82 from its 25-day parent strontium-82 have some disadvantages. The elution from Bio-Rex-70 using 30-60 ml/min of 2% to 3% NaCl precludes its continuous administration to cardiac patients because of salt and fluid overload problems. The alternative procedure using Chelex-100 and as eluant 0.1 M $\text{NH}_4\text{Cl-NH}_4\text{OH}$ at pH 9.3 also requires large volumes and is unusable clinically because it causes severe pain at the site of intravenous administration. A new approach is to use an alkaline NaCl solution, Chelex-100 of a finer mesh size, a shorter column and a lower flow rate. From a 2.0x0.9 cm column of 200-400 mesh Chelex-100, rubidium was eluted almost quantitatively in ~ 5 ml, using 0.1 M NaOH in 0.2 M NaCl. Elution of rubidium was little affected under these conditions as flow rate was changed from 4 to 16 ml/min. Strontium breakthrough with 750 μg of added carrier was below 10^{-7} of column activity/5 ml at 4 ml/min, and was more than an order of magnitude greater at 20 ml/min. Flow is maintained constant with a metering pump and the eluant can be neutralized by metering 0.1 M HCl into the line, giving a final product in isotonic saline. The new approach reduces the amount of salt and water administered so that constant infusion may be maintained for a reasonable time to produce an equilibrium image. Quantitative positron emission tomographic imaging under these conditions permits measurements of regional perfusion since the perfusion $F/V = \lambda_D C_T / EC_a$. λ_D is the physical decay constant, E is the extraction ratio and C_T and C_a are tissue and arterial concentrations of activity.

MANUFACTURE OF THE KRYPTON-81m GAS GENERATOR FOR LUNG VENTILATION STUDIES. J.F. Lamb, G.A. Baker, A. Khentigan, H.A. Moore, W.C. Neesan, and H.S. Winchell. Medi-Physics, Inc., Emeryville, California.

Krypton-81m gas generators have been commercially produced for clinical trials for assessing regional lung ventilation since September 1976. The generator consists of

cyclotron-produced rubidium-81 absorbed on a cation exchange column from which the Kr-81m may be eluted by passage of humidified oxygen. Krypton-82, bombarded with protons, produces rubidium-81 with a maximum reaction cross section of 500 mb at 22 MeV proton energy. The ranges of protons in krypton gas are estimated to be 1.8 g/cm² at 22 MeV and 0.4 g/cm² at the 14 MeV reaction threshold, so that thick target yields of approximately 15 mCi/ μAh can be realized from a 70% isotopically enriched Kr-82 target. The Rb-81 activity is removed from the target with distilled water, the radioactive bromine impurities removed by an Al_2O_3 column and the generators prepared by equilibrating the carrier-free Rb-81 solution with cation exchanger for 2-3 minutes. The exchange is essentially quantitative. Pure carrier-free krypton-81m may be eluted with an efficiency greater than 90% by passage of humidified oxygen at a pressure less than 5 psi and a flow rate greater than 200 cm³/minute. The optimum flow rate for a lung ventilation study is determined by the nature of the administration system (i.e., face mask, mouthpiece, etc.) and by the respiration rate and volume of the patient. Our recommended protocol has resulted in greater than 200,000 counts in four minutes per view for a study performed on a healthy volunteer with a 700 μCi generator, using a Nuclear Chicago Pho Gamma III camera with a 250 keV collimator. Results from lung ventilation studies of more than 100 patients indicate that the krypton-81m gas generator may be a useful diagnostic aid.

Ta-178 - A NEW SHORT-LIVED RADIONUCLIDE FOR LOW ENERGY GAMMA CAMERAS: PRODUCTION AND SEPARATION. B. Leonard Holman, Alun G. Jones, Gale I. Harris and Rudi Neirinckx. Department of Radiology, Harvard Medical School and Peter Bent Brigham Hospital, Boston, MA, and Department of Radiology and Cyclotron Laboratory, Michigan State University, East Lansing, MI

Low energy imaging systems such as the multiwire proportional counters and Fresnel zone plate tomographic cameras are inefficient for photon energies greater than 100 keV. Ta-178 (half life, 9.4 min), the daughter of W-178 (half life, 21.5 d), has promising physical characteristics for use with such low energy camera systems. It decays mainly by electron capture (99%) with 1% β^+ positron emission, 59% to the ground state and 35% to the 93.2 keV state of stable Hf-178, with the remaining 6% to excited levels between 1.2 and 1.6 MeV. The gamma ray spectrum is dominated by characteristic hafnium x-rays (55-65 keV). W-178 was produced with the MSU 50 MeV, variable energy, sector focussed cyclotron using a target consisting of a stack of five 0.005 inch thick Ta sheets. The runs were performed at a proton energy of 40 MeV for a total exposure of 2.9 $\mu\text{A-hr}$. Gamma ray spectra were obtained with a Ge(Li) detector. Optimum production of W-178 occurred at $E_p=34-35$ MeV at an effective activity of 80 $\mu\text{Ci}/\mu\text{A-hr/MeV}$ of target thickness for the 93.2 keV gamma ray. W-178 is isolated from the irradiated foils and loaded onto an ion exchange column. Elution of this column with dilute HCl shows Ta-178 yields of approximately 50% of the theoretical maximum in volumes of 3-4 ml, with an elution time of 2 minutes. W-178 breakthrough is calculated as a maximum of 0.005%/ml of eluant. This separation may therefore form the basis of a generator system for this short-lived radionuclide.

PANCREAS SPECIFICITY OF IODO AND BROMO ALIPHATIC AMINO ACID ANALOGS. Hank Kung, Syed Gilani and Monte Blau. State University of New York at Buffalo, Buffalo, N.Y.

Substitution of a halogen atom (bromine or iodine) for a methyl group in natural compounds often does not impair biological activity, e.g., iododeoxyuridine for thymidine and various bromo and iodo steroids. We have synthesized and studied the biological distribution of iodo and bromo aliphatic amino acid analogs for possible use as pancreas localizing agents.

Rather than using the short-lived gamma-emitting isotopes of bromine suitable for scanning, we prepared the C-14 labeled compounds. The valine analog β -bromo- α -aminobutyric acid was synthesized from C-14 labeled L-threonine and its distribution was studied in rats.

Contrary to expectations, this compound showed no pancreas uptake or any other amino acid behavior. Similar failure of aliphatic bromo-compounds to resemble their methyl analogs has been reported for fatty acid uptake in heart (Stöcklin et. al.), although iodo-fatty acids are taken up (Robinson). The failure of these bromo for methyl substituted compounds to be metabolized is rather surprising in view of the good match in size, electro-negativity and lipophilicity.

Iodo analogs of leucine (γ -iodo- α -aminopentanoic acid) and valine (β -iodo- α -aminobutyric acid) have been prepared with I-125 labels. These compounds proved to be quite unstable and were rapidly deiodinated in vivo.

It is clear that halogen analogs of aliphatic amino acids are not useful as pancreas localizing agents.

POLYCYCLIC AROMATIC MERCURIALS AS MYOCARDIAL INFARCT IMAGING AGENTS. Robert N. Hanson, Michael A. Davis and B. Leonard Holman, Joint Program in Nuclear Medicine, Harvard Medical School, Boston, MA.

External imaging agents offer the most rational approach to assessing the efficacy of cardioactive drugs. Using the heat lesioned rat heart model we screened a series of Hg-203-hydroxymercurifluoresceins and -phthaleins and Hg-203-hydroxymercurifluorescein and -phenolphthalein complexes. The hydroxymercuri- group appears necessary for uptake (% ID/g MI) and for specificity (MI/normal), as I-131-rose bengal, (0.7, 7.8), H-3-fluorescein (0.2, 2.4) and H-3-phenolphthalein (0.2, 3.2) had low values for both these ratios. The Hg-203-mercuric nitrate had an uptake comparable to the Hg-203-hydroxymercurifluoresceins and -phthaleins (7.1 vs. 3.4 and 15.8) but the tissue selectivity was lower indicating that the polycyclic organic nucleus may impart tissue specificity. In the fluorescein series the introduction of halogen substituents at the 2'7' or 4'5' positions reduced the selectivity of the agent (24.7 and 25.4, respectively) compared to the non-halogenated compound (51.5). The replacement of the carboxylic acid in hydroxymercuriphenolphthalein with a sulfonic acid moiety and removal of the 10'-oxygen of hydroxymercurifluorescein reduced infarct specificity from 34.1 to 23.9 and from 51.5 to 34.1 respectively indicating the introduction of substituents may reduce infarct selectivity. Hg-203-hydroxymercurifluorescein and -phenolphthalein complexes revealed no significant difference at one hour after administration. Tc-99m-fluorescein complex showed decreased uptake and specificity (0.5, 6.4) as expected due to the absence of Hg. Testing of the analogous Tc-complex containing Hg is in progress.

THE SYNTHESIS OF TELLURIUM-123m LABELED STEROIDS.* F. F. Knapp, Jr. and A. P. Callahan, Radioisotope Dept., Oak Ridge National Laboratory, Oak Ridge, Tenn.

This investigation explored methods for the preparation of Te-123m labeled steroids which may be potential endocrine imaging agents. Tellurium-123m (120 d) has ideal imaging properties, 84% abundance of 159 keV photons. Fabrication of the 24-nor-23-(alkyl tellura) steroid sidechain was chosen as a novel route for the introduction of the Te-123m nuclide because of the availability of lithocholic and allolithocholic acids which are readily converted to the corresponding norbromides via a Hunsdiecker-type degradation. The steroidal norbromides were coupled with sodium alkyl tellurols which were formed by reduction of dialkyl ditellurides. The dialkyl ditellurides were prepared by reaction of alkyl iodides with sodium ditelluride generated *in situ* by the reaction of sodium and tellurium in liquid ammonia. Examples of steroids prepared in this manner include: 24-nor-23-(isopropyl tellura)- and 23-(isopentyl tellura)-5 β -cholan-3 α -ol and 24-nor-23-(isopropyl tellura)- and 23-(isopentyl tellura)-5 α -cholan-3 β -ol. The chemical and physical properties of these unique compounds were consistent with the proposed structures. The Te-123m labeled 24-nor-23-(alkyl tellura) steroids were prepared from reactor produced Te-123m. A general three-step method has been developed for the preparation of Te-123m labeled 24-nor-23-alkyl tellura) steroids in reasonable yield from

elemental Te-123m. The synthesis and subsequent purification can be easily completed in a single day.

*Research sponsored by U. S. Energy Research and Development Administration under contract with Union Carbide Corporation.

TISSUE DISTRIBUTION OF 5-THIO-D-GLUCOSE IN HAMSTERS BEARING PANCREATIC TUMOR MODELS. Arnold M. Markoe, Victor R. Risch, Ned D. Heindel, Jacqueline Emrich, Wendy Lippincott, and Luther W. Brady, Hahnemann Medical College and Hospital, Philadelphia, Pa.

5-thio-D-glucose (5-TDG) has been shown by others to exert profound biochemical and biological effects on rapidly metabolizing tissues including the pancreas. Because of our interest in delineating pancreatic neoplasms, we undertook to study the tissue distribution of S-35-labeled 5-TDG in hamster pancreatic tumor models after i.v. injection prior to using 5-TDG as a model compound for the synthesis of more clinically useful imaging agents. The tissue distribution was determined at various times after injection using liquid scintillation techniques. In normal hamsters, initial uptake of 5-TDG into kidney and liver was high. The normal pancreatic uptake was never greater than 0.6% of the injected activity per gram tissue. However, in all of our tumor models, 5-TDG uptake into tumor was in excess of that normal pancreatic tissue, up to 2 hr. after injection in the case of the functional insulinoma, up to 6 hr. for the Pan No. 1 acinar tumor and for over 24 hr. in the pancreatic duct tumor. For this latter model, an average tumor to pancreas ratio of 4.87 was maintained from 15 min to 24 hr. after injection.

TIME	DUCT TUMOR/ORGAN RATIOS				
	Liver	Kidney	Blood	Muscle	Pancreas
2 hr	3.47	0.96	5.47	5.31	5.01
6 hr.	2.24	1.16	5.62	4.12	3.63
24 hr.	2.32	2.31	23.24	1.31	5.94

These studies have provided impetus for using 5-TDG as a model compound for the synthesis of potentially useful agents for the clinical detection of pancreatic tumors. (A.M.M. is a S.N.M. Student Research Fellow.)

A NEW CLASS OF PANCREATIC IMAGING AGENTS: AROMATIC AMINO ACID DERIVATIVES OF SELENOPHENE. Michael A. Davis, Torbjorn Frejd, Roger W. Giese and Salo Gronowitz, Harvard Medical School and Northeastern University, Boston, MA and University of Lund, Lund, Sweden.

Carcinoma of the pancreas is responsible for the death of 7000 persons annually in this country. Although surgical resection techniques for this organ have been perfected, their success relies heavily on early diagnosis. Unfortunately, early diagnosis is rarely achieved because the current radiopharmaceutical used for pancreatic imaging, Se-75-L-selenomethionine (SeM), has several shortcomings, prominent among which is a low pancreas to liver concentration ratio (P/L). Recent work has focused on the synthesis and biologic evaluation of several selenium containing aliphatic amino acids which normally do not contain a sulfur atom. All agents of this type tested thus far have proved inferior to SeM. A survey of the H-3 and C-14 amino acid literature led us to hypothesize that aromatic amino acids would achieve a higher P/L ratio. We report here the successful testing of our hypothesis with the sulfur containing aromatic amino acid, thienylalanine, labeled with C-14 and the synthesis and evaluation of 2 selenium derivatives of phenylalanine obtained by the substitution of the phenyl or thienyl ring with the analogous 5 membered selenophene moiety. In our first series of experiments we compared SeM with commercially available C-14-thienylalanine in the rat 1 hour after injection. The P/L ratios were 3.0 and 6.0 respectively confirming our belief concerning the aromatic amino acids. Recent experiments with the 2- and 3-isomers of selenylalanine gave P/L ratios of 2.0 for SeM and 4.2 for the selenylalanines. These results have encouraged us to initiate biodistribution and toxicity studies in primates prior to a contemplated clinical trial.

TUESDAY, 4:00 p.m.-5:30 p.m.

CHICAGO ROOM

CARDIOVASCULAR 4

Chairman: John A. Burdine
Co-Chairman: Salvador Treves

RADIONUCLIDE VENOGRAPHY (RVN) IN THE PRACTICE OF NUCLEAR MEDICINE. Wil B. Nelp. University of Washington, Seattle.

This report summarizes experience with Tc-99m-MAA lower extremity (L.E.) and pelvic venography in 250 pts. I) 117 pts. with suspected acute pulmonary embolus (P.E.) without clinical evidence of deep venous occlusive disease (DVD), II) 46 pts. with evidence of DVD and no suspicion of P.E., III) 35 pts. with clinical evidence suggesting both P.E. and DVD, and IV) 52 pts. with swollen leg(s) with equivocal signs of DVD or with suspected IVC disease.

RVN was done with bilateral injections of 25 ml. of saline-MAA and imaging from IVC to popliteals. Lung imaging was done in each case. 306 studies were analyzed (250 original, 57 repeat) in conjunction with all data from ancillary diagnostic tests and patients' medical records.

88 original RVNs (99 legs) showed occlusive DVD. The SFV was involved most (89%) but pelvic veins were occluded in 52%.

In Group I, a final Dx. of P.E. was made in 30 pts. and 37% showed unsuspected DVD. In the other 87 pts. DVD was uncovered in 8%. In Group II, 38 pts. (83%) had a final Dx. of DVD, with 95% abnormal RVN. Unexpected P.E. were seen in 12 (29%). In Group III 20 pts. had acute or chronic DVD, with 90% positive RVN. 12 pts. (60%) had acute P.E. with (11/12) positive RVN. In Group IV, 16 pts. (31%) had DVD and positive RVN with RVN being the diagnostic determinate in pelvic and IVC disease. 3 pts. had unexpected P.E. Overall correlation of abnormal Doppler flow signals with RVN areas of obstruction in extremities was 90%.

RVN with lung imaging demonstrated the ease and sensitivity for detecting DVD, particularly in the pelvis. The relatively high detection rate of unsuspected DVD and P.E. in Group I and II type patients was diagnostically and therapeutically rewarding.

ASSESSMENT OF ANTICOAGULANT THERAPY FOR THROMBOPHLEBITIS BY I-123-FIBRINOGEN SCINTIGRAPHY. Sally J. DeNardo, Gerald L. DeNardo, and Anne-Line Jansholt. University of California at Davis, Sacramento Medical Center, Sacramento, CA.

Our earlier work in 300 patients confirmed the usefulness of I-123-fibrinogen for the diagnosis of thrombophlebitis, especially in the pelvis and thighs. 31 patients were studied on more than 1 occasion (2-5 times) while on heparin or coumadin treatment for thrombophlebitis. In 11 patients, abnormal I-123-fibrinogen venous uptake progressively disappeared (normalized) on several studies and this correlated with an uneventful recovery.

Persistence of significant I-123-fibrinogen incorporation after 10 days of heparin therapy or over one month of coumadin, was related to pulmonary embolus or thrombophlebitis if therapy was discontinued at that time.

This preliminary data suggest that: 1) normalization of I-123-fibrinogen images should be seen before ceasing therapy and; 2) that continuation of significant incorporation of fibrinogen warrants more vigorous therapeutic approaches.

Further evaluation of I-123-fibrinogen as a unique tool in accessing the short and long-term success of heparin and coumadin for thrombophlebitis therapy is justified.

(This research was supported by ACS grant #DT-45).

MYOCARDIAL IMAGING WITH I-123 HEXADECENOIC ACID. N.D. Poe, G.D. Robinson, Jr., F.W. Zielinski, W.R. Cabeen, Jr., J.W. Smith, and A.S. Gomes. University of California, Los Angeles, California.

Myocardial imaging with I-123 hexadecenoic acid (HA) was performed in 21 patients undergoing cardiac catheterization. Of 13 patients with CAD, the 6 with proven infarction

showed perfusion defects as did 5 of 6 anginal patients without infarction. The infarct group had corresponding wall motion disturbances by ventriculography while the anginal group usually did not. The remaining patient whose only symptom was an arrhythmia had no perfusion defect. The non-CAD group was comprised mostly of patients with valvular diseases with image patterns similar to those reported with other radiopharmaceuticals.

Using a pinhole collimator and 5 mCi doses of HA, count rates in excess of 100K/min are produced. Satisfactory perfusion images can be acquired in 3 min with a 4 projection study completed in less than 20 min post injection. Speed is important as HA has a myocardial T 1/2 of 25 min. However, by obtaining a selective single 10 min view (separately or as part of a complete study) sufficiently high total counts can be collected for determination of regional clearance rates. Presumably, clearance from hypoxic or injured myocardium will be slower than normal.

Myocardial imaging with HA provides qualitative perfusion information similar to that obtainable with potassium analogs but with the advantage of higher count rates which permit quantitative measurements plus low patient radiation dose. Preliminary evidence suggests that perfusion deficits in asymptomatic angina patients can be identified without induction of stress. The degradation of HA is rapid enough to determine clearance rates and may prove useful for evaluating myocardial metabolism on a regional basis.

LOCALIZATION OF A SPECIFIC I-131 ANTIBODY TO MYOGLOBIN IN MYOCARDIAL TISSUE AND FACTORS WHICH INFLUENCE MYOGLOBIN RELEASE FROM CARDIAC CELLS. R.W. Parkey, L.M. Buja, P. Kulkarni, M.J. Stone, and J.T. Willerson. Univ. of Texas Health Science Center at Dallas, Dallas, TX.

Previously we have shown that acute myocardial infarction is associated with the development of marked increases in serum myoglobin, presumably as a consequence of myoglobin liberation from damaged cells with severe membrane permeability alterations. The present study was performed to determine whether cardiac myoglobin release is a consequence of myocardial necrosis or whether milder forms of myocardial injury produce severe enough membrane permeability alterations to result in significant myoglobinemia. Twenty-nine awake unsedated dogs with balloon occluder devices positioned around their proximal left anterior descending coronary artery (LAD) and RV pacing electrodes were studied. Animals were assigned to groups of either fixed LAD occlusion for 24 hours, temporary LAD occlusion for 15 min followed by reperfusion for 24 hrs, sham LAD occlusion or rapid ventricular pacing (250 beats/min) without LAD occlusion for 90 min. Sera for myoglobin determination were obtained prior to and at graded intervals following each intervention; the samples were analyzed for myoglobin utilizing a radioimmunoassay we have previously described. An additional 7 awake dogs with permanent LAD occlusion were injected intravenously 24 hrs after LAD occlusion with an I-131 labeled antibody for canine cardiac myoglobin (reared in rabbits). The results indicate that (1) rapid ventricular pacing for 1 1/2 hrs and brief temporary coronary occlusion followed by reflow do not significantly increase serum myoglobin values and (2) fixed LAD occlusion results in marked increases in serum myoglobin within 2 hrs and peak increases by 6 hrs after occlusion; peak serum myoglobin values correlate with the histological extent of infarct size ($r=0.83$). The antibody against cardiac myoglobin was selectively concentrated in the area of gross infarction 48-72 hrs after LAD ligation. The greatest antibody concentration was in the subendocardial portion of the infarcted area (8:1 infarct to normal tissue ratio). It was also possible to identify the infarct region in the closed chest dog with the labeled myoglobin antibody as a "hot spot" on myocardial scintigrams using a Pho Gamma Scintillation camera and computer processing. Thus, the data suggest that significant release of myoglobin from myocardial cells and uptake of a specific antibody against cardiac myoglobin occur only after severe and probably irreversible myocardial cell membrane permeability alterations and cellular necrosis. The data also indicate that a labeled antibody against cardiac myoglobin may be utilized as another means of obtaining "hot spot" myocardial scintigrams in experimental animals with myocardial necrosis.

THE PROGNOSTIC IMPLICATIONS OF ACUTE MYOCARDIAL INFARCT SCINTIGRAPHY. B. Leonard Holman, Robert J. Chisholm, and Eugene Braunwald. Harvard Medical School and Peter Bent Brigham Hospital, Boston, MA

The predictive value of myocardial scintigraphy with Tc-99m pyrophosphate was studied in 100 patients admitted to the coronary care unit with suspected acute myocardial infarction. None of the 21 patients with normal scintigrams had acute myocardial infarction by other criteria. Fifty-five percent of patients with diffuse uptake (pattern B), 73% of patients with focal uptake (pattern C) and all patients with intense focal uptake (pattern D) and massive uptake (pattern E) had acute infarction. The complication rate in the hospital and after discharge (mean followup: 6.1 months) for patients with pattern E was 88% compared to 42% for D, 30% for C, 36% for B and 10% for patients with

normal scintigrams (A). For patients with acute infarction with patterns C, D and E, the complication rate rose with increasing size of the myocardial uptake on the anterior view. Thus, patients with uptake of less than 16 square cm had no complications, while patients with uptake of 16-40 square cm had a complication rate of 68% and a mortality rate of 12%. Patients with uptake of more than 40 square cm had a mortality rate of 67%. In addition to its diagnostic potential, acute infarct scintigraphy provides prognostic information which is potentially useful for patient triage and for therapeutic decisions early in the evolution of the infarct.

PREOPERATIVE, POSTOPERATIVE, AND LATE FOLLOW-UP Tc-99m PYROPHOSPHATE MYOCARDIAL SCINTIGRAPHY AND CORONARY ARTERY BYPASS SURGERY. Kenneth P. Lyons, Harold G. Olson, John H. Kuperus, Wilbert S. Aronow, and Edward A. Stemmer. Veterans Administration Hospital, Long Beach, Calif.

To evaluate Tc-99m Pyrophosphate myocardial scintigraphy in coronary artery bypass surgery, 71 patients had a scintigram before surgery (average 2.7 days), 58 had a repeat study postoperatively (average 7.7 days), and 27 had a third, follow-up scintigram (average 4.7 months).

Preoperatively, 18 of 37 (49%) patients with Functional Class IV angina and 12 of 33 (36%) with Class III angina had positive scintigrams. From the 58 postoperative scintigrams, seventeen of 22 (77%) abnormal preoperative scintigrams improved with surgery. At follow-up, 13 of 15 patients with Class I angina had negative scintigrams, however, 9 of the 12 with Class II and III angina also had negative studies.

Eight patients had ECG criteria of perioperative myocardial infarction. In 6, the infarct was seen on postoperative scintigraphy.

There were 8 surgical deaths among the 71 patients (11%). Six of these had positive preoperative scintigrams. The surgical mortality of the 30 patients with positive preoperative scintigrams was 20%. Four of 17 patients with Class IV angina and a positive scintigram died (24%) compared to no deaths among the 20 Class IV angina patients with negative preoperative scintigrams.

In conclusion: (1) a positive preoperative scintigram especially in patients with Class IV angina carries an increased risk of surgery; (2) scintigrams tend to become negative after surgery and remain so irrespective of the clinical state; and (3) scintigraphy is useful in demonstrating perioperative infarcts.

PREDICTIVE VALUE OF MYOCARDIAL PERFUSION IMAGING FOR AORTOCORONARY BYPASS SURGERY. Michael J. Chamberlain, William J. Kostuk. University Hospital, London, Ontario.

Evaluation of patients (pts) for aortocoronary bypass (ACB) surgery is dependent on the findings at cardiac catheterization. Left ventricular (LV) angiography cannot distinguish between reversible and irreversible myocardial dysfunction. In 82 pts macroaggregates of human serum albumin labeled with iodine-131 were injected before operation into the right coronary artery and technetium-99m labeled microspheres were injected into the left coronary artery. Two weeks after operation similar technetium-99m and iodine-131 injections were made into the native vessels and grafted vessels respectively. Myocardial distribution of the 20 μ particles was visualized with a rectilinear scanner. Sixty-seven pts had normal myocardial perfusion scans (MPS) preoperatively even though wall motion was abnormal in 34. There was substantial improvement in the LV function of these 34 pts; the mean ejection fraction increased from 56 to 65% ($p < .01$). Fifteen pts had abnormal MPS; improvement in LV function in this group occurred only if the bypass graft was made to an area with normal regional perfusion preoperatively. Thus, an adequate capillary bed is present if the MPS is normal, regardless of the degree of critical stenosis or abnormal wall mo-

tion. The pt with a completely occluded coronary artery and a normal MPS should be a good candidate for ACB and will show improved LV contraction.

TUESDAY, 4:00 p.m.-5:30 p.m.

LINDHEIMER ROOM

IN VITRO AND RADIOASSAY 1

Chairman: Howard J. Dworkin

Co-Chairman: Eileen Nickoloff

BERSON-YALOW AWARD PAPER

RADIOMETRIC ESTIMATION OF THE REPLICATION TIME OF BACTERIA IN CULTURE: AN OBJECTIVE AND PRECISE APPROACH TO QUANTITATIVE MICROBIOLOGY. Edward U. Buddemeyer, Glynn M. Wells, Robert Hutchinson, and Gerald S. Johnston. Division of Nuclear Medicine, University of Maryland Hospital, Baltimore Md.

In a recently-developed, two compartment liquid scintillation vial, the evolution of $^{14}\text{CO}_2$ resulting from bacterial metabolism of labeled glucose was measured sensitively, cumulatively and automatically in a liquid scintillation counter. In each of seven species tested, a period of log-linear expansion of cumulative counting rate with time was observed. The exponential increase in cumulative counting rate was related to cell replication time by the integral of a first-order differential equation. Within a given species the radiometrically measured replication time was found to be remarkably constant, unaffected by a four-fold variation in the activity of added labeled glucose, insensitive to the presence of carrier glucose and independent of the number of bacteria in the initial inoculum over a range of five orders of magnitude. Precise measurements of growth inhibition were obtained by noting the prolongation of cell replication in the presence of antibiotics. These experiments demonstrate that the replication rate of an organism in culture is a highly-reproducible characteristic that is susceptible to precise radiometric measurement in fundamental units of time under a variety of experimental conditions.

THE USE OF INDIUM-111 FOR STUDIES OF CYTOTOXICITY MEDIATED BY LYMPHOCYTES OR BY ANTIBODIES AND COMPLEMENT. Janez Ferluga, Anthony C. Allison and Mathew L. Thakur. Division of Cell Pathology, Clinical Research Centre, Harrow and MRC Cyclotron Unit, Hammersmith Hospital, London, England.

The mechanism by which tumour cells in man and animal are killed by lymphocytes or antibodies and complement has long been a subject of investigations. Tritiated thymidine I-125 Deoxyuridine (IUDR) and Cr-51 chromate have been used to label tumour cells and radioactivity released from the cells has been used as a measure of cell death. However, the spontaneous release of Cr-51 is excessively high and the thymidine and IUDR which are incorporated into DNA are inconvenient to use. Mouse lymphoma cells (P815/CRC) in Hank's solution were incubated with In-111 oxine. Greater than 95% of the radioactivity was associated with the cells. Cells were also labeled with IUDR and Cr-51. Fourtyeight hours after incubation of the labeled cells in culture medium 40% of the Cr-51 and approximately 20% of

the In-111 and IUDR radioactivity was found in the supernatant. The IUDR radioactivity is known to be released only from dead cells. This confirms that there is no spontaneous release of the In-111 which is known to be bound to cytoplasmic components in cells. On the other hand, when the tumour cells are lysed using sensitized lymphocytes or rabbit antibodies and guinea-pig complement, the release of In-111 is similar to that of Cr-51.

These results together with the high labeling efficiency and ease of detectability make the In-111 oxine an attractive agent for cytotoxic studies on tumour cells.

AUTOMATED RIA USING RECYCLABLE ANTIBODY. LaVell R. Johnson, K. LaMont Hadfield, and Bill B. Barnett. Auto-Assay, Division of Becton, Dickinson and Company, Salt Lake City, Utah.

To automate and conserve valuable antibody, techniques were investigated which made it possible to recycle antibody for analytical purposes. Constant volume aliquots, 0.3 ml of antigen solution (eg. cortisol, estriol) containing either H-3 or I-125 tracer, are pumped at controlled rates through an antibody chamber. The antibody chamber is a micro-column containing specific antibody covalently bound to solid beads. The free antigen passes on to either a liquid or a crystal scintillation detector. The bound antigen is eluted quantitatively with appropriate buffers. Individual antibody chambers have been used for over 1000 cycles without change in antibody characteristics. The mean for an overall 8-fold proportional dilution study (40 cycles) for extracts of plasma estriol sample was 21.0 ng/ml and the CV was 7.1% for eight levels. Intra-assay reproducibility of a 12.3 ng/ml plasma estriol sample ranged from a CV of 4.8 to 9.6% (n=121) over five days. The inter-assay CV for the means on the five days was 5.8%. The concentration range for the estriol assay is 0.25 - 16 ng/ml. The %B ranged from 60% with estriol-H-3 tracer to 6% at 16 ng/ml. The antisera for estriol cross reacts 43% with estriol-3-sulfate, 14% with estriol-3-glucuronide and less than 1% with estrone, estradiol, and other estriol derivatives. For cortisol, a simple direct plasma dilution (50-200 fold) in pH 3.5 sample buffer is all that is needed for a plasma assay. The concentration range is 0.25-16 ng/ml. 11-Deoxycortisol is the significant cross-reacting (5%) steroid. In conclusion, we have developed an automated 3-minute assay for steroids using a continuously recyclable antibody.

AUTOMATED RADIOIMMUNOASSAY: EVALUATION OF A SYSTEM FOR THYROXINE AND TRIIODOTHYRONINE DETERMINATIONS. Stanley J. Goldsmith, Helena Lpyszyc, Jeffrey Schultz, Felice Korn & George Schussler. Mt. Sinai Medical Center, New York, N.Y.

An automated RIA system (Centria, Union Carbide) for Thyroxine (T4) and Triiodothyronine (T3) was evaluated. The system consists of lyophilized reagents, an automatic pipetting station, a timed centrifugal mixer-incubator-

separator and a 3 probe counter-microprocessor. Separation is achieved by Sephadex column filtration during centrifugation. Bound fraction is counted; microprocessor generates standard curve values and sample (S) concentration. Pipetting coefficient of variation (COV) was 1.68% vs. 1.39% (experienced tech-manual pipette).

	T4			T3		
	Lo	Mid	Hi	Lo	Mid	Hi
Centria	6.90	5.91	2.53	-	6.79	5.97
Inhouse	-	2.57	5.57	-	2.66	4.30

Mean and standard deviation in a normal population:

	T4 (N=32)		T3 (N=29)	
	Lo	Hi	Lo	Hi
Centria	81.50	32.74	1.80	0.84
Inhouse	84.50	29.26	1.83	0.60

Over a wide range, correl. coeff. of 274 clinical S for T4 vs. Inhouse=0.93; of 123 T3 S=0.70. 308 T4 or 277 T3 patient S in duplicate could be assayed and results calculated in an 8 hour day.

T4 Auto RIA is a highly reliable, easy to perform method comparing favorably with the precision and reproducibility of an inhouse manual method. T3 Auto RIA had a greater degree of variability but the accuracy of the method would permit its use in a clinical setting.

PERFORMANCE CHARACTERISTICS OF CONCEPT 4 AUTOMATIC RADIO-ASSAY. Orwin L. Carter. Micromedic Systems, Horsham, Pa.

Concept 4TM Automatic Radioassay totally automates T4 (RIA), T3 (RIA), T3 Uptake, Digoxin, and Cortisol radioassays from the pipetting of the patient sample through the calculation of patient values. The Autopak^R test delivery systems for these five assays use treated tube technology with a single reagent addition of ¹²⁵I labelled antigen in buffer. Tubes are incubated, aspirated, and washed twice without operator intervention. Quantitation is done automatically in a dual detecting gamma counter with on line data reduction performed on a Hewlett Packard 9815A.

A summary of performance characteristics is shown below:

	T4 (RIA)	T3 (RIA)	T3 Uptake	Digoxin	Cortisol
Intraassay CV(%)	2.6	5.5	2.7	7.4	7.4
Interassay CV(%)	5.7	5.5	3.4	6.5	9.2
Average Recovery(%)	98.2	118.7	---	102.1	109.4
Sensitivity (95% B/B ₀)	0.25	0.25	---	0.08	0.1
Crossreactivity(%)	0.02	0.001	---	0.05	0.146
Substance	T3	T4	---	Digitoxin	11-deoxycortisol
Normal Range	4.5-12.0 ug/dl	0.0-2.0 ng/ml	35-45 %	1.0-2.0 ng/ml	3.0-18.0 ug/dl (AM)

Precision Values are shown for pools at the midpoint of the normal range.

WEDNESDAY, JUNE 22, 1977

WEDNESDAY, 8:30 a.m.-10:00 a.m.

CHICAGO ROOM

NEUROLOGY 1

Chairman: C. Douglas Maynard
Co-Chairman: John F. Lindeman

ACCURACY OF CURRENT NEURODIAGNOSTIC TESTS IN THE DETECTION OF CEREBROVASCULAR DISEASE. G. T. Krishnamurthy, K. N. N. Murthy, K. Paramesh, S. D. Dand, and W. H. Blahd. VA Wads-

worth Hospital Center, and UCLA School of Medicine, Los Angeles, Calif.

The diagnostic accuracy of the qualitative and quantitative radionuclide brain perfusion, static brain images, CAT scan, and angiogram was studied in 39 patients with CVA. In 33 patients, interval between the onset of lesion and diagnostic test was less than 10 days; in the other 6 patients, the interval was 10-30 days. The perfusion study was made in the anterior view with 15-20 mCi of Tc-99m-DTPA and the images were recorded at 2-sec intervals. Data were computer recorded at 0.5 sec/frame for 36 sec. For analy-

sis, 6 regions of interest (3 pairs) were chosen. Right/left ratio (in percent) for each pair of curves was obtained during transit time. CAT scans were obtained in 14 patients before and after the infusion of contrast agent. True positivity for the static brain image study, the CAT scan, the qualitative brain perfusion study, and the angiogram were 33, 50, 54, and 69%, respectively. The addition of quantitative data increased the true positive rate of radionuclide perfusion studies to 62%. The overall accuracy of the radionuclide studies (including static images) was 72% as against 50% by CAT scan. The radionuclide true positive rate for 14 patients who also had CAT scans was 80% versus 50% by CAT scan alone. In 6 patients whose CAT scans were negative, the radionuclide study was positive; the reverse was true in one patient. It is concluded that for cerebrovascular lesions, the radionuclide triple test should be the screening test, and the CAT scan or angiogram should be used in selected cases where additional detailed information is required for therapy.

RADIONUCLIDE AND COMPUTERIZED TOMOGRAPHY SCANS IN EVALUATION OF HEAD INJURED PATIENTS. Abass Alavi, Barbara P. Uzzell, David E. Kuhl, and Robert A. Zimmerman. Hospital of the University of Pennsylvania, Philadelphia, Pa.

Transmission computerized tomography (CT) was used to study 234 patients with head trauma, and 80 of these were evaluated with radionuclide (RN) scans. The CT scans were obtained by using an EMI head unit. In 21 patients with final diagnoses of chronic subdural (SD) hematoma, 18 were positive with both tests. Two patients had positive CT and negative RN studies. In 1 patient the CT was negative for SD, while RN study appeared positive. Of 13 patients with intracerebral hematoma (ICH) shown immediately on CT scans, 11 had a positive RN scan. In these patients, RN scans were positive 6 days or more after insult in all but one case which was demonstrated in 3 days. In 9 patients with evidence of cerebral contusion on the CT scan, the RN studies were positive in 8. CT scans accurately diagnosed epidural hematoma in all 13 patients. None of the 21 patients with acute SD hematoma were studied with RN scans. All were accurately diagnosed by CT scans. In 25 patients post-operative for SD hematoma, the CT scans were of great value in detection of residual hematoma or reaccumulation of blood. In conclusion, although RN studies were quite sensitive in detection of chronic SD, ICH of several days duration and cerebral contusion, the CT scans were most sensitive and specific means of diagnosis of intracranial hematomas immediately after head injury and post-operatively.

PARAMETRIC IMAGING OF THE BRAIN WITH POSITRON CT SCANNING. J.O. Eichling, C.S. Higgins, M.J. Welch, M.M. Ter-Pogossian. Department of Radiology, Washington University School of Medicine, St. Louis, Missouri.

The capability of positron CT scanning to accurately yield the regional in vivo concentrations of a radionuclide within an organ on a quantitative basis provides the impetus for exploration of new areas in nuclear medicine. This capability, unique to reconstruction techniques, permits positron CT scanning to be employed for the regional determination of a wide array of physiological quantities, i.e., parametric imaging, in which the display represents the regional distribution of the computed quantity. Proposals for the brain include regional determination of blood volume, blood flow, tissue hematocrit, lipid content, tissue pH, partition coefficients, and tissue metabolism. We have tested the viability of this concept by (1) demonstrating that the output of the imaging system is linear with the concentration of radionuclide contained in the region of interest, (2) by calibrating the system's response to provide a means of determining the regional radioactivity concentration in vivo and (3) by employing rela-

tively atraumatic methods to determine several quantities. We have measured cerebral blood volume and cerebral hematocrit by employing carbon-11-carboxyhemoglobin and carbon-11-methyl albumin as vascular labels in rhesus monkeys and in normal human volunteers. The data predict a normocarbic (PaCO₂=37mmHg) mean CBV of 3.8 ml/100g for 8 rhesus monkeys with a normocarbic tissue hematocrit prediction of 0.87, and a mean rCBV of 3.9±0.4 for 10 human volunteers. In addition, computed tissue:blood partition coefficients for C-11-methanol and octanol are 0.95 and 1.3 respectively, for the rhesus monkey brain. All the data are in agreement with corresponding values obtained with conventional methods.

DETERMINATION OF LOCAL CEREBRAL GLUCOSE UTILIZATION BY MEANS OF RADIONUCLIDE COMPUTED TOMOGRAPHY AND (F-18)-2-FLUORO-2-DEOXY-D-GLUCOSE. D.Kuhl, M.Reivich, A.Wolf, J.Greenberg, M.Phelps, T.Ido, V.Casella, J.Fowler, B.Gallagher, E.Hoffman, A.Alavi and L.Sokoloff. University of California, Los Angeles, Los Angeles, Calif. University of Pennsylvania, Philadelphia, Pa. Brookhaven National Laboratory, Upton, N.Y.

The purpose of this study was to adapt to man the established (C-14)-deoxyglucose [(C-14)-DG] autoradiographic technique for measuring local cerebral glucose consumption in animals. In the (C-14)-DG method, the intravenously injected tracer is taken up in the brain at a rate proportional to that of glucose; utilization is calculated after autoradiographic measurement of the localized metabolic products.

Both (C-14)-FDG and (F-18)-FDG were synthesized for various parts of the project, the latter requiring a new synthetic route via direct fluorination. In-vitro studies and studies in animals confirmed the validity of (F-18)-FDG as a tracer and as a substitute in the (C-14)-DG model.

In man, Mark IV tomography was performed 30 minutes after intravenous injection of 5mCi of (F-18)-FDG and the distribution of F-18 activity was determined from cross-sectional images. With knowledge of the arterial time-course of specific activity of (F-18)-FDG and previously determined constants related to FDG kinetics, the local metabolic rate for glucose was determined for each part of the brain.

Representative values expressed in mg/100g/min agree with values reported in the literature. These are: visual cortex 7.36, sensory-motor cortex 6.51, frontal cortex 6.19, parietal cortex 5.84, thalamus 6.71, and subcortical white matter 2.48.

This new ability to measure local brain metabolism should be an important aid to understanding cerebral function in health and disease.

REGIONAL CEREBRAL BLOOD FLOW STUDY WITH AUTOFLUOROSCOPE SYSTEM-70 AND ITS APPLICATION TO PRE- AND POSTOPERATIVE EVALUATION OF ARTERIOVENOUS MALFORMATION PATIENTS. Yasuo Kawamura, Tadahisa Kurimoto, Kuniyuki Soneda, Hiroshi Matsumura, Akira Kasahara, and Magiochi Matsuda. Kansai Medical University, Osaka, Japan.

This study was performed to evaluate the effect of surgery on regional cerebral blood flow (rCBF) and to determine the relationship of rCBF to the neurologic signs in patients with arteriovenous malformations (AVM). The rCBF was measured in 5 patients with AVM by injecting 5 mCi of Xe-133 with radiocontrast into the internal carotid artery and imaging with a computerized multi-crystal scintillation gamma camera (Autofluoroscope System-70) before and after surgical intervention. The activity recorded from the 294 minidetectors was manipulated using a height over area calculation and immediately displayed as a functional color image on a television screen. An approximate 20-24 percent decrease of the preoperative rCBF was observed in and around the AVM and correlated with improvement in the neurologic deficits. In addition to the localized decrease in rCBF the surgery apparently altered the general distribution of rCBF. The maximum increase in rCBF was 49 percent. Following surgery in one patient with an occipital AVM the pre-operative homonymous quadransopia disappeared completely with improvement (decrease) in the rCBF.

We conclude that due to its abnormal large flow the AVM causes an "intercerebral steal phenomenon" that rapidly diminishes rCBF in its contiguous areas.

WEDNESDAY, 8:30 a.m.-10:00 a.m.

JANE ADDAMS ROOM

INSTRUMENTATION 3

Chairman: Robert N. Beck
Co-Chairman: Michael E. Phelps

MOTION CORRECTED HEPATIC SCINTIGRAPHY: IMPROVED DIAGNOSTIC RESULTS. D.A. Turner, E.W. Fordham, A.A. Ali, P.D. Rubin, R. Muehrcke, A.N. Sukerkar, G.J. Novetsky and D.P. Dalia. Rush Medical College, Chicago, Ill. B.E. Oppenheim and N.J. Yasillo, University of Chicago, Chicago, Ill. F.B. Hoffer, University of California, San Francisco, Cal.

Oppenheim has described a digital method of correcting hepatic scintigrams for respiratory motion. Hoffer et al. have reported preliminary experience with an analogue version. This communication reports an objective test of the latter. A motion correction device was built for an Ohio Nuclear Series 100 camera. Corrected and uncorrected images were simultaneously recorded on Polaroid film during routine hepatic scintigraphy of 1100 patients, selected without known bias. Autopsy, liver biopsy or inspection at laparotomy shortly before or after scintigraphy was considered to have established the "true" state of the livers of 49 patients with hepatic tumors and 53 normals. Five observers of varying experience in nuclear medicine independently evaluated the scintigrams for the presence of mass lesions, using a five category rating scale, without knowledge of the true states. Results were expressed as receiver operating characteristic curves. For all observers, performance was better with motion correction or when interpreting corrected and uncorrected studies together than when interpreting uncorrected studies alone. Motion correction is an inexpensive, efficacious method of improving the diagnostic quality of hepatic scintigrams.

A SURVEY OF THE MEASURED DEAD TIME OF SCINTILLATION CAMERAS. Ralph Adams*, Gerald J. Hine**, and C. Duane Zimmerman*. *Loma Linda University, Loma Linda, Calif., and **Boulder, Colo.

This investigation was undertaken to evaluate the dead time performance of current models of scintillation cameras. Measurements were made under simulated clinical conditions using a protocol developed by the authors. We show that in the presence of a scattering medium the newer scintillation cameras behave very close to the paralyzable model. We define "paralyzing dead time (T)" under simulated clinical conditions" in terms of a paralyzable system and specified parameters of scatter, analyzer window (20%), and counting rate (20,000/sec per source). The protocol employs two Tc-99m sources in a plastic phantom which provides 5 cm forward scatter and 10 cm back scatter. The spectral emission from it closely approximates that from Tc-99m in the myocardium in the 30° LAO view. The sources do not require accurate calibration, and the result is easily computed with a pocket calculator. The method is reproducible to a small fraction of 1 μsec and sufficiently sensitive to detect a change of less than 1 volt in the high voltage supply.

The survey demonstrates significant differences in dead time performance from one manufacturer to another. These differences are somewhat masked by widely differing performance between individual instruments of a given model. We also show a marked improvement in current models over the previous generation of cameras (typically 6 μsec vs. 15 μsec). The numerical values we obtain are greater by a factor of 2 or 3 than those advertised by most manufacturers, who employ various other methods to specify dead time.

COMPUTER-ASSISTED CINEMATIC DISPLAYS IN NUCLEAR MEDICINE. Henry N. Wagner, Jr., Mattheus G. Lotter, Lloyd G. Knowles, T.K. Natarajan and Kenneth H. Douglass. The Johns Hopkins Medical Institutions, Baltimore, Md.

One of the most significant improvements in cardiovascular nuclear medicine is imaging the beating of the right and left ventricles by motion-picture display of the intraventricular distribution of technetium-99m albumin during 16 or more phases of the cardiac cycle. Stimulated by our results in viewing ventricular function as a motion picture, we have begun to make other "fast motion" pictures of a whole variety of body functions, including the cerebral circulation, pulmonary perfusion and ventilation, biliary excretion, and renal and testicular blood flow. We have compressed data obtained over periods of minutes, hours and days into 16 frames per second. These "compressed time images" are shown over and over in monochrome and color displays and have been found to improve our perception of regional dysfunction. Comparison of the new techniques with prior methods, i.e., inspection of a series of individual images and functional images, has resulted in improvement in observer performance in terms of both false positives, false negatives and degree of certainty of diagnosis. A specific example is the improvement in thallium-201 images of the myocardium when synchronized motion picture display is used. The cinematic-display improves perception partly by doing away with the blurring effect on the usual type of static images of moving structures, such as the heart, and in revealing small changes in regional function in studies of the cerebral circulation, liver and biliary systems, bones, and kidneys and testes.

A QUANTITATIVE RESOLUTION PHANTOM. Barry S. Brunsten, Robert N. Beck, Elbert L. Lands, and Bhailal Patel. University of Chicago Hospitals and the Franklin McLean Memorial Research Institute, Chicago, Ill.

A quantitative parallel line phantom, capable of measuring Anger camera resolution to <1mm, has been developed. It consists of two identical parallel line grids which generate, by a Moiré effect, the pattern frequency to be imaged. The spacing of this line pattern may be varied from <4mm to >400mm, and the setting accuracy improves at small spacings.

Previous resolution phantoms may be placed in two categories. The four-quadrant bar and similar types have only a few pattern spacings and test only a portion of the image area at one time. Uniform phantoms (Ples, etc.) which test the entire image area must be designed for an individual camera in a particular mode of operation to effectively indicate change of resolution.

Using the Moiré phantom in studies of intrinsic resolution, 4 settings within a 2mm range show resolution of the pattern: over the entire, most, a small part, or none of the image area. Once the resolution limit has been determined for a camera, images at 3 settings around this limit allow even minor fluctuations to be observed.

Since 11/1/76, weekly intrinsic resolution measurements have been performed on two Pho-Gamma IV's, a mobile Pho-Gamma IV, and a Searle LFOV to compare resolution and uniformity with frequency of service.

The Moiré-type phantom provides accuracy in measurement, compatibility with cameras of differing resolution, simplicity, and modest measurement time. It is also suitable for indicating spatial distortion and measuring resolution of most collimators.

TECHNIQUES FOR MEASURING REGIONAL AND TOTAL-BODY BONE MINERAL MASS. Ronald R. Price, Kenneth H. Larsen, Juan J. Touya, and A. Bertrand Brill. Nuclear Medicine Division Vanderbilt University Hospital, Nashville, TN.

A rectilinear scanning system utilizing a modified whole-body scanner has been developed to make quantitative scans of regional and whole-body bone mineral content (BMC). The system employs the two photon attenuation technique utilizing a Gd-153 transmission source. Computer generated images of the derived BMC (g/cm²) are now being analyzed

and evaluated for their utility in detecting and monitoring bone demineralizing diseases. These techniques are being used with a modified Ohio Nuclear Scanner to collect and compare the BMC images to quantitative scans of Tc-99m labelled bone agents to produce bone uptake to BMC ratios in suspected lesions.

Scans of the lumbar spine take approximately 10 minutes and deliver a radiation dose of less than 10 mrad. Lower resolution whole-body BMC scans take 20 minutes and also deliver a dose of about 10 mrad. Measurements on a group of normal volunteers and a group of patients with suspected and confirmed osteoporosis have been encouraging and suggest that the vertebral BMC scans will be a sensitive indicator of bone disease.

The experience we have gained from the use of parameter images derived from the ratio of emission bone scan images to BMC images suggests that these images may prove to be an important adjunct to the routine emission bone scan. (Supported in part by ERDA # EY-76-S-05-2401).

COMPARATIVE PERFORMANCE STUDY OF LARGE FIELD SCINTILLATION GAMMA CAMERAS: AN UPDATE. Chun B. Lim, Paul B. Hoffer, David Rollo and David L. Lilien, University of California, San Francisco, Ca.

There has been significant progress in the basic imaging performance of large field gamma cameras since we reported our comparative evaluation last year. Two recently introduced cameras (Picker 4/15 and Ohio-Nuclear 410) were studied and compared with previous results on Searle LFOV and Ohio-Nuclear 110. Specific parameters studied for 140keV gamma imaging were: 1) intrinsic resolution and sensitivity, 2) system collimator sensitivity and resolution, 3) count rate capability and influence of count rate on resolution, 4) energy resolution, 5) field uniformity and linear distortion. One production model of each instrument was tested. Each instrument was interfaced with identical PDP-11 computer units for resolution measurements to insure uniformity of comparison. The concise results of the comparison for 1) intrinsic resolution (140keV FWHM), 2) max. count rate (20% window), 3) count rate at 10% data loss, and 4) energy resolution (FWHM) were as follows:

Searle LFOV	ON-110	ON-410	Picker 4/15
1) 6.7 mm	6.5 mm	5.5 mm	4.7 mm
2) 145K/sec	92K/sec	92K/sec	112K/sec
3) 70K/sec	68K/sec	68K/sec	68K/sec
4) 15%	15%	15%	12%

Field uniformity and linear distortion performances of Searle and ON cameras were slightly better than that of the Picker 4/15. Subjective evaluation of Rollo phantom images reveals little apparent resolution difference when comparing similar collimators and scatter material thicknesses.

INITIAL EXPERIENCE WITH A HIGH QUALITY VIDEO DISPLAY FOR NUCLEAR MEDICINE IMAGING. David M. Shames, Robert E. L. Farmer and William O'Connell, University of California, San Francisco, Ca.

In order to assess the value to nuclear medicine imaging of a high quality digital image video display, we interfaced the DeAnza Systems display to our Gamma 11 (DEC) computer. The basic hardware characteristics of this display include a 256x256x12 bit image buffer, programmable intensity transformation table and color or black and white image presentation. Software has been written to allow images to be placed on the screen in a number of different formats. While the most visually appealing format is that of a single 128x128 image or several of these up to four, we also have the capability of displaying a single 256x256 image or up to sixteen 64x64 images simultaneously. Linear or non-linear contrast enhancement is performed at the keyboard through the intensity transformation table. Each element of the display memory is 12 bits deep, allowing a capability of 1024 gray shades plus two graphics overlays. Software has also been written to place characters anywhere on the face of the display and to edit these characters by simple keyboard operations.

The images obtained from this display at 128x128 are of analogue quality, and quite suitable for clinical interpretation at 64x64. We have found the display particularly

useful for placing multiple images from the same or different studies on the display at the same time with each image individually contrast enhanced and annotated with any desirable characters. Display images can be dumped to the Microdot (Searle) for clinical and archival purposes and photographed with poloroid for the patient's and referring physician's records.

COLLIMATOR EVALUATION FOR MYOCARDIAL IMAGING WITH Tl-201. H Nishiyama, DW Romhilt, CC Williams, RJ Adolph, VJ Sodd, M Gabel, JT Lewis and EL Saenger, Nuclear Medicine Laboratory, BRH, FDA, and Cincinnati General Hospital, Cincinnati, Ohio.

Myocardial imaging with Tl-201 is most often obtained using the high-resolution parallel-hole collimator (HRC), which frequently misses the small non-transmural infarction. Based on this observation, evaluation of collimator resolution was made by both in-vitro and in-vivo studies. The collimators evaluated by line spread function (LSF) were HRC, low energy converging collimator (CONV) and pinhole collimator (PHC). A cylindrical heart phantom with three different sizes of myocardial infarctions was evaluated in both endocardial and epicardial location. The best resolution was obtained with PHC, followed by HRC and CONV, with both LSF and phantom studies. All collimators showed better delineation of the epicardial lesion than the endocardial of the same size. Further, 10 dogs with an induced acute myocardial infarction (AMI) were imaged, and later, results of image evaluation were correlated with postmortem findings. The most accurate detection of AMI in dogs was obtained by PHC as LSF indicated. The sensitivity of the collimators is in reverse order of the resolution. A reasonable compromise in the clinical setting is to use HRC in standard projections, and then obtain one or two selected views by PHC. This procedure increased overall diagnostic accuracy from 70% using HRC alone to over 90% using PHC in experimental study.

WEDNESDAY, 8:30 a.m.-10:00 a.m.

LINDHEIMER ROOM

ONCOLOGY 2

Chairman: Andrew T. Taylor, Jr.
Co-Chairman: Stanley M. Levenson

COMPARISON OF GALLIUM SCAN AND CHEST X-RAY EVALUATION FOR MEDIASTINAL SPREAD OF CARCINOMA OF THE LUNG. Naomi P. Alazraki, Paul J. Friedman, Andrew Taylor, Jr. Joseph W. Ramsdell, Richard M. Peters, and Gennaro Iasi. VA Hospital and University California, San Diego, CA.

A comparative study of the accuracy of gallium scans and chest x-rays in predicting mediastinal involvement by tumor in patients with lung carcinoma was performed. The study protocol included only preoperative patients with suspected lung carcinoma, subsequently diagnosed by either mediastinoscopy, thoracotomy, or autopsy (two patients) and excluded patients with known metastatic disease or oat cell carcinoma.

Gallium scans were performed using 5 millicuries of 67-gallium injected intravenously. Imaging was done at 72 hours following injection on a rectilinear scanner with anterior, posterior, and oblique camera views of the chest, when indicated. The gallium scans were always compared with chest x-rays taken within a few days of the scan. Oblique views and chest tomograms of the mediastinum were obtained when warranted by either radiological or clinical opinion. Mediastinal exploration (by mediastinoscopy or anterior thoracotomy) was used as the definitive criterion

for presence or absence of mediastinal tumor.

The results on 25 patients indicated that the gallium scan was slightly more sensitive in the detection of mediastinal tumor than the chest x-ray, while both were equally specific. There were no false negative results for gallium and two false negatives for chest x-ray. The results support the possibility of considering omitting the mediastinoscopy prior to thoracotomy when the gallium scan shows no involvement of the mediastinum with tumor.

STEROID INDUCED SUPPRESSION OF GALLIUM UPTAKE IN TUMORS OF THE CENTRAL NERVOUS SYSTEM. Alan D. Waxman, John R. Beldon, William R. Richli, Doina E. Tanasescu, and Jan K. Siemsen. LAC/USC Medical Center, Cedars-Sinai Medical Center, Los Angeles, Calif.

Isolated case reports have indicated that steroids may reduce technetium uptake in tumors of the central nervous system. We have evaluated Tc-99m glucoheptonate (TcGH) as well as Gallium uptake in vivo and have found the affect of steroids on technetium uptake to be minimal, while the affect on Gallium is profound.

Delayed TcGH and Gallium brain scans were done on 61 patients with proven central nervous system tumors. Technetium scans were done 2 - 4 hours following a 15 mCi injection. Gallium scans were done 2 - 7 days following a 5 mCi injection. The patients were broken down into a steroid group and a nonsteroid group. The steroid group were those patients who were on steroids at greater than replacement levels. TcGH and Gallium brain scans were compared using lesion to calvarial ratios. The results are shown on the following table:

	Tc Pos Ga Neg	Tc > Ga	Tc = Ga	Tc < Ga	Tc Neg Ga Pos	Tc Neg Ga Neg
Steroids	12	16	10	1		3
Nonsteroids	1	2	10	4	2	

In addition, 4 patients had Gallium brain scans prior to steroid therapy, and again after being on steroids for one week. The Gallium brain scan, in all cases showed either a disappearance of Gallium uptake or a reduction of Gallium uptake in tumor. The TcGH brain scan was either not affected, or affected only slightly.

We conclude that steroids have a profound affect on Gallium uptake in tumors of the CNS, while affecting TcGH uptake minimally.

COMPARISON OF THE BIOLOGIC DISTRIBUTION OF THREE COMMERCIALLY AVAILABLE Ga-67 CITRATE PREPARATIONS IN NORMAL AND DISEASED RATS. Michael A. Davis, Rebekah A. Taube and Alice D. Carmel, Children's Hospital Medical Center and Joint Program in Nuclear Medicine, Harvard Medical School, Boston, MA.

Gallium-67 citrate enjoys widespread popularity as a radiodiagnostic imaging agent for sites of inflammation, infection and malignancy. Most of the radiopharmaceutical used in this country is obtained from three commercial suppliers. Recent reports suggest that a difference may exist in the biologic distribution and diagnostic efficacy of the three products. Two studies, each using a different source of Ga-67, came to opposite conclusions concerning the accuracy of the agent for stroke diagnosis. Another project employing two commercial suppliers of Ga-67 to investigate malignant diseases concluded that the variations in product formulation were responsible for observed discrepancies in biologic distribution. Analysis of the three products indicated that one manufacturer had a preservative present and another eight times the citrate concentration of the other two. Experiments were designed and carried out to ascertain whether these differences in formulation had any effect upon the biologic distribution in normal and pathologic states. Normal rats, rats bearing a transplanted subcutaneous glioblastoma and rats with a turpentine induced abscess served as models for this evaluation. The animals were killed at 1 and 48 hrs after intravenous injection of the test agent. Data for complete organ distribution and total body retention at both 1 and 48 hrs showed no statistically significant differences among the three products in either normal or diseased animals. We conclude that the differences in formulation of the three commercial preparations have no significant effect on the biologic distribution of Ga-67 in the rodent models used in this investigation.

CLINICAL TUMOR SCANNING WITH Tl-201 CHLORIDE. Norihisa Tonami, Takatoshi Michigishi, Hisashi Bunko, Masami Sugihara, Tamio Aburano and Kinichi Hisada. Kanazawa University School of Medicine, Kanazawa, Japan.

A case of lung cancer was incidentally found, in which the primary lesion of cancer was clearly visualized on the Tl-201 scintigrams taken for myocardial evaluation. Following the experience, tumor scanning with Tl-201 chloride was performed to investigate its diagnostic value. Fifty-one patients with untreated malignant lesion and 29 with benign disorder, mostly thyroid disease, were studied with Tl-201 which were given intravenously as thallium chloride in a dose of 1.5-2.0mCi. To compare the detection rate of malignant lesion, Ga-67 scanning was also performed in 18 patients. Of the 51 malignant lesions, 36 (71%) were visualized as positive with Tl-201, whereas 13 of 18 lesions (72%) were positively delineated with Ga-67. High positive results with Tl-201 in malignant lesions were obtained in thyroid cancer: 14 of 15 (93%), lung cancer: 10 of 14 (72%) and primary hepatoma: 3 of 4 (75%). Poor positive result was in metastatic liver cancer: none of 8 (0%). Of the 19 benign cold thyroid nodules 6 were positively visualized with Tl-201. However, Tl-201 did not accumulate in the other 13 benign nodules, 11 out of which were confirmed to have cystic degeneration. All of five with chronic thyroiditis and all of three with hot nodule showed positive accumulation of Tl-201. The data suggests that if the thyroid nodule is found to have negative accumulation of Tl-201, malignancy can be ruled out except a small microscopical lesion. Tl-201 scanning also appears to be useful to differentiate primary hepatoma from metastatic liver cancer.

RADIOPHARMACOKINETICS OF ANTITUMOR AGENTS: FLUORINE-18 5-FLUOROURACIL. Walter Wolf, Jashovam Shani, David Young, and Elizabeth Vine. Radiopharmacy Program, University of Southern California, Los Angeles, CA.

Previous work on the distribution of 5-Fluorouracil (5-FU) labeled with C-14 and F-18 suggested little, if any, specificity in the localization of this radiopharmaceutical in a number of murine tumors [JNM 16:582 (1975)]. We wish to report here our results on the differential distribution of F-18 5-FU in sensitive vs. non-responsive L-1210 lymphocytic leukemia in mice, as a potential model for prediction of chemotherapeutic response to 5-FU.

The mice were injected with F-18 5-FU, sacrificed at 2 and 12 hrs., dissected, and the activities measured in over 15 organs and tissues. The tumor/blood ratios between the 5-FU responsive vs. the non-responsive lines are:

	2 hours	12 hours
Responsive	1.90 ± 0.12	20.69 ± 1.87
Non-responsive	0.96 ± 0.27	4.04 ± 0.66

Studies currently in progress are evaluating whether these differential kinetics of distribution also occur in patients, what are the optimal times for measurement, and whether indeed the use of F-18 5-FU can differentiate responsive from non-responsive tumors in man, as well as whether it is feasible to monitor and optimize dose regimens using this radioactive chemotherapeutic agent. (This work was supported by NCI grant P01 CA-19438)

COBALT-BLEOMYCIN A2: A BETTER RADIOLABELED TUMOR LOCALIZING AGENT. Jack N. Hall, James M. Woolfenden, Joseph D. Chen, and Dennis D. Patton. University of Arizona Health Sciences Center, Tucson, Az.

Several investigators have indicated that cobalt-57 Bleomycin is more readily taken up by malignant tissue than any of the other radiolabeled bleomycins. In addition, Eckelman, et al have isolated bleomycin components by high performance liquid chromatography (HPLC) into four major fractions (A1, A2, IMA2, B2) and studied their biological distribution using cobalt-57 as a label. Their results suggested that the major components, A2 and B2 are the most useful fractions for tumor localization. Consequently, the purpose of this study was to evaluate the artificial bleomycins produced by fermentation rather than

HPLC to eliminate the potential for undesirable chemical reactions (e.g. transformation of the A2 by the solvent system used).

The tumor model used in this study was an AKD-2 mouse bearing a ridge osteogenic sarcoma which is sensitive to bleomycin. Biological distribution studies were performed at 1, 4, 24, and 48 hrs. for the commercially available and three artificial bleomycins (A2, A5, B2). At 24 hours the following tumor to muscle and tumor to blood ratios were obtained.

Co-57 Agent	T/M	T/B
Bleomycin (mixture)	23	36
Bleomycin A2	57	99
Bleomycin A5	27	37
Bleomycin B2	47	28

The high tumor-to-nontumor ratios of radiolabeled bleomycin A2 suggests that a search for a shorter half-life radionuclide as a label for this antineoplastic agent should be continued.

[O-16(He-3,p)F-18], crown ether (18-Crown-6) and 21-hydroxypregn-4-ene-3,20-dione methanesulfonate. The maximum radiochemical yield based on total activity present after workup was 18%.

The distribution of 21-fluoroprogesterone-F-18 was studied in rats given intravenous injections and sacrificed in groups of three at 5, 10, 15 and 30 minutes after administration. The adrenal glands contained a higher concentration of radioactivity than any other organ at all times studied. The highest tissue concentration found was 0.075% dose/g in the adrenal glands, 5 min. after administration. The adrenal/blood concentration ratios were 42, 21, 17 and 7 at 5, 10, 15 and 30 minutes after administration respectively.

In summary, 21-fluoroprogesterone has been prepared in an overall radiochemical yield of 18% from KF-18. Initial distribution studies in rats indicate that the compound may be useful as an adrenal imaging agent.

A NEW GERMANIUM-68/GALLIUM-68 GENERATOR. Gary J. Ehrhardt and Michael J. Welch. Department of Radiology, Washington University School of Medicine, St. Louis, Missouri.

A germanium-gallium generator producing EDTA-free Ga-68 rapidly and conveniently would permit the synthesis of a broad spectrum of Ga-radiopharmaceuticals difficult or impossible to produce from the strong EDTA-Ga-68 complex provided by current generators and would therefore greatly facilitate the wide application of positron tomography. A solvent extraction generator system producing the weak gallium-68,8-hydroxyquinoline complex free of EDTA has been investigated by attempting the extraction at various pH values and with various solvents in standard separatory funnels. The conditions for optimum yield and minimum Ge-68 breakthrough were found to be extraction from pH 4.8 Ge-68 solution (.01M Ge) with an equal volume of chloroform, followed by a backwash with a similar, non-radioactive aqueous phase in a second separatory funnel, and finally evaporation of the chloroform to dryness. This system gave Ga-68 yields of 70-80% and Ge-68 breakthrough values of <0.003% in the final product. In addition, the gallium-68 oxine is readily convertible to other radiopharmaceuticals, contains only a small quantity of oxine (<50 µg) and is conveniently delivered dry. The extraction system is simple and amenable to automation. The 275 day half-life of Ge-68 and the low germanium loss rate of <0.01% per milking should provide a generator with a long useful lifetime.

COVALENT ATTACHMENT OF CHELATING GROUPS TO HUMAN SERUM ALBUMIN. Gary E. Krejcarek and Karen L. Tucker, Medical Products Div., 3M Co., 3M Center, St. Paul, MN.

In 1974, Sundberg and co-workers synthesized the bifunctional chelating agent, 1-(p-benzediazonium) EDTA. When coupled to proteins, this reagent created specific metal binding sites on macromolecules. In this communication, an alternate procedure is described which attaches DTPA to proteins using reagents common in peptide synthesis. The technique is considerably easier to carry out and does not require the synthesis of any intermediates.

The mixed carboxycarbonic anhydride of DTPA was prepared from pentatriethylammonium DTPA and isobutylchloroformate. This anhydride was added to an HSA solution which was cooled in an ice bath and buffered at pH 7.5. After 20 hours at 4°C, the reaction mixture was dialyzed and the protein fraction corresponding to DTPA covalently coupled to HSA was isolated by gel chromatography. DTPA-HSA, in glycine-HCl buffer pH 3.4, was labeled with In-113m resulting in a labeling yield of greater than 98%.

Distribution studies in mice with In-113m labeled DTPA-HSA showed a blood clearance rate similar to I-125 HSA. The amount of isotope in the liver was nearly identical for the two proteins indicating that the HSA was not denatured during the modification and labeling procedure.

This technique allows coupling of DTPA to a variety of proteins of physiological interest. The DTPA modified proteins could be labeled with other metal isotopes such as Ga-68 and In-111.

WEDNESDAY, 10:45 a.m.-12:15 p.m.

CHICAGO ROOM

RADIOPHARMACEUTICAL 3: FLUORINE, GALLIUM, AND INDIUM

Chairman: Raymond L. Hayes
Co-Chairman: Harry Saul Winchell

BIODISTRIBUTION IN NORMAL AND TUMOR BEARING ANIMALS OF F-18-2-DEOXY-2-FLUORO-D-GLUCOSE (F-18-DG): A NEW AGENT FOR MEASURING MYOCARDIAL GLUCOSE TRANSPORT AND METABOLISM. P. Som, A.N. Ansari, H. Atkins, V. Casella, J. Fowler, B. Gallagher, T. Ido, C. Wan, A. Wolf and D. Kuhl. Brookhaven National Laboratory, Upton, N.Y. and UCLA, Los Angeles, CA.

Transport of sugar in metabolically active organs such as brain and heart is known to be high. Enhanced sugar transport and metabolism by transformed cells has also been documented. This study was undertaken to determine the biodistribution of F-18-DG, a γ -emitting glucose analog with a view toward using this agent to probe local glucose metabolism in these organs as well as in tumors. In normal mice heart uptake reached a maximum value of ~ 32%/gm by ½ hr which remained constant up to 2 hrs. Liver, lungs, kidneys, small intestine and blood showed very rapid clearance. At 2 hrs, heart/lung and heart/liver ratio was 12 and 32 respectively. In dogs 2.8-4.1% dose accumulated in the heart at 1 hr. The highest activity in the heart was in the left ventricle and interventricular septum.

The brain uptake reached a maximum of 6%/gm by 15 min in mice and decreased slowly over 2 hrs. In dogs, the brain activity (2.14%/organ) showed non-uniform distribution, highest activity being in the cerebral cortex, followed by cerebellum and medulla. The gray matter showed 2-3 times higher activity than the white matter. The blood clearance showed a fast T½ of 3-4 min at which time >80% cleared. At 2 hrs ~ 50% activity was found in urine, the predominant chemical form of which although unidentified, was not fluoride. Preliminary studies in tumorous animals (spontaneous breast tumors in rats, eye melanomas in hamsters) showed tumor/normal tissue ratios of > 3 (CA breast/normal breast) at 1 hr and 4.6 (melanoma/normal eye) at 2 hrs.

21-FLUOROPROGESTERONE-F-18 AS AN ADRENAL IMAGING AGENT. Larry A. Spitznagle and Carol A. Marino. Department of Nuclear Medicine, University of Connecticut Health Center, Farmington, Conn.

This laboratory has been interested in developing techniques for labeling potential radiopharmaceuticals with fluorine-18. A method has been developed to prepare 21-fluoroprogesterone labeled with F-18. The method utilizes F-18 obtained from a cyclotron with a water target

GALLIUM-68 LABELING OF PROTEINS. S.J. Wagner, L.C. Knight, G. Krejcarek* and M.J. Welch. Department of Radiology, Washington University School of Medicine, St. Louis, Mo.; *3M Co., St. Paul, Minn.

Due to the large stability constant of gallium-transferrin in order to form a protein labeled with the positron-emitting radionuclide gallium-68 it is necessary to first couple a strong chelate to the protein. In this study we used the reaction developed by Krejcarek in which DTPA is coupled to proteins by the formation of an amide. Using human serum albumin as a model the efficiency of the chelation of HSA with the mixed acid anhydride of the quaternary triethyl ammonium salt of DTPA and the butyl formate was studied by isotope dilution in order to determine the efficiency of the labeling reaction. Carrier Ga(III) was added and the variation in Ga-binding studied with an acid anhydride/protein molar ratio of 70. The labeling yield was ~5%, the final albumin-DTPA containing ~3 moles of DTPA per mole of albumin. After purification of the DTPA labeled HSA we have shown that it is possible to prepare gallium-68 labeled albumin in high yield by chelation with the DTPA labeled protein. Chelation will occur when the gallium is in the form of either the chloride or the 8-hydroxyquinoline complex. In vitro stability studies have been carried out using the long-lived gallium-67 and indium-111 to determine the exchange of the metal ion from the DTPA protein to transferrin. Using physiological concentrations of transferrin exchange of only a few percent per day has been observed. The use of this type of reagent extends the number of available positron-emitting radiopharmaceuticals.

THE RELATIVE BINDING AFFINITY OF GALLIUM-67 FOR LACTOFERRIN AND TRANSFERRIN. Paul B. Hoffer, John P. Huberty and Hassan Khayam-Bashi. University of California, San Francisco, Ca.

We have previously demonstrated that gallium-67 in human colostrum is bound to the lactoferrin-albumin protein fraction. Lactoferrin is also present in other tissues which concentrate gallium-67. The purpose of these studies was to compare the affinity of gallium-67 for lactoferrin versus transferrin.

Gallium-67 citrate was incubated with partially purified human transferrin and human lactoferrin at various hydrogen ion concentrations. The free gallium-67 was separated from the protein bound fraction by extraction with cation exchange resin. Control studies were also performed in the absence of protein.

In a second study, gallium-67 citrate was incubated with apotransferrin, the unbound fraction was extracted by cation exchange resin and the transferrin bound gallium-67 was incubated with apolactoferrin for 2 hours at 37° C at pH 6.0. The transferrin and lactoferrin fractions were then separated by immunoelectrophoresis and the relative activity in each fraction determined by counting the activity in the precipitin bands.

Gallium-67 has greater affinity for lactoferrin than for transferrin. This differential affinity is especially marked at lower pH values. Transferrin bound gallium-67 migrates to lactoferrin when the latter protein is added. During a two hour incubation with approximately equal initial protein concentrations, about 85% of the radionuclide transferred from the transferrin to the lactoferrin.

These findings suggest that gallium-67 localization in tissues and secretions containing lactoferrin can be explained by the preferential affinity of gallium-67 for lactoferrin versus transferrin.

MECHANISM OF GALLIUM LOCALIZATION IN INFLAMMATORY LESIONS. Min-Fu Tsan, William Y. Chen, Ursula Scheffel, Shameen Menon, and Henry N. Wagner, Jr. The Johns Hopkins Medical Institutions, Baltimore, Md.

The mechanism of ionic gallium-67 (Ga-67) localization in inflammatory lesions was studied. Human granulocytes (PMN) had higher Ga-67 uptake than lymphocytes, while red blood cells had no affinity for Ga-67. Ga-67 uptake by PMN showed temperature dependence, was independent of Ga-67 concentration, and was not inhibited by metabolic inhibitors.

However, its binding to PMN could be removed by trypsin but not by neuraminidase. These results are consistent with the hypothesis that plasma membrane serves as a diffusion barrier and Ga-67 only binds to the surface of the PMN plasma membrane. When this membrane permeability barrier was disrupted, as in heat-killed PMN, Ga-67 uptake increased markedly. Ga-67 also was taken up by a variety of microorganisms. *S. aureus* had the highest affinity, followed by *Sal. typhimurium*, *E. coli*, *Enterococcus*, and *L. leichmannii*. *S. epidermidis* and *C. albicans* had low affinities for Ga-67. Experimental abscesses were induced with *E. coli* or turpentine in rabbits. Twenty-four hours after intravenous injection, only 20% of Ga-67 in abscesses was in fractions containing intact PMN, cell debris or bacteria; the remainder was in a soluble, non-cellular fraction (2,500 g supernatant). This soluble fraction may represent cellular components of the necrotic pus cells. It is concluded that Ga-67 localization in the inflammatory lesions is due to its uptake by PMN as well as the offending microorganisms.

WEDNESDAY, 10:45 a.m.-12:15 p.m.

LINDHEIMER ROOM

HEMATOLOGY 1

Chairman: R. Edward Coleman

Co-Chairman: Barry A. Siegel

INDIUM-111 LABELED CELLULAR BLOOD COMPONENTS: MECHANISM OF LABELING WITH SPECIAL REFERENCE TO STUDIES WITH HUMAN NEUTROPHILS. Mathew L. Thakur, Anthony W. Segal, Louis Louis, Michael J. Welch and Timothy J. Peters, MRC Cyclotron Unit, Hammersmith Hospital, Clinical Research Centre, Harrow, England and Washington University School of Medicine, St. Louis USA.

Neutrophils were isolated from blood and labeled with In-111 oxine. The labeled cells were incubated up to 2 hours in plasma and in 0.15M NaCl. No release of radioactivity from the cells occurred during this period. However, oxine assayed spectrophotometrically was rapidly released in suspending medium. The labeled cells were homogenized with a tight fitting pestle in a 0.2M sucrose containing 0.1mM sodium citrate pH 6.8. The homogenate free of nuclei and undisrupted cells was subjected to sub-cellular fractionation by sucrose density gradient centrifugation. When the neutrophils were incubated for 10 or 60 minutes with In-111 oxine, 80% or 40% respectively of the radioactivity remained in the cytosol. Only approximately 3% of the activity in the cytosol was extractable in chloroform, 18% was dialysable and about 5% was precipitable with trichloroacetic acid. The cytosol solution was analysed at 4 degree C on 3cm x 100 cm Sephadex G-200 column using citrate buffer pH 8.6 as an eluent. The results indicated that the radioactivity was associated with cytoplasmic components of apparent mol.wt. 540,000, 80,000, 3,600. The work therefore suggests that the In-111 oxine complex crosses the cell membrane and dissociates. The oxine may leave the cells where as the In-111 firmly binds to cytoplasmic components.

INDIUM-111 LABELED AUTOLOGOUS LEUKOCYTES IN MAN. Mathew L. Thakur, J. Peter Lavender, Rosemary N. Arnot, David J. Silvester and Anthony W. Segal, MRC Cyclotron Unit, Royal Postgraduate Medical School, Hammersmith Hospital, London England.

Autologous leukocytes isolated by three different techniques have been labeled with In-111 oxine and administered to 15 patients suspected of inflammatory disease. Focal accumulation of radioactivity was detectable in 12 patients and subsequent confirmation of sepsis was obtained. From 3 such patients samples of abscesses were recovered

which showed markedly higher radioactivity than that in the same weight of blood. In the other 3 patients a normal distribution of radioactivity was observed, and subsequent prolonged clinical examination failed to sustain any evidence of sepsis.

The stability of the label has been demonstrated and the in vivo kinetics and distribution of the labeled cells studied. The distribution is influenced by the type and viability of the cells in the preparation. Generally, the distribution of leukocytes administered intravenously and measured as In-111 radioactivity showed initial accumulation in the lungs. Approximately half of this radioactivity cleared in 15 minutes and the remainder slowly in four hrs post injection. Twentyfive to 50% of the radioactivity subsequently distributed in the spleen, liver and bone marrow. The relative count rate in the spleen was higher than in the liver. The radioactivity in the liver and spleen did not show appreciable change with time up to 48 hours post injection. The In-111 radioactivity administered as labeled leukocytes free from erythrocytes cleared from the circulating blood with a half time of 7.5 hours.

NUCLEAR SCANNING WITH INDIUM-111 LABELLED CIRCULATING LYMPHOCYTES IN ANIMALS. Philip Frost, Heiner Frost, and Julian Smith. Wayne State University School of Medicine and Harper Hospital, Detroit, Mich.

It is the purpose of this study to determine if Indium-111 labelled lymphocytes recirculate normally and whether they distribute normally to lymphatic tissues. The goal is to evaluate the scanning potential of such labelled circulating cells. The initial part of these investigations determined that lymphocytes can indeed be labelled with Indium-111 and that labelling follows first order kinetics. The incubation of mouse lymphocytes with as little as 10 μ Ci of Indium-111 results in 2.5 million cpm per 10 million cells. Cells labelled with Indium-111 distribute in a manner identical to chromium labelled cells into the lymphoid organs of the mouse and rat. In addition, these cells recirculate normally in the rat as evidenced by the thoracic duct cannulation studies we have performed. Extremely high doses of Indium (in excess of 100 μ Ci per 100 million cells) is toxic to the cells. Early experiments have demonstrated that utilizing a rectilinear nuclear scanner, we can delineate the spleen, the liver, the cervical and probably the mesenteric and periaortic lymph nodes. We are presently modifying our procedures and technique in an effort to demonstrate smaller lymph node groups. We foresee the potential use of this methodology as a means of studying lymphocyte recirculation in man as well as attempting to delineate lymphatic tissue by nuclear scanning. This has potential uses in a variety of patients, including those with neoplasia or connective tissue diseases. (This work is supported in part by NIH Grant No. CA1642603 and the Harper Hospital Medical Staff Trust Fund.)

INVIVO DISTRIBUTION OF INDIUM-111 LABELED LYMPHOCYTES. COMPARISON WITH Cr-51 AND Tc-99m LABELS IN ANIMALS AND MIGRATION IN MAN. Mathew L.Thakur, Gordon H.Rannie, Williams L.Ford, John M.Goldman, Kate Murray, Rosemary Arnot, Diana Park and Peter Lavender, MRC Cyclotron Unit, Royal Postgraduate Medical School, Hammersmith Hospital, and Manchester University Medical School, England.

Rat Lymphocytes were obtained from thoracic duct by cannulation, purified, washed with 0.15M NaCl and re-suspended in culture medium or in 0.15M NaCl. The cells in culture medium were incubated for 1 hr with Cr-51 chromate, and Tc-99m pertechnetate and for 10 minutes in normal saline with In-111 oxine. Approximately 5% of the Cr-51 and Tc-99m and 85% In-111 radioactivity was associated with the cells. At 24 hrs after i.v. injection of labeled cells to syngeneic rats 30.8% of In-111 activity was found in lymph nodes compared to 26% of Cr-51 and 3.6% of Tc-99m. Cr-51 and In-111 radioactivity in the spleen decreased to 31% at 24 hrs from 56% at 2 hrs post injection. During 18 hrs after injection 30% In-111, 26% Cr-51 and 0.6% Tc-99m radioactivity recirculated from blood into lymph

collected from thoracic duct. The In-111 and Cr-51 radioactivity was much lower in all nonlymphoid tissues amounting to only 10% in the liver. Only 0.3% of the In-111 circulating in blood was found in plasma. These results signify the viability and the physiological redistribution of the In-111 labeled lymphocytes. In a small group of patients with Hodgkins disease autologous lymphocytes separated from blood and labeled with In-111 were administered intravenously. Whole body scans showed radioactivity in the spleen, liver and bone marrow together with the recirculated radioactivity in lymph nodes.

EVALUATION OF THE IN VIVO PROCESS FOR PREPARING Tc-99m RED BLOOD CELLS. John F. Harwig and Adel G. Mattar. Washington University School of Medicine, St. Louis, MO.

Preliminary reports of in vivo labeling of red blood cells (RBC) with Tc-99m appear promising but have left several mechanistic questions unanswered. To further elucidate the in vivo labeling process we have studied quantity of Sn(II), time interval between administration of Sn(II) and pertechnetate, labeling efficiency, clearance rate from blood, optimum early and delayed scan times, and chemical form of non-RBC bound activity. Quantities of Sn (II) from 0.5 μ g/kg to 50 μ g/kg body weight were generated electrolytically and injected intravenously into 1-3 kg rabbits 5-30 min preceding injection of 1-5mCi pertechnetate. Serial blood samples were drawn 5 min - 24 hr after pertechnetate administration to determine % whole blood activity bound to RBC (labeling efficiency) and % injected dose (ID) remaining RBC bound (clearance). Plasma samples were analyzed by gel chromatography to determine nature of non-RBC bound activity. When $>2 \mu$ g Sn(II)/kg is injected 20 min prior to pertechnetate, the labeling efficiency reaches 95% 15 min later, by which time 90% ID is RBC bound. Non-RBC bound activity is largely in a reduced chelated form. The labeling efficiency remains $>95\%$ for at least 24 hr, which corresponds to the half-clearance time. Below 2 μ g Sn(II)/kg labeling efficiency ranges from 30% - 80% at 15 min with only 25% - 70% ID being RBC bound, the remainder largely in the form of free pertechnetate. The labeling efficiency slowly climbs to $>95\%$ as the pertechnetate clears.

These results indicate that in vivo RBC labeling is a function of well-defined conditions which can readily be manipulated to provide excellent properties for routine use.

WEDNESDAY, 2:00 p.m.-3:30 p.m.

CHICAGO ROOM

GASTROINTESTINAL 1

Chairman: Robert C. Stadalnik

Co-Chairman: Robert S. Hattner

THE RELATIVE IMPORTANCE OF BLOOD FLOW AND LIVER PHAGOCYTTIC FUNCTION IN THE DISTRIBUTION OF TECHNETIUM-99M SULFUR COLLOID. John W.B. Bradfield and Henry N. Wagner, Jr. The Johns Hopkins Medical Institutions, Baltimore, Md.

Imaging of the liver and spleen by Tc-99m sulfur colloid (T-SC) depends both on blood flow and on the ability of phagocytic cells to take up the colloid. This study was done in mice to find out whether abnormal organ distribution of T-SC could be caused by severe depression of Kupffer cell function. Kupffer cell blockade was produced using i.v. dextran sulfate. Blockade was measured by quantitating the distribution of i.v. Cr-51 labeled sheep red blood cells (Cr-SRBC). In control mice 90% of the test Cr-SRBC were recovered from liver and less than 5% from spleen. In blocked mice liver uptake was reduced to 10% whereas splenic uptake was increased to 40% of the injected dose and the activity in the bone marrow was increased 37-fold. In contrast the distribution of T-SC in blocked mice was only slightly disturbed by the most severe block-

ade. When T-SC was injected i.v. in a dose equivalent to 1000 times that used in humans, there was no evidence of Kupffer cell saturation when tested with Cr-SRBC or T-SC.

Three conclusions are drawn: 1) We find no evidence that abnormalities in the distribution of T-SC to liver and spleen are caused by depressed function of hepatic phagocytes. 2) T-SC is not a suitable agent for measuring Kupffer cell function. 3) Kupffer cell blockade cannot be used to increase the localization of this scanning agent in other organs such as spleen or bone marrow.

BIOLOGICAL DISTRIBUTION OF VARIOUS SIZE COLLOIDAL PARTICLES IN DISEASED STATES. John J. Coupal, Frank H. DeLand, and Eulshin E. Kim. Veterans Administration Hospital and University Medical Center, Lexington, Ky.

The purpose of this study was: (1) to measure the variation in colloidal particle size in preparations of stannous chloride (SC1) and sulfur colloid (SC) (labeled with Tc-99m) (2) to evaluate the effect of particle size on biological distribution in normals and diseased states. Particle size was measured in 29 preparations of S-C and six of SC1 by polycarbonate membrane filters of various pore sizes. Mean particle size of the S-C was $0.42\mu\text{m} \pm 0.1$; of the SC1 90% was greater than $0.8\mu\text{m}$. In sixty patients the biological distribution was judged from radionuclide images by: (1) relative concentration in liver and spleen, (2) concentration in bone and lung, and (3) level of body background activity. Normal images were observed in nine patients although the S-C preparations varied in particle size ($0.2-0.8\mu\text{m}$) and the stannous chloride preparations were all greater than $0.8\mu\text{m}$. In those patients (19) with bone marrow activity, if spleen activity/unit volume exceeded that of the liver, liver disease was always present, but if they were equal, liver disease was not present. In nine patients with prominent bone marrow activity there was no increased splenic activity. Lung activity was found in 13 patients, six with liver disease. Of nine patients with lung activity greater than bone marrow activity, only three had liver disease. Of 12 patients receiving SC1, five showed lung activity; only one had liver disease. We conclude that within the particle size range of RES imaging commercial preparations that no size relationships could be established relative to lung, bone marrow, and splenic activity, except for increased lung activity with SC1.

THE ROLE OF GA-67 CITRATE IMAGING AND DIAGNOSTIC ULTRASOUND IN PATIENTS WITH SUSPECTED ABDOMINAL ABSCESSSES. Bharath Kumar, Philip O. Alderson, G. Geisse Mallinckrodt Institute of Radiology, St. Louis, Mo.

A prospective comparison of Ga-67 Citrate imaging and abdominal sonography was performed in 50 patients with suspected abdominal abscesses. Each patient had both a dual probe rectilinear Ga-67 scan (48 and 72 hour views) and an Ultrasound study (Bistable N=22, Grey Scale N=28) within a 48 hour period. Both studies were negative in 19 patients and subsequent follow-up demonstrated no evidence of a focal inflammatory process. 15 patients were proven to have an intra-abdominal abscess. Ga-67 images were positive in 13 (87%) of these patients while the sonograms identified the abscess in 11 (73%). In one patient, false positive results were obtained by both procedures. The remaining 15 patients had positive Ga-67 images and negative sonography. These Ga-67 studies demonstrated abnormalities other than abscesses. 6 patients had renal disease, (3 pyelonephritis, 1 vasculitis, 1 renal vein thrombosis, 1 ATN) and 9 patients had other types of inflammatory disease (3 subacute bacterial endocarditis, 2 lower extremity cellulitis, 3 injection abscesses, 1 Crohn's disease). In 12 of these patients these sites of inflammation proved to be the source of fever. There are no statistically significant differences in the sensitivity or specificity of Ga-67 imaging and sonography for detecting abdominal abscesses. An advantage of Ga-67 imaging is its ability to detect non-abscess sites of inflammation within and outside the abdomen.

THE USE OF ULTRASOUND TO ENHANCE THE DIAGNOSTIC UTILITY OF THE EQUIVOCAL LIVER SCINTIGRAPH. Daniel C. Sullivan, Kenneth J. W. Taylor, and Alexander Gottschalk. Yale University, New Haven, Connecticut.

Using state-of-the-art 37 tube cameras, we have undertaken a prospective study on 75 patients with equivocal hepatic scintigraphs adding grey-scale echography to see if diagnostic accuracy could be improved using the combined modalities. The ultrasound study was usually performed immediately, and in all cases no later than 2 days after the hepatic scintigraph. The nuclear studies were categorized on the basis of the initial reading as: 1). "equivocal, probably normal", 2). "equivocal, equivocal", or 3). "equivocal, probably abnormal". The echographic findings were summarized as: 1). "normal", 2). "equivocal", or 3). "abnormal" with respect to the specific question raised by the nuclear image. In the 75 patients studied, 84 equivocal radionuclide findings were identified as follows: non-homogeneity (35); enlarged porta hepatis (19); edge defect (19); left lobe abnormality (5); enlarged renal fossa (4); or enlarged hepatic vein confluence (2). Satisfactory proof is available in 45 instances.

Based upon these 45 proven findings, the following conclusions can be drawn: 1). When the liver scintigraph is equivocal in any way and the ultrasound is normal - the liver is normal with high reliability [25/28 or 89% in this series]. 2). When the liver scintigraph is "equivocal - probably abnormal" and the ultrasound in abnormal - the liver is abnormal, [12/12 - 100% in this series]. 3). All other combinations have limited reliability. Five of six patients in this study fell into category 1). or 2). above, and the increased accuracy of the equivocal liver scintigraph with ultrasound is statistically significant ($p < .01$) compared to the radionuclide study alone.

THE SOURCE OF FECAL GALLIUM-67 IN RATS. Andrew Taylor, Steve Mullen, Neil Chafetz, Wallace Hooser. Veterans Administration Hospital, San Diego, Ca.

Bowel preparation prior to gallium-67 scanning often consist of cathartics, a liquid diet, enemas or some combination of the above. A liquid diet apparently presupposes Ga-67 excretion by the liver into the bile; presumably, the liquid diet would minimize the emptying of the gallbladder. This investigation was undertaken to determine the contribution made by the liver to Ga-67 excretion via the gut.

The bile duct was ligated and severed in 30-Sprague-Dawley rats and sham operations were performed in an additional 30 rats. All 60 rats received a tail vein injection of 20-30 microcuries of Ga-67 citrate and were housed in metabolic cages where three successive 24 hour collections of urine and feces were obtained. Ten rats respectively from the control and experimental animals were sacrificed at 24, 48, and 72 hours for tissue distribution studies.

At all time periods, the tissue distribution of Ga-67 in the experimental animals was similar to that in the controls. The 72 hour fecal excretion of Ga-67 in the control animals was 13.3% compared to 11.3% in rats with the severed bile ducts. Clearly, the contribution by the liver to fecal excretion of gallium was minimal. Based on these studies, it would probably be unnecessary to deprive a patient of solid food since the liver contribution to gut excretion was minimal and a liquid diet would be unlikely to facilitate gallium transit through the bowel.

WEDNESDAY, 2:00 p.m.-3:30 p.m.

LINDHEIMER ROOM

BONE/JOINT 2

Chairman: James M. Woolfenden

Co-Chairman: Dennis D. Patton

GALLIUM SCANNING IN PAGET'S DISEASE OF BONE: A SUPERIOR PARAMETER IN FOLLOWING THE RESPONSE TO CALCITONIN THERAPY. A. D. Waxman, J. K. Siemsen**, and F. Singer. LAC/USC

Medical Center, Los Angeles, Calif.

Conventional bone scans have been used along with biochemical parameters and x-rays in the evaluation of patients with Paget's disease of bone. We have compared the above parameters with Gallium scans of the skeletal system before and after calcitonin therapy in patients with known Paget's disease.

Eleven patients with Paget's disease had serial bone scans with Tc-99m diphosphonate (TcDP) before and after calcitonin therapy, while 8 patients had Gallium skeletal surveys. All patients had serial serum alkaline phosphatase and 24 hour urinary hydroxyproline determination.

The pretreatment Gallium scans all showed skeletal abnormalities similar to the TcDP bone scans. The TcDP bone scan was a poor indicator of calcitonin induced improvement in moderate to severe disease when compared with the serum alkaline phosphatase and urinary hydroxyproline determinations. Gallium scans done within a week of the bone scans, however, showed dramatic improvement in all cases, and appeared to parallel the changes demonstrated biochemically.

We conclude that calcitonin has a profound effect on Gallium uptake by pagetic bone. The results suggest that Gallium scanning is a much more sensitive parameter in following patient response to calcitonin than the conventional bone scan.

FRACTURE HEALING: EVALUATION UTILIZING RADIONUCLIDE BONE IMAGING. Lewis Gumerman, Stewart Fogel, Mark Goodman, Edward Hanley, George Kappakas, Geoffrey Levine, Akio Kikuike. University of Pittsburgh, Pgh., Pa.

Radionuclide bone imaging was performed in a rabbit model to observe the course of fracture healing and establish criteria for distinguishing delayed and non-union from normal healing.

Tc-99m Methylene Diphosphonate gamma camera (pinhole collimator) images were collected and subjected to computer data analysis. Sequential imaging continued until healing or non-union was established clinically and radiographically. Four groups were established: 1) Control - immobilization; 2) Normal Fracture - osteotomy; 3) Delayed Union - osteotomy plus periosteal stripping; 4) Non-Union - osteotomy, periosteal stripping and polymethyl methacrylate interposed between fracture fragments.

Histogrammic representation of absolute count rates along the rabbit tibia one week after osteotomy had the configuration of two peaks with a central valley at the fracture line. At two weeks a broad single or biphasic peak was present. No healing was demonstrable by radiograph. At three weeks the peak had narrowed and callus was detectable. By four weeks the peak was narrower, callus was detectable and the fractures were clinically stable. In the Delayed Union group the sequence was similar but delayed up to three months. The Non-Union group demonstrated no recognizable pattern of healing.

Sequential bone scanning with quantitative data analysis has potential for indicating the course of healing in fractures. Absence of a peak at each fracture end may be an early predictor of non-union.

VALUE OF TECHNETIUM-99m PYROPHOSPHATE BONE IMAGING IN EQUINE ORTHOPEDICS. Gottlieb Ueltschi. Klinik für Nutztiere und Pferde, Berne Switzerland.

This study was undertaken to evaluate the usefulness of bone imaging techniques in early navicular disease, tarsal degeneration and spinal disorders. The equine skeleton can be demonstrated using a scintillation camera, 2-4 hours after i.v. administration of 100 mCi Tc-99m-PP. All diseased navicular bones (102) showed increased uptake of the bone label, whereas the sound ones (98) showed little or no uptake. 9 horses with increased uptake and no lameness showed lesions of navicular disease at autopsy. 26 horses showing increased uptake and no lameness are being examined regularly to determine, if the scintigraphic findings are an early sign of navicular deterioration. Of 344 tarsal joints examined 149 showed increased tracer uptake and radiological changes, 188

normal uptake and no other changes, 74 an increase in uptake but no radiological alterations and 19 normal uptake with marked radiological changes. The 14 horses with increased tracer uptake but no other alterations are under observation to see, if the scintigraphic findings are an early sign of osteoarthritis. In 20 horses the vertebral column was studied. In 3 horses with back pain increased accumulation of the tracer was observed on one side of the iliosacral junction. In 5 other horses with back problems abnormal uptake in the thoracolumbar spine could be demonstrated. Bone imaging is an extremely helpful method for the evaluation of radiological changes and there is some evidence that this technique could be used for the early detection of navicular disease and joint affections.

WEDNESDAY, 2:00 p.m.-3:30 p.m.

JANE ADDAMS ROOM

IN VITRO AND RADIOASSAY 2

*Chairman: Danielle J. Battaglia
Co-Chairman: Kent Painter*

AUTOMATIC PAPER-STRIP RADIOASSAY. I. DETERMINATION OF THYROXINE BY A ONE-STEP PROCEDURE. Marshall E. Deutsch and Louis W. Mead. Thyroid Diagnostics, Inc., Bedford, MA.

Our objective was to demonstrate if it is possible to carry out radioassay by allowing a developing solution to traverse a strip of paper on which a sample has been deposited, thus bringing the sample into successive contact with a series of reagents previously impregnated on the paper. Advantages are greater stability of reagents (they are kept dry until the moment of reaction), simplicity of operation (the complex whose radioactivity is to be measured is brought to a spot where the measurement can be made without manipulation of the paper; i.e., decantation and centrifuging are obviated), obviation of timing (the reaction automatically stops when the strip has been completely traversed) and removal of various interferences because of differing Rf's.

By use of a developing solution containing thimerosal and salicylate to inhibit unwanted binding, we have been able to construct such a paper for radioassay of thyroxine. The paper is 19 cm long by 6 mm wide, with a bend at 10 cm, and it is supported on a plastic strip. Antibody is immobilized by adsorption on polystyrene latex at the bend and, 2 cm below this a solution of I-125 labelled thyroxine is dried on the paper. Twenty µl of serum is applied below this and the test is started by dipping the strip in developing solution. Indicator at the end of the strip shows when the test is completed.

After an hour, the strips are inverted and counted in a shield which permits counting of the end 1.6 cm only. The test has a sensitivity of about 0.5 µg% and a coefficient of variation of about 3%.

Conclusion: feasibility of the method has been shown.

THYROXIN RADIOASSAYS UTILIZING ALBUMIN MAGNETIC MICROPARTICLES. Dionyssis S. Ithakissios and David O. Kubiatowicz. Medical Products Division, 3M Co., 3M Ctr., St. Paul, MN., 55101.

Advantages of utilizing magnetic microparticles in radioassays have been described [Clin. Chem. 22, 1165 (1976)]. We extended this approach by preparing a variety of magnetic microparticles which were useful both in non-immune (NIR) and immune (RIA) T₄ assays. The microparticles were composed of a water insoluble protein matrix containing barium ferrite. The protein matrix was made insoluble through chemical crosslinking with glutaraldehyde. Two different compositions of particles were made according to their utilization in radioassays: a) the protein matrix consisted of BSA containing T₄ antibody or TBG b) the matrix was made of albumin only or included a second sub-

stance such as charcoal, silicates or anion exchange resin. The first type of particle used was in solid phase RIA and NIR. The second type was used in assays requiring separation of free from bound T_4 . The utilization of these particles in radioassays was found to provide fast and precise results (less than 60 min to perform: CV less than 4%) with minimum manipulations.

This method had potential application to other assays as was demonstrated by using albumin magnetic microparticles in T_3 Uptake and vitamin B-12 radioassays.

SOLID PHASE RADIOASSAY FOR "THYROTROPIN-DISPLACING IMMUNOGLOBULINS." Michael Okerlund, Judy Duh, and Francis S. Greenspan. University of California Medical Center, San Francisco, California.

Human thyroid plasma membranes were attached to polyvinyl cups and displacement of human thyrotropin(TSH)-125I by serum gamma globulin extracts studied by a new solid phase method. A summary of the data:

Group	Number	Range	Mean±S.D.	%Pos.
Normal pool	--	---	100±5	---
Graves, never treated	40	35-91	68±9	80.0
Graves, treated	30	41-105	71±7	75.0
Graves on thionamide	18	55-101	76±8	88.9
Other thyroid disease	45	65-124	103±11	17.8

Positive test=90% binding level of normal globulin pool. 90% of patients with untreated Graves' disease had positive tests, with levels not correlated with goiter size, thyroid antibodies or severity. Euthyroid ophthalmopathy patients had positive tests, as did 90% of cases on antithyroid therapy for Graves' disease and most up to 1 year after treatment with radioiodide or surgery. 20% of patients with Hashimoto's thyroiditis were positive and several with nodules or cysts. "Thyrotropin-displacing-immunoglobulins" are a relatively specific test for Graves' disease and our finding of similar TSH binding to both normal and hyperthyroid membranes suggests a primary importance of this immunologic factor in thyroid activation. The higher proportion of unexplained positive tests in patients with thyroid diseases such as adenomas and cysts than in normal people may indicate either an immunologic factor in some of these disorders or that such immunoglobulins are a genetic marker requiring other unknown factors for actual thyroid activation.

INTERNAL SAMPLE ATTENUATOR. A NEW METHOD FOR COUNTING OF BOUND AND FREE ACTIVITY IN RADIOIMMUNOASSAY WITHOUT PHYSICAL SEPARATION OF PHASES. Jan I. Thorell, Dept of Nuclear Medicine, University of Lund at Malmö General Hospital, Malmö, Sweden.

Radioimmunoassay and related procedures are based on measurement of the distribution of the radioactivity between antibody bound and free fractions. To permit counting of either (or both) of them, one fraction is usually turned into a non-soluble form, e.g. by precipitation or adsorption. Then, the two phases are physically separated, usually by removal of the soluble phase. This step is one of the single major sources of error in the assay, in some assays quite time-consuming and not suitable for automation.

The dominating radionuclide in radioimmunoassays is ^{125}I . Its low energy gamma-radiation (27-35 keV) is effectively attenuated by elements with moderately high Z-numbers. If such an attenuator in powder form is added to the incubation tube, and is mixed with the solid phase the radiation is attenuated and the sample would only emit radiation from the soluble phase, despite the presence of both phases within the tube.

Theoretical considerations and practical testing showed that Cadmium and Tungsten were effective attenuators. The system was tested in a double antibody insulin assay, a hPL ethanol precipitation assay and a solid phase-antibody insulin assay. Tungsten powder was added to the tubes before and/or after centrifugation of the samples after which the

samples were counted without further separation of phases. The results showed standard curves with identical sensitivity and improved precision in comparison with assays involving a conventional separation step with counting of individual phases.

DOUBLE-ANTIBODY RADIOIMMUNOASSAY FOR HUMAN PRE-ALBUMIN. Hsieh Fu Cheng, Sue Keller, and Richard E. Peterson, Nuclear Medicine, University of Iowa Hospitals and Clinics, Iowa City, Iowa.

Pre-albumin (TBPA), one of the serum proteins which bind thyroid hormones, should be included in studies of protein-binding problems affecting thyroid function. Since two-thirds of the flux in free thyroxine is due to release and binding of the hormone by TBPA, measurement of acute and chronic changes in serum TBPA can be of value in selected thyroid function studies. For this reason, we sought to develop a fast and sensitive TBPA assay.

The double-antibody radioimmunoassay (RIA) for TBPA is based on a competitive reaction between I-125-TBPA and TBPA (standards or serum) for the binding site of an immunobinding reagent (IBR). The precipitable IBR is prepared from the interaction between rabbit antiserum against TBPA and goat anti-rabbit gamma globulin. A RIA kit for human TBPA has been developed, consisting of purified human TBPA, I-125-TBPA, and the IBR. I-125-TBPA is allowed to react with IBR at 4°C for 24 hours. The precipitate is conveniently separated by membrane filtration, washed, and measured for radioactivity, which represents the antibody-bound form of the TBPA. An acceptable standard log-log curve relating antibody-bound I-125-TBPA to added standards of TBPA can be readily obtained. Unknown TBPA values in samples being assayed can be read off the standard curve.

Our normal serum pre-albumin range approximates 350 µg/ml (35 mgm/dl)(5.0 µmole/L) in agreement with earlier results using electrophoretic techniques. This double-antibody, pre-precipitate RIA procedure is readily applicable to CSF, milk, etc. Assay results from patients with a variety of thyroid disorders will be presented.

RADIOMETRIC MICROBIOLOGICAL ASSAY OF FOLATE AND NIACIN. Judith A. Kertcher, Marianne F. Chen, Patricia A. McIntyre and Henry N. Wagner, Jr. The Johns Hopkins Medical Institutions, Baltimore, Md.

There is a need for sensitive, specific and reliable assays for folates and niacin. A radiometric method, originally developed for assaying vitamin B12 in serum, has been extended to measure levels of these vitamins present in biological fluids. Lactobacillus casei was used for the assay of folic acid. In the presence of C-14-gluconic acid, the production of C-14 CO₂ by this bacterium was proportional to the amount of 5 methyl tetrahydrofolic acid present. Preliminary studies of ten normal sera assayed by this method showed a mean of 6.48 ± 1.86 ng/ml, with a range of 4.5 to 10.8 ng/ml. The normal range for serum folate is 5 to 21 ng/ml.

Niacin was assayed using Lactobacillus plantarum with U-C-14 malic acid. C-14-CO₂ production was found to be proportional to the amount of niacin present. In early studies, it was not necessary to separate precipitated serum proteins or debris from whole blood hemolysate, resulting in the elimination of several steps necessary for the conventional microbiological assay. Further simplification is possible if lyophilized bacteria are substituted in the assay. Use of lyophilized bacteria obviates the need for routine subculture of the organisms. Values obtained from comparison of standard and lyophilized cultures showed excellent agreement for the 20 sera tested to date.

These semi-automated radiometric microbiological assays may be applicable not only to measuring vitamin B12, folates and niacin levels in biological fluids, but also to determining their levels in foodstuffs.

THURSDAY, JUNE 23, 1977

THURSDAY, 10:45 a.m.-12:15 p.m.

JANE ADDAMS ROOM

**RADIOPHARMACEUTICAL 4:
TECHNETIUM RADIOPHARMACEUTICALS**

Chairman: Gerald D. Robinson

Co-Chairman: David R. Allen

THE INFLUENCE OF STRUCTURAL CHANGES ON BIODISTRIBUTION OF Tc-99m LABELED N-SUBSTITUTED IDA DERIVATIVES. Gopal Subramanian, John G. McAfee, Robert W. Henderson, Marilyn Rosenstreich and Linda Krokenberger. Upstate Medical Center, Syracuse, New York.

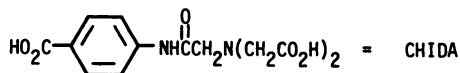
A variety of N-substituted IDA derivatives were synthesized and labeled with Tc-99m using stannous chloride. Substitution groups for the iminohydrogen included: I. acetamide; 2, hydroxyethyl; p-hydroxy acetophenone & methyl. II. Substituted acetanilides: 2,6 Dimethyl; 2,6 Diethyl; 2,6 Diisopropyl; 2,4,6 Trimethyl; p-ethyl; p-isopropyl; p-butyl; p-ethoxy; p-butoxy & o-butoxy. III. Acetobenzylamine.

Imaging and biodistribution studies were performed with these compds. in rabbits. Group I compds. were excreted predominantly through kidneys with minimal localization in the liver. The converse was true for Group II compds. and the Group III compd. was excreted equally by both organs.

As the lipophilicity of the substituent group increased, the biliary excretion also increased and the urinary excretion decreased. Group II compds. which had a fast transit time in the liver also showed a high urinary excretion. As the substituent group was changed in the 2,6 positions from methyl to isopropyl, the 15 minute urinary excretion decreased (5.2% to 1.6%) the concentration in the liver increased (9.8% to 44.5%), and the excretion to the bile decreased (69.7% to 35.4%). Similar differences in distribution were seen for substituents at the para position. The p-butyl derivative had the least urinary excretion (<1% at 1 hr), the highest retention in the liver (10% at 1 hr) and a relatively slow rate of biliary excretion. Thus, the relative concentrations and rates of clearance by the liver and kidney can be markedly altered by selecting different substituents for coupling IDA.

RELATIONSHIP BETWEEN MOLECULAR STRUCTURE AND BILIARY EXCRETION OF TECHNETIUM-99m HIDA AND HIDA ANALOGS. Donald Burns, Luigi Marzilli, David Sowa, David Baum and Henry N. Wagner Jr. Division of Nuclear Medicine and Department of Chemistry, Johns Hopkins University, Baltimore, Md.

In order to gain information on the relationship between molecular structure of technetium radiopharmaceuticals and their biodistributions, a detailed investigation of Tc-99m-HIDA was undertaken. A new synthesis of HIDA was developed which involves reaction of 2,6-xylidene with nitrilotriacetic acid in the presence of acetic anhydride to give a 70% yield of HIDA in 4 hours. Several analogs of HIDA were prepared by this reaction including:



Mixed liquid experiments with HIDA and CHIDA demonstrated that these compounds form bis-complexes with technetium, i.e., two molecules of ligand are bound per technetium. Identical complexes (as evidenced by electrophoresis, chromatography and biodistribution) were obtained when sodium borohydride or stannous chloride were used as reducing agents, indicating that tin is not incorporated into the complexes. The charges on the complexes were determined using ion exchange and electrophoresis. The biodistributions of five of the complexes, including one mixed ligand complex Tc(HIDA)(CHIDA), in mice revealed a linear

relationship ($r = 0.994$) between biliary excretion and $\ln|MW/Z|$ where:
MW = the molecular weight of the technetium complex
Z = the net charge on the technetium complex

TECHNETIUM-99m:3-HYDROXY 4-FORMYL PYRIDINE:GLUTAMIC ACID COMPLEX. A NEW RAPID CHOLESCINTIGRAPHIC AGENT. Akira Kohno Tatsuo Maeda, Hiroyuki Shiokawa, Yoshiharu Karube and Yoshikazu Matsushima. Kurume University, Kyushu Cancer Center and Kyushu University, Fukuoka, Japan.

A new radiopharmaceutical, Tc-99m:3-hydroxy 4-formyl pyridine(HFP):glutamic acid(G) complex(Tc-99m-HFPG) underwent more rapid biliary excretion in animals and gave more clear scintigrams than Tc-99m-pyridoxylidene-glutamate. In normal rabbit, the gall bladder was clearly visualized scintigraphically 10 min after iv injection. The radioactivity in the intestine kept increasing and 1 hr after injection most of the injected radioactivity was present at the intestinal region. The renal excretion was a minor path. Thyroid was not visualized scintigraphically. When the bile was collected from the common bile duct by cannulation, about 85% of the radioactivity injected was present in the bile and no radioactivity in the duodenum and the intestine within 1 hr. The complex was prepared by heating an aqueous solution (pH 6.5-7.5) of HFP, G, and pertechnetate-99m for 10-15 min at 90-100°. The simple method may be applicable for a kit preparation. The toxicity test is going in these laboratories. No serious objection for clinical use has been found so far.

PREFERENTIAL LOCALIZATION OF LIPOSOMES [Tc-99m DTPA] IN THE LIVER. George H. Hinkle, Gordon S. Born, Wayne V. Kessler, and Stanley M. Shaw. Purdue University, School of Pharmacy and Pharmacal Sciences, West Lafayette, IN.

Liposome formulations composed of different lipids were studied in order to achieve an efficient entrapment procedure for the production of liposomes [Tc-99m DTPA]. The entrapment efficiency was studied using gel filtration column chromatography. An evaluation of the particle size range of the prepared liposomes was conducted using electron microscopy. Entrapment techniques and separation procedures led to a liposome [Tc-99m DTPA] preparation with particles in the colloidal size range. Dramatic differences in the organ distribution of the liposome [Tc-99m DTPA] preparation in mice were produced when different particle size ranges of liposomes were injected. Liposomes [Tc-99m DTPA] eluted in the first fraction after the void volume led to a maximum uptake by the liver of greater than 90% of the injected dose ten minutes after intravenous injection. The colloidal size range liposomes of the first fraction provided a greater degree of localization in the liver than the liposomes of the pooled fractions. For pooled fractions, blood levels remained elevated indicating the presence of very small diameter liposomes [Tc-99m DTPA].

With appropriate techniques, a liposome [Tc-99m DTPA] preparation was obtained which cleared rapidly from the blood, produced low background tissue levels, and a high degree of liver localization. Tc-99m DTPA liver clearance values indicated that the liposome [Tc-99m DTPA] preparation may be useful as an agent for determination of liver function.

ARE TWO PHOSPHATE GROUPS NECESSARY FOR BONE LOCALIZATION OF Tc-99m COMPLEXES? Hank Kung, Robert Ackerhalt and Monte Blau. State University of New York at Buffalo, Buffalo, New York.

All of the Tc-99m bone scanning agents in current use are complexes containing at least two phosphate groups.

It is not clear whether this is a requirement for localization or just a reflection of the fact that the first Tc-99m bone scanning agents were polyphosphates.

We have prepared a new bone scanning agent, phosphonoacetic acid (PAA) containing only a single phosphate group. This compound was chosen because it represents the simplest monophosphate which would be expected to complex Tc. PAA is a new antiviral agent which specifically inhibits virus-induced DNA polymerase by interacting with it at the pyrophosphate binding site.

Labeling was carried out in the usual manner with Sn(II) reduced Tc-99m pertechnetate. Yields were high and paper chromatography showed less than 1% free Tc-99m pertechnetate. Organ distribution studies were done in rabbits and rats. At two hours the femur uptake was 1.2% in rabbits and 0.93% in rats. This corresponds to a total bone uptake of about 30% and 23% respectively. The corresponding data for Tc-99m pyrophosphate are 0.80% and 0.98% in femur and 20% and 25% in total bone.

We conclude therefore that monophosphates do localize in bone. This new class of Tc complexes may have some advantages over di- and polyphosphates for myocardial infarct localization.

DISSOCIATION CONSTANTS OF Tc-99m CHELATES WITH SERUM PROTEIN. Mrinal K. Dewarjee and Paul M. Brueggemann. Mayo Clinic and Mayo Foundation, Rochester, MN.

After showing the relationship of protein binding and the localization of Tc-99m chelates into infarcted myocardium, we realized the importance of the nature of interaction between serum protein and Tc-99m chelates in biodistribution and imaging with Tc-labeled compounds and determined the dissociation constants of Tc-chelates and human serum albumin by the modified Hummel-Dreyer technique and equilibrium dialysis.

The Sephadex G-50 column was equilibrated with dilute solutions of different Tc-99m chelates, e.g. Tc-diphosphonates (HEDP and MDP), Tc-glucoheptonate, Tc-DMSA and Tc-DTPA. Variable amount of human serum albumin (25, 50, 125 and 250 mg) was added to the column and washed with the same solution of Tc-chelate. The extent of extraction, i.e. the amount of radioactivity in the crest is a measure of the strength of interaction between human serum albumin. From the known amount of human serum albumin added and the amount of Tc-chelates in the crest, the dissociation constants have been determined. The dissociation constants of Tc-MDP, Tc-P2O7, Tc-DMSA, Tc-glucoheptonate and Tc-DTPA are 2.2×10^{17} , 2.7×10^{16} , 8.4×10^{16} , 1.1×10^{16} , and 1.4×10^{17} respectively. These results are in conformity with the blood clearance of Tc-MDP, Tc-HEDP and Tc-P2O7. These results will be useful in the kinetics of distribution and compartmental analysis of Tc-labeled compounds in biological system.

POLAROGRAPHY OF Tc(IV) AND Re(IV) COMPLEXES. George H. Carey, Alun G. Jones, Alan Davison, Harvey S. Trop, Bruno V. DePamphilis and Michael A. Davis, Department of Radiology, Harvard Medical School, Boston, MA and Dept. of Chemistry, Massachusetts Institute of Technology, Cambridge, MA.

The chemical form of technetium in radiopharmaceuticals is the subject of some debate. Because reduction from the heptavalent state appears to be the first step in the formation of many of the compounds in use in nuclear medicine, a clearer understanding of the accessibility of oxidation states +3, +4, +5 and +6 in aqueous solution as a function of ligand donor sets is required. This understanding is hampered by the lack of a large body of systematic chemistry for both this element and its congener rhenium, and by the ease of hydrolysis in aqueous solution of simple technetium complexes in the most stable of the reduced states, (+4), to technetium dioxide dihydrate. Polarographic studies of well characterized technetium (+4) complexes and their rhenium analogs have been carried out in acetonitrile. These studies have provided information on the inherent ease of oxidation and reduction of these species as a function of ligand donor sets in the absence of complications due to hydrolysis. Using a rotating platinum electrode, halide and pseudo-halide (+4) complexes as the tetraalkyl

ammonium salts undergo reversible one electron oxidations to the +5 state. These oxidations, with the exception of SCN^- , are very difficult for both Tc and Re. The rhenium complexes are easier to oxidize than those of technetium, e.g. $E_{1/2}^0(Re, X = Cl^-) = 1.18$ volts vs. SCE, but $E_{1/2}^0(Tc, X = Cl^-) = 1.94$ volts vs. SCE. In addition, one electron reduction reactions to the +3 states have been studied using a dropping mercury electrode. It is concluded that the one electron oxidation and reduction of hexacoordinate Tc(IV) complexes containing halide ligands is extremely difficult.

THURSDAY, 10:45-12:15 p.m.

LINDHEIMER ROOM

PULMONARY 2

Chairman: Roger H. Secker-Walker
Co-Chairman: Norman D. Poe

PULMONARY VENTILATION, PERFUSION AND RADIOAEROSOL DEPOSITION IN DOGS FOLLOWING HEMITHORAX IRRADIATION WITH CO-60 OR FAST NEUTRONS. P.C. Alderson, E.W. Bradley, M.E. Bradley, K.G. Mendenhall and B.A. Siegel. Armed Forces Radiobiology Research Institute, Naval Medical Research Institute, Bethesda, MD and George Washington University, Washington, DC.

To assess the effects of therapeutic doses of radiation on regional pulmonary function, 31 dogs had serial chest radiographs and quantitative Xe-133 ventilation, Tc-99m perfusion and Tc-99m phytate aerosol studies following hemithorax irradiation with Co-60 photons or fast neutrons. Each dog also had serial spirometry and compliance measurements. All doses of radiation were delivered in a 24-treatment course, 4 doses per week for 6 weeks. Integral photon doses of 3000, 4500, or 6750 rads were delivered; neutron doses were 1000, 1500, or 2250 rads. All studies were repeated 3, 6, 9 and 12 months after irradiation and compared to baseline studies obtained prior to irradiation. Dogs in the high-dose photon and neutron groups and the medium-dose neutron group showed spirometric evidence of decreased lung volume and had decreased compliance. These dogs showed marked reductions of perfusion and aerosol deposition in the irradiated lung. The single-breath Xe-133 distribution and radioaerosol deposition pattern agreed more closely with the perfusion pattern than did Xe-133 equilibrium or clearance studies. Although several dogs had focal areas of mild Xe-133 retention, overall clearance rates of Xe-133 were increased. The results provide information about alterations of regional lung function in (primarily) restrictive pulmonary disease, and demonstrate that neutrons are 4-5 times as damaging to normal lung as photons.

Kr-81m VERSUS Xe-133 FOR VENTILATION IMAGING IN SUSPECTED PULMONARY EMBOLISM. Paul M. Weber and L.V. dos Remedios, Kaiser-Permanente Medical Center, Oakland; Robert Schor and David Shames, University of California, San Francisco, CA.

For suspected pulmonary embolism (PE) we used Tc-99m microspheres to evaluate perfusion (Q), and compared Kr-81m with Xe-133 for ventilation (V) imaging. First in a single position (usually posterior sitting), Xe V equilibrium (generally rebreathing 1-4 min) and washout images were taken. Then microspheres were injected with patient supine, and Kr-81m eluted by O₂ from Rb-81 generator was delivered as needed by mask. Corresponding pairs of Q and Kr V images were taken in all positions including obliques by spectrometer switching. Final diagnosis was based on clinical outcome. Of 30 patients, V and Q were normal in 2 without lung disease. Of 9 with PE, 2 had no other pulmonary disease (OPD), and both Kr and Xe V were normal. Of the other 7 (PE & OPD), Kr V multiple views differentiated regional V/Q mismatches (PE) from adjacent matched lesions (OPD) in 3 where Xe showed matched V/Q only (3 PE missed). In 3 others with PE & OPD, Kr showed V defects in 2 not seen with Xe, while in 1 Xe showed more V defects than Kr.

The other 19 (no PE) had OPD or heart failure and Kr was more sensitive in 2 (Xe false positive PE in 1) and Xe in 4 for showing some V lesions. Kr-81m (190 keV, $T_{1/2} = 13$ sec) with better resolution, low radiation dose, ease of use and capacity for quick multiple paired V/Q views results in greater sensitivity than Xe for diagnosis of PE especially when associated with OPD. Longer Xe equilibration may improve its sensitivity but is time consuming. Xe may show small areas of OPD better because washout lesions are positive. With Kr, defects are always photopenic and may be obscured by normal activity.

PULMONARY VENTILATION AND PERFUSION MEASUREMENTS USING Kr-81m; BASIC METHODOLOGY. Peter J. Kenny, Denny D. Watson, John C. Clark, Ronald D. Finn and Albert J. Gilson. Mount Sinai Medical Center, Miami Beach, FL.

Kr-81m from a Rb-81 → Kr-81m generator has been used to measure changes in regional ventilation (\dot{V}/V), regional perfusion (\dot{Q}/V) and regional ventilation perfusion ratio (\dot{V}/\dot{Q}) in 20 dogs in the control state and following lobar occlusion and/or drug intervention. Data from this work were analyzed to provide a basis for the use of Kr-81m for similar measurements in pulmonary function studies in humans. Serial quantitative images were obtained during the equilibrium and washout phases for both ventilation and perfusion studies using a scintillation camera-computer system. A method was developed for measuring \dot{Q}/V and \dot{V}/\dot{Q} by constant intravenous infusion of Kr-81m in a dextrose solution. In this case, the equilibrium concentration of Kr-81m in any region depends on the values of \dot{Q}/V and \dot{V}/V in that region. \dot{V}/V was measured from ventilation washout studies. From this, separate quantitative determinations of \dot{Q}/V and \dot{V}/\dot{Q} , as well as \dot{V}/V , for the whole lung and selected regions were made. Because of the short half-life and short equilibration times for Kr-81m distribution in the lungs, it was possible to make repeated determinations of these quantities at intervals of a few minutes to assess the effects of intervention. For example, within minutes of lobar occlusion, perfusion reduction averaging 50% was shown to have occurred in the hypoxic region, as expected, presumably due to reflex vasoconstriction. The techniques developed provide a basis for the use of Kr-81m in combined ventilation and perfusion studies for the measurement of \dot{V}/V , \dot{Q}/V and \dot{V}/\dot{Q} in humans.

A CLINICAL COMPARISON OF Xe-127 AND Xe-133 FOR VENTILATION STUDIES. Harold L. Atkins, Herbert Susskind, Johannes F. Klopper, Azizullah N. Ansari, Powell Richards, and Ralph G. Fairchild. Brookhaven National Laboratory, Upton, N.Y.

Xenon-127 is currently available from Brookhaven National Laboratory for pulmonary diagnostics. A clinical comparison of Xe-127 and Xe-133 was therefore carried out to evaluate whether the theoretical advantages secondary to the physical decay characteristics of Xe-127 could be realized in a clinical situation.

Nineteen male patients with a variety of pulmonary problems were studied. A large field-of-view gamma camera was used with medium resolution 280-keV and medium sensitivity 140-keV collimators for the Xe-127 and Xe-133 studies, respectively.

The theoretical advantages of Xe-127 over Xe-133 were shown to exist in practice. The principal advantages of Xe-127 are higher count rates per millicurie and improved resolution. The ratio of Xe-127/Xe-133 in counts recorded over the chest wall per millicurie of radioactivity in the lungs averaged 1.22 at equilibrium and 1.39 for the initial inspired breath. Use of the highest sensitivity collimators would result in a further gain, thereby increasing this ratio to 2.20 and 2.50. Markedly improved resolution of Xe-127 was demonstrated by measurement of a line phantom, but this was not apparent on subjective appraisal of scintiphotos, except in the washout phase. Other advantages of Xe-127 are an excellent shelf life and a lower patient

radiation dose. Furthermore, a prior perfusion study using a Tc-99m radiopharmaceutical does not affect the quality of the Xe-127 ventilation study. The use of Xe-127 therefore permits the selection of only those patients with suspected pulmonary embolism requiring ventilation studies and eliminates unnecessary radiation exposure.

PATTERNS OF VENTILATION IN PATIENTS WITH CARDIOMEGALY OR HEART FAILURE. R.H. Secker-Walker, T. Toban and J.E. Ho. St. Louis University School of Medicine, St. Louis, Mo.

Patterns of regional ventilation in patients with heart failure have received little attention, although such patients are often referred for ventilation-perfusion studies.

We have studied patients suffering from ischemic heart disease (11), hypertensive heart disease (16), and other cardiomyopathies (16), who had no history of chronic obstructive pulmonary disease. Each had a ventilation study using serial images of the washin and washout of ¹³³Xe, and a perfusion scan using (Tc-99m)HAM.

Twenty one patients with evidence of peripheral edema had significantly larger hearts ($P < 0.01$) than those without edema, but their age and mean arterial blood pressures were not significantly different. A defect related to the heart was seen at the left base at the end of the washin in 23 patients, but there was no significant relationship between the size of, or filling of the left lung compared to the right with respect to heart size, or the presence or absence of peripheral edema.

Eighteen patients had clear lung fields by 4 min. (mean 2.5 ± 0.93 min) while the remainder had delayed clearance (mean 6.0 ± 2.5). The presence of rales at the bases was significantly associated with delayed clearance ($\chi^2 = 6.75$, $P < 0.01$). There was no difference in the clearance time between the left and right lungs in any group.

These findings indicate a wide range of clearance patterns in patients with cardiomegaly or heart failure. The highly significant association of rales with delayed clearance is consistent with the suggestion that edema of the terminal bronchioles is one of the mechanisms underlying impaired gas exchange in these conditions.

REGIONAL O₂-CO₂ PARTIAL PRESSURES AND PULMONARY VENOUS CONTENTS FROM VENTILATION-PERFUSION SCANS. B.R. Line, J.D. Fulmer, B.D. McLees, R.G. Crystal, A.E. Jones, and J.J. Bailey. National Institutes of Health, Bethesda, Md.

Ventilation-perfusion ratio (V/Q) images are of importance in providing a quantitative measure of the matching of blood and gas pools, but contain insufficient information to determine the adequacy of gas exchange. To evaluate the effect of V/Q imbalance on O₂-CO₂ transfer, we have combined scintigraphic V/Q studies with a model of alveolar gas exchange adapted from Kelman (Res. Phys. 4:260, 1968). The model algorithm, implemented in Fortran II on a minicomputer (HP 5407A), uses a two stage iterative approach to compute V/Q ratio relationships to O₂-CO₂ blood contents and alveolar partial pressures utilizing patient hgb, hct, pH, temperature, mixed venous contents and inspired gas compositions. Model data is combined with scintigraphic V/Q determinations in over 1500 small regions of lung to generate images of regional O₂-CO₂ partial pressures, O₂-CO₂ blood contents, respiratory quotient and volumes of O₂ uptake-CO₂ release.

To validate this approach, seven patients with biopsy proven pulmonary fibrosis underwent upright cardiac catheterization and upright posterior ventilation (Xe-127) and perfusion (Tc-99m MAA) studies. The blood oxygen content (CaO₂) values (range 17.7-25 vol%) predicted from perfusion and O₂ content images differed from the actual CaO₂ values by $4.15 \pm 4.42\%$ (mean \pm sem). We conclude that: (1) a physiologic model of pulmonary gas exchange can be applied to scintigraphic data to estimate regional alveolar pressures and capillary contents and (2) the functional images produced may be useful to detect regions most significant in derangement of pulmonary gas exchange.

ACUTE TOXICITY AND SAFETY FACTORS OF LUNG IMAGING AGENTS AS A FUNCTION OF PARTICLE SIZE. Michael A. Davis, Georgia M. Frieswick and Arnold Mandelstam, Joint Program in Nuclear Medicine, Harvard Medical School, Boston, MA.

Estimates of the safety factor for macroaggregated human serum albumin (MAA) and human albumin microspheres (HAM) used in pulmonary perfusion scintigraphy vary widely. This investigation was designed to elucidate the safety factor as a function of the particle size. The particles were injected into the tail vein of non-anesthetized albino CD rats and mice. The LD-50 (24 hrs) was determined for 5 discretely sized microspheres composed of 3 different materials. For each particle type and size survival curves were plotted to show the relationship between the percentage of animals surviving and the number of particles injected per gram body weight. The materials of which the particles were composed had little or no effect on the acute biologic response as evidenced by identical LD-50 values for albumin and latex spheres of the same size. Results indicated that the acute LD-50 (24 hrs) in rats varied from 710 to 154,000 particles/gram body weight and in mice from 695 to 96,500 particles/gram body weight for 90 to 13.5 μ m particles respectively. The slope of the killing curve showed the minimum lethal dose (MLD) to be 25 to 30% lower than the LD-50 value. When extrapolated to the clinical situation these data yield safety factors (MLD) of 1,000 to 10,000 for injected doses of 100,000 to 1,000,000 microspheres (28 \pm 12 μ m). The safety factor drops dramatically to 25 with equivalent doses of 90 μ m particles. It has been previously proposed that the ideal particle size for pulmonary perfusion scintigraphy is 13.5 \pm 1.5 μ m. Particles of this dimension have a safety factor 5 times greater than that obtained with the currently used 28 \pm 12 μ m microspheres.

THURSDAY, 2:00 p.m.-3:30 p.m.

CHICAGO ROOM

HEMATOLOGY 2

Chairman: Patricia A. McIntyre

Co-Chairman: Michael J. Welch

STUDY OF THE KINETICS AND IN VIVO DISTRIBUTION OF IN-111-LABELED PLATELETS: A COMPARISON WITH CR-51 LABELED PLATELETS IN RABBITS. Ursula A. Scheffel and Patricia A. McIntyre. The Johns Hopkins Medical Institutions, Baltimore, Md.

In 1976 Thakur et al. described In-111-oxine as a suitable agent for labeling platelets. The present study was undertaken to evaluate In-111 labeled platelets with respect to their physiological behavior. A method, recently recommended for its maximum yield of viable platelets and least damaging effect on the cells during labeling with Cr-51, was modified and optimized for use with In-111-oxine. Although platelets were labeled in the presence of plasma a reasonably good efficiency of 27%-67% was achieved.

The recovery and mean survival time of In-111 and Cr-51-labeled platelets were compared in rabbits (8 animals each). The percent of circulating platelets at 20 minutes after infusion was significantly higher ($p < 0.001$) for In-111 labeled platelets (82.9 \pm 7.1) than for Cr-51-labeled platelets (56.2 \pm 8.7) (mean \pm 1 s.d.). For the estimation of the mean survival time three different mathematical models were used. No significant difference ($p < 0.5$) was noted in the survival of In-111 and Cr-51-labeled platelets.

The fate of In-111 labeled platelets was followed by gamma camera imaging at various times after injection for a period of 6 days. Within the first hour there was an increase in splenic radioactivity. At later times, as cardiac activity decreased, liver activity increased.

Our results indicate that In-111 is, in addition to its more advantageous physical characteristics, a better label

for platelets than Cr-51. In-111-labeled platelets should provide a valuable tool for the study of platelet kinetics in human health and disease.

COMPARISON OF IN-111 LABELED PLATELETS AND IODINATED FIBRINOGEN FOR THE DETECTION OF DEEP VEIN THROMBOSIS.

L.C. Knight, J.L. Primeau, B.A. Siegel, M.J. Welch.

Department of Radiology, Washington University School of Medicine, St. Louis, Missouri.

Iodinated fibrinogen is widely used for detection of deep vein thrombosis by the fibrinogen uptake test. If I-131 or I-123 is used as a label, scintigraphic visualization of thrombi may be accomplished. Unfortunately, fibrinogen is not efficiently taken up by older thrombi in which fibrin deposition has slowed, and a high thrombus-to-blood ratio of radioactivity is necessary for imaging, especially in areas of large blood pool. We have previously reported the use of In-111 labeled platelets for the visualization of thrombi and shown that thrombi as old as 96 hours can be visualized. In this study the uptake of In-111 labeled platelets in thrombi is compared to that of iodinated fibrinogen. Freshly isolated platelets were labeled by mixing them with 8-hydroxyquinoline lipid soluble complex of In-111. The platelets were then administered to dogs in whom venous thrombi had been induced by alteration of the intima by an electric current. Dogs with thrombi of various ages (1-24 hr) were studied and I-125-fibrinogen (IC1 method, <0.5 I atoms per molecule fibrinogen) was injected at the same time as the platelets. Twenty-four hours after injection, the thrombi were removed and the associated radioactivity compared with that of equal weight of blood (thrombus: blood ratio). Thrombus: blood ratios as high as 32:1 were obtained for indium labeled platelets; i.e. as much as 2x as high as for iodinated fibrinogen. For thrombi of all ages, good scintigraphic images were obtained from 1-24 hours after injection of the agent (best images at 12-15 hours post-injection) even when the thrombi were not visible by contrast venography.

DIAGNOSIS OF EXPERIMENTAL PULMONARY EMBOLI WITH INDIUM-111 LABELED PLATELETS. G. McIlmoyle, H.H. Davis, M.J. Welch, J.L. Primeau, L.A. Sherman, and B.A. Siegel. Edward Mallinckrodt Institute of Radiology, St. Louis, Mo.

A simple, noninvasive method for the direct visualization of pulmonary emboli would be of considerable value for the diagnosis of this common disorder, especially in patients who have underlying parenchymal lung disease or are too ill to undergo pulmonary angiography. For this purpose, we have investigated the accumulation of In-111 platelets in acute pulmonary emboli. Radiolabeled venous thrombi were produced in 6 dogs by the injection of human thrombin and Tc-99m sulfur colloid into occluded segments of both jugular veins. One hour later, the thrombi were released and images demonstrating the position of the Tc-99m labeled pulmonary emboli were obtained. Autologous platelets labeled with In-111 oxine were injected and sequential images were obtained for one hour. The dogs were then sacrificed, and the emboli and tissue samples were removed and assayed for activity. Sixteen pulmonary emboli containing Tc-99m sulfur colloid were seen by imaging and 14 of these were detected with In-111 platelets; 5 emboli were visualized immediately and uptake in the remaining 9 appeared on later images. In all animals, at least one embolus was detected by imaging. Mean embolus weight was 538 mg, mean In-111 uptake was 1.09% dose/g embolus, and mean embolus/blood ratio was 16.1. In 2 animals, images showed additional foci of increased In-111 uptake, distal to an embolus containing Tc-99m; this uptake may reflect thrombus propagation. Our results demonstrate that acute pulmonary emboli in dogs can be readily detected by imaging with In-111 labeled platelets.

TECHNETIUM-99m-OXINE AND INDIUM-111-OXINE LABELED AUTOLOGOUS PLATELETS: DEMONSTRATION OF FRESH EXPERIMENTAL VENOUS THROMBI IN THE RABBIT AND DOG. Brian W. Wistow, Zachary D. Grossman, Gopal Subramanian, John G. McAfee,

Robert W. Henderson, Marsha L. Roskopf. Upstate Medical Center, Syracuse, N. Y.

Utilizing In-111-oxine platelets (Thrombosis Res. 9, 345, 1976), Thakur has visualized experimental canine deep vein thrombi produced by electrical damage to vessel walls. With both Tc-99m-oxine platelets and In-111-oxine platelets we have imaged dog and rabbit venous thrombi produced by magnetically controlled intravascular iron particles.

Thrombi were created by i.v. injection of iron particles 1.2 μ in diameter suspended in Renografin-76, with an external magnet positioned proximal to the injection site. After 30 minutes, the magnet was removed and radiographs demonstrated that the iron particles remained stationary. Gross examination of dissected veins revealed the clumped particles enmeshed in clot.

Platelet suspensions were prepared by a "button-less" centrifugation method and labeled. Thrombi formed following labelled platelet injection were easily visualized as were thrombi created 1 to 3 hours prior to platelet injection. However, older thrombi - formed 18-24 hours before platelet injection - were not usually detected. Controls with Tc-99m pertechnetate as well as Tc-99m-oxine incubated with whole blood and with platelet-poor-plasma were negative.

In conclusion, Tc-99m-oxine platelets and In-111-oxine platelets are useful agents for fresh venous thrombus localization. However, in this experimental model, their value for demonstrating older thrombi is limited.

VISUALIZATION OF FRESH ENDARTERIAL DAMAGE BY TECHNETIUM-99m-OXINE AND INDIUM-111-OXINE LABELED AUTOLOGOUS PLATELETS. Zachary D. Grossman, Brian W. Wistow, Gopal Subramanian, John G. McAfee, and Robert F. Rohner, Upstate Medical Center, Syracuse, New York.

Following McAfee and Thakur's introduction of oxine for cell labeling (JNM,17,480,1976), Thakur utilized In-111-oxine labeled platelets to visualize canine venous thrombi and mechanically damaged arterial intima (Thrombosis Res., 9,345,1976). We have demonstrated deposition of both Tc-99m and In-111 platelets on minimally injured endarterial surfaces, without thrombosis.

Rabbit ear arteries were punctured distally, an angiographic wire guide inserted, and an electric current passed between the wire and a distant soft tissue electrode. Platelets suspended in saline were incubated with either Tc-99m stannous oxine or In-111-oxine for 20 minutes at room temperature. Labeling efficiency for In-111-oxine varied from 85 to 99%; for Tc-99m, from 11 to 34%. Platelets were then injected intravenously into the contralateral ear at various intervals following arterial damage.

Both In-111-oxine platelets and Tc-99m-oxine platelets successfully imaged arterial injury 1, 3, and 6 hours old. Injury 24 hours old, however, was only faintly demonstrated. Tissue sections of successfully imaged arteries showed slight endothelial edema and disruption of the intimal cell layer; however, integrity of the internal elastic lamella and luminal patency were maintained.

Therefore, Tc-99m and In-111-oxine labeled platelets accumulate selectively in sufficient numbers to permit gamma camera imaging, on minimally damaged endarterial surfaces, even in the absence of thrombosis.

THE USE OF In-111 OXINE LABELED PLATELETS FOR LOCALIZATION OF VASCULAR THROMBI IN HUMANS. David A. Goodwin, Jerrold T. Bushberg, Paul Doherty, Martin J. Lipton, Frances K. Conley, Carol I. Diamanti, and Claude F. Meares, Veterans Administration Hospital and Stanford University, School of Medicine, Palo Alto, CA, *Department of Chemistry, University of California at Davis.

In seven patients with suspected vascular thrombi, platelets obtained from 70ml of citrated blood by serial centrifugation were labeled with In-111 oxine using the method of Thakur et al*. The procedure took approximately 4 hours and the labeling yield averaged $66.8\% \pm 13.2$ for 5 patients. The overall yield (including chelation of oxine and extraction in chloroform) was $26.2\% \pm 8.0\%$. An

average of 300 uc was injected and whole body scans and spot views obtained 2, 24 and 48 hours after injection. Blood disappearance was followed up to one week. The average biological half life was $3.52 \pm .20$ days in 2 patients. The labeled platelets were concentrated in the liver and spleen on both early and 24 and 48 hour scan. In one patients concentration of labeled platelet on the scan was noted in the femoral arteries corresponding to the areas which had been previously entered with a catheter for angiography. Patients with advanced arterio-sclerosis shown by angiography had no uptake of platelets in the corresponding arteries on the scan. One patient with cellulitis of one leg had no platelet uptake in the affected limb. This relatively simple labeling technique provides viable radiolabeled platelets suitable for imaging intravascular thrombi in humans.

*Indium-111 Labeled Platelets:Preparation, Function Studies and In Vivo Evaluation. M.L.Thakur, M.J.Welch, J.Heinrich Joist and R.E. Coleman, J.Nucl.Med.17:561,June 1976.

INDIUM AND IRON AS KINETIC TRACERS FOR EARLY ERYTHROPOIESIS. Barbara J. McNeil, Marjorie K. Jeffcoat and Michael A. Davis. Harvard Medical School, Harvard Dental School and the Joint Program in Nuclear Medicine, Boston, Mass.

External visualization and delineation of functional bone marrow is important for diagnostic, prognostic and therapeutic purposes. Radionuclides of iron are the most logical choice for assessment of erythropoietic activity but the usable isotopes have long half lives, poor decay characteristics or limited availability. Indium-111 chloride has therefore been used for marrow imaging although the site of its cellular localization is unclear. In this investigation we attempted to solve the problem of cellular localization by employing an animal model which selectively damages hematopoietic cells. Fe-55, an Auger electron-emitting radionuclide, delivers a lethal intracellular radiation dose to erythropoietic cells with minimal damage to surrounding reticuloendothelial cells.

In the rat we have shown that the absolute marrow uptakes of indium and iron were different whereas the absolute uptakes of indium and sulfur colloid were the same. However, in animals whose erythroid activity was partially ablated with Fe-55, the relative uptakes of iron and indium were the same and corresponded to the extent of remaining erythroid activity. In addition, during an in vitro separation of marrow cellular elements with iron carbonyl, both iron and indium remained in the erythroid-rich supernatant whereas sulfur colloid was in the precipitate.

These results indicate that in the rat, indium-111 chloride is an effective in vivo marker of bone marrow erythropoietic activity.

CLINICAL IMAGING OF MARROW. Rashid A. Fawwaz, Lester Hollander and James McRae. Donner Laboratory, University of California, Berkeley, California.

We have used 3 isotopes for marrow imaging: 52-FeSO₄, 111-InCl₃ and 99mTc-S-colloid.

When evaluation of splenic erythropoiesis was necessary, 52-Fe was used since 111-In and 99mTc-S-colloid localize normally in the spleen. Examples of marrow imaging in this category include: (1) the staging of patients with polycythemia vera, (2) the presurgical evaluation of the potential value of splenectomy in patients with myeloid metaplasia and increased splenic sequestration of red cells, (3) the differentiation of patients with end stage polycythemia with myelofibrosis from those with aplastic anemia. Splenic erythropoiesis occurs in the former but not the latter, and (4) the differentiation of benign eosinophilias from eosinophilic leukemias. In the former 52-Fe marrow distribution is normal. In leukemias, extramedullary hematopoiesis is observed early.

When hematopoietic reserve was being evaluated, 52-Fe or 111-In was utilized. Radiocolloids were not used because phagocytic activity does not always reflect erythropoietic activity. Examples of the value of marrow imaging in this category include: 1. Predicting the value of androgen therapy in patients with aplastic anemia where the hematologic

response correlates with the degree of residual marrow present. In cases of myelofibrosis a similar predictive value can be ascribed to $^{52}\text{-Fe}$ but not to $^{111}\text{-In}$ imaging, since the latter, in these instances, does not accurately reflect erythropoiesis. 2. The assessment of marrow toxicity in patients receiving chemo- or radiotherapy.

When evaluation of localized marrow replacement was sought, $^{99\text{m}}\text{Tc-S}$ -colloid was used due to the superior images obtained.

THURSDAY, 2:00 p.m.-3:30 p.m.

JANE ADDAMS ROOM

ENDOCRINE/METABOLISM 2

Chairman: Stanley J. Goldsmith

Co-Chairman: Steven M. Larson

THYROID FUNCTION IN CHRONICALLY DIALYZED UREMIC PATIENTS. Martin L. Musynowitz, Prentice Thompson, Stephen R. Plymate, and Douglas Daniels. William Beaumont Army Medical Center, El Paso, Texas.

Thyroid function in uremic patients undergoing chronic hemodialysis has been extensively studied, but disparate results have been reported in some of the parameters investigated. We have evaluated ten such patients who had no overt clinical evidence of thyroid dysfunction. Serum concentrations of Thyrotropin (TSH), Protein Bound Iodine (PBI), and Triiodothyronine Uptake (T3U) were normal and 24-hour I-131 uptake was also normal. Thyroxine as iodine (T4I), Free Thyroxine Index (FTI), Triiodothyronine (T3), Free Triiodothyronine Index (FT3I), Reverse Triiodothyronine Index (FRT3I) were significantly reduced, and Serum Inorganic Iodide (SII) and Nonhormonal Iodoprotein (SIP) were elevated. Thyroxine Binding Globulin Capacity was normal. The ratios T4I/T3 and FTI/FT3I were normal, but T4I/RT3 and FTI/FRT3I were reduced. TSH administration caused significant increases in T4I, T3, T3U, FTI, FT3I, and RT3 as compared to baseline, but the increases were less than normal in regard to T4I, T3, T3U, FTI, and FT3I. The TSH stimulated rises in RT3 and FRT3I were normal. These results strongly suggest that in chronically dialyzed uremic patients (1) a hypophyseal defect with regard to TSH secretion is present (2) a primary intrathyroidal defect is also present, but whether this is due to the elevated SII or not is indeterminate, (3) the peripheral binding of circulating thyroid hormones is essentially normal, and (4) there appears to be a shift in the peripheral conversion of thyroxine from T3 to RT3.

USE AND MISUSE OF THE SERUM T₃ CONCENTRATION AND FREE T₃ INDEX. C.M. Abreau, A.G. Vagenakis, L. Fournier, and L.E. Braverman. U. Mass. Medical School, Worcester, Ma.

The measurement of serum triiodothyronine by RIA has led to advantages and problems in interpreting results obtained in patients with suspected thyroid disease. An indirect serum free T₃ concentration can be calculated as the product of the serum T₃ (Seralute) and the resin T₃ uptake ratio (Trilute), i.e., the free T₃ index (FT₃I). The serum concentrations of T₃ and T₄ (Tetralute) and the free T₃ and T₄ indexes were measured in 74 normal subjects, 48 hyperthyroid patients, 12 patients with T₃ hyperthyroidism in whom serum T₄ concentration is normal, 41 hypothyroid patients, 20 patients with non-thyroidal systemic illness, 20 pregnant women, and 14 patients with an hereditary increase or decrease in serum TBG. Serum T₃ and FT₃I were strikingly elevated in all patients with T₄ hyperthyroidism and elevated, but less so, in patients with T₃ hyperthyroidism. During pregnancy, the serum T₃ concentration was elevated due to the increase in TBG but the FT₃I was normal. The serum T₃ and FT₃I were low in patients with overt hypothyroidism. In the 20 patients with systemic illness, the serum T₃ and FT₃I were decreased in 14 and the serum T₄ and FT₄I were increased in six. Serum T₃ was increased and FT₃I normal in patients with an here-

ditary increase in TBG. Serum T₃ and FT₃I were decreased in patients with an hereditary absence of TBG while serum T₃ was low or normal and FT₃I normal in patients with partial TBG deficiency. These studies suggest that the serum T₃ concentration and FT₃I are useful in diagnosing all forms of hyperthyroidism but are falsely low in many patients with systemic illness due to a defect in the peripheral conversion of T₄ to T₃. Abnormalities in TBG can also be detected by measuring the serum T₃ and FT₃I.

ENDOGENOUS SERUM TSH LEVELS AND METASTATIC SURVEY SCANS IN THYROID CANCER PATIENTS USING TRIIODOTHYRONINE WITHDRAWAL. Neil D. Martin. David Grant USAF Hospital and Kettering Medical Center, Kettering Ohio.

In order to use I-131 for imaging and treating thyroid cancer patients, high serum thyroid stimulating hormone (TSH) levels must be present. We wished to determine if high endogenous serum TSH levels could consistently be generated from a hypothyroid state produced by using the triiodothyronine withdrawal principle described by Stein and Nicoloff, and where possible, observe if any differences existed between images obtained by this method and those obtained by using bovine TSH injections. 6 weeks before scanning, those patients with differentiated thyroid cancer were switched from thyroxine to 25 mcg. of triiodothyronine (cytomel) t.i.d. 4 weeks later the cytomel was discontinued and 10-14 days later, one mCi of I-131 was given after blood was obtained for the determination of serum T₄, TSH, and T3R by radioassay methods. The patients were scanned 2-3 days later. A total of 55 studies were performed on 37 patients from 1973 through 1976 and only one did not demonstrate an elevated TSH level. 10 of the 37 patients had scans positive for metastatic tissue. 9 of the 37 patients had metastatic survey scans performed using both bovine TSH and endogenous TSH stimulation. 2 had positive images and 6 had negative images. No differences were noted between the two sets of scans. The serum T₄ levels were below normal in all 55 studies. The T3R results were normal in 11 of 30 studies reflecting the lack of sensitivity of this test. It is concluded that triiodothyronine withdrawal does induce high endogenous TSH levels and that under normal circumstances bovine TSH injections are not required for metastatic scans.

HUMAN REACTION TO BOVINE TSH. G. T. Krishnamurthy and W. H. Bland. VA Wadsworth Hospital Center, and UCLA School of Medicine, Los Angeles, Calif.

Thyrotropin (TSH) stimulation test is commonly employed to enhance the uptake of I-131 by the tumor or thyroid remnant during therapy for thyroid cancer. Often an allergic reaction to bovine TSH is noted. However its true incidence and its relation to dose have not been reported. Twenty-five years ago a study was initiated to follow the therapeutic course of thyroid cancer patients. Diagnostic followup scans were obtained with 5 mCi of I-131 yearly for 5 years, and once every two years thereafter. During each followup scan, 10 units of bovine TSH was given daily for 3 days. Local erythema or swelling larger than 4 cm in diameter, generalized urticaria, or anaphylactic shock (rare) were considered allergic reactions.

A total of 42 patients were treated in this fashion. The cumulative TSH dose varied from 50-500 units, with a mean of 192 units. Eighteen of 42 patients (43%) showed reactions to TSH. The cumulative mean dose of TSH in these 18 patients was 116 units. The reaction rate rose steadily up to a dose of 150 units and reached a plateau thereafter. Twenty-four patients (57%) showed no reaction to TSH and have continued to receive it. The cumulative dose range in these patients is 30 to 490 units, with a mean of 200 units. It is concluded that human reaction to bovine TSH is quite frequent (43%). An allergic reaction is generally found before reaching a cumulative dose of 150 units of TSH. Beyond this amount, a reaction is not dose related.

AN EVALUATION OF SEVERAL DIAGNOSTIC PROCEDURES AS PROGNOSTIC GUIDES FOR THIONAMIDE-TREATED HYPERTHYROIDISM. S. Nagataki, H. Ikeda, F. Matsuzaki, T. Yamaji, T. Tsushima, H. Uchimura,

Y. Imai, M. Maeda, N. Kuzuya, S. C. Chiu, N. Sasaki and L. F. Kumagai. The Third Department of Internal Medicine, Faculty of Medicine, University of Tokyo, Tokyo, Japan.

T₃-suppressibility (T₃-suppr) is a useful prognostic guide during drug therapy for hyperthyroidism. Other procedures which do not require *in vivo* radioactivity were studied to see if they could be substituted for T₃-suppression. T₃-suppr, serum T₄ changes after T₃ and TSH and prolactin responses to TRH were evaluated in hyperthyroid patients during drug therapy. Serum T₄, T₃ and TSH were normal at the time of testing. T₃-suppr was defined as 20 min thyroidal ¹³¹I uptake of <8% after T₃ (75 µg/d) for 14 days. No significant correlation was observed between T₃-suppr and peak serum TSH responses to TRH in 52 patients; 5 of 25 suppr and 14 of 27 nonsuppr patients failed to show a TSH rise of >5.4 mU/ml to TRH. Prolactin responses to TRH were normal or increased in all 36 patients tested regardless of their T₃ suppr or TSH responses to TRH. Serum T₄ changes after T₃ correlated significantly with T₃ suppr in 58 patients; T₄ levels in 36 suppr patients before and after T₃ for 2 weeks were 9.9 ± 0.3 µg/dl and 6.1 ± 0.3 µg/dl, respectively, p <.001. In 22 nonsuppr patients, T₄ changes were not significant before and after T₃, 10.1 ± 0.4 µg/dl and 9.3 ± 0.5 µg/dl, p >.05.

These data indicate (1) T₃-suppressibility and TRH responsiveness in hyperthyroidism during drug therapy are regulated by different mechanisms, so TSH or prolactin responses to TRH are not useful prognosticators. (2) Changes in serum T₄ after T₃ may be substituted for T₃-suppression tests obviating the use of parenteral isotopes and may be especially useful in children and during pregnancy.

DIFFERENTIAL DIAGNOSIS OF HYPERCALCEMIA BY MEASURING PARATHYROID HORMONE, CALCITONIN AND 25-OH-D₃. Rikushi Morita, Masao Fukunaga, Shigeharu Dokoh, Itsuo Yamamoto and Kanji Torizuka. Department of Radiology and Nuclear Medicine, Kyoto University, Kyoto, Japan.

We have measured blood levels of parathyroid hormone (iPTH), calcitonin (iCT) and 25-OH-D₃ in 24 cases with a variety of causes of hypercalcemia and estimated the usefulness of the assays of these calcium regulating hormones in differentiating hypercalcemic conditions. In primary hyperparathyroidism, iPTH levels were markedly high. The iCT levels, however, were within normal range except for one case with renal failure. In 7 cases with bone metastases from primary neoplasms iPTH levels were characteristically low, presumably being suppressed by hypercalcemia, whereas iCT levels were higher than normal. Four patients with remote malignant tumors produced a PTH like substance with resulting hypercalcemia. In these not only iPTH but also iCT levels were markedly high and 25-OH-D₃ levels were within normal range. From tissue assays the primary tumors, PTH like substance was identified but not CT. In a case with hypercalcemic multiple myeloma, iPTH, iCT, ionized Ca⁺⁺ and 25-OH-D₃ were distributed within normal range. This increased serum calcium level was thought to be due to large amounts of myeloma protein which bound additional calcium. Two cases with Vitamin D intoxication were easily differentiated by extremely elevated serum 25-OH-D₃ levels with normal iPTH and iCT.

THURSDAY, 2:00 p.m.-3:30 p.m.

LINDHEIMER ROOM

NEUROLOGY 2

Chairman: Kenneth A. McKusick
Co-Chairman: Gilbert H. Isaacs

LONGITUDINAL MULTIPLANE EMISSION TOMOGRAPHY OF THE BRAIN USING NITROGEN-13 AMMONIA. Malcolm Cooper, Karim Rezaizadeh, James L. Lehr, John F. Mullan, Bruce Mock, Eugene

E. Duda. University of Chicago Hospitals, Chicago, Ill.

Nitrogen-13 ammonia has been suggested as a means of measuring regional brain metabolism. Its differential diagnostic value has been tested in patients with inflammatory, degenerative, neoplastic, or ischemic brain lesions. Correlative imaging studies were obtained using Tc-99m pertechnetate, Ga-67 citrate, and CTT. The N-13 ammonia was produced using the ¹⁶O(p,α)¹³N reaction on water.* Twelve patients received ¹³NH₃, Tc-99m, and CTT studies. Seven patients also received Ga-67. Nuclide studies were performed using the Anger scanning camera (Pho/Con, Searle Radiographics, Inc.) with appropriate collimators. Six-plane vertex view tomograms or 12-plane anterior or lateral view studies were obtained. The N-13 ammonia brain images, obtained in 4-20 min. per view, showed relative increased uptake in cerebral cortex and cerebellar hemispheres. Intense uptake observed in two patients with meningioma was absent in a third with a cerebellar-pontine angle meningioma. Decreased or absent uptake was found in the following: abscess-2, ischemic stroke-1, radiation gliosis-1, post-surgical tissue loss-2, glioma-1, cerebral edema/cerebritis-1. Lung metastases-2, distinguished by other nuclide and CTT studies, could not be identified on the ¹³NH₃ images. Imaging of brain perfusion and metabolism using ¹³NH₃ was useful in determining regional dysfunction and distinguishing postsurgical change from tumor regrowth, but did not provide differential diagnostic information in primary or metastatic neoplastic disease.

(* Funded under ERDA contract # EY-76-C-02-0069)

CRITICAL EVALUATION OF Tc-99m GLUCOHEPTONATE AS A BRAIN SCANNING AGENT. Doina E. Tanasescu, Ralph S. Wolfstein, and Alan D. Waxman. Cedars-Sinai Medical Center, Los Angeles, California

The purpose of this study was to determine the accuracy and sensitivity of Tc-99m glucoheptonate brain scintigraphy.

Brain imaging consisted of a 15 mCi Tc-99m glucoheptonate dynamic flow study with both immediate and delayed (2 - 4 hours) static images obtained. All imaging was done using an Anger camera (Searle HP). Patient documentation was by angiography, surgery, autopsy, or clinical followup greater than one year.

794 patients were included in this study. 599 were proven normal, while 195 were proven abnormal. Of the abnormal group, 162 patients had abnormal static imaging, and an additional 20 had abnormal perfusion studies. 51 patients were found to have neoplasm, 44 CVA, and 67 other lesions. Without inclusion of perfusion results, overall sensitivity was 83%, and accuracy 95.5%. With inclusion of the perfusion studies, overall sensitivity was 93% and accuracy 98%. Sensitivity for CVA was 62%, and for tumor 94%. With inclusion of the perfusion studies, sensitivity for CVA increased to 90%.

Subdural hematoma and infection were also readily detectable with very high sensitivity values. However, this group was quite small in total number.

We conclude that Tc-99m glucoheptonate is an excellent radiopharmaceutical for brain scanning, with extremely high sensitivity and accuracy for the detection of central nervous system abnormalities.

COMPARATIVE STUDY OF TECHNETIUM-99m GLUCONATE AND FOUR OTHER TECHNETIUM COMPLEXES (PERTECHNETATE, DTPA, CITRATE AND BLEOMYCIN) IN THE DIAGNOSIS OF METASTATIC BRAIN TUMORS. Manfred Akerman, G. de Tovar, and Diana B. Chorny. Hopital Foch, Suresnes, France.

Technetium-99m gluconate has been proposed as a brain tumor-scanning agent. In order to evaluate its usefulness in the diagnosis of cerebral metastases we have compared its results with those of 1) pertechnetate, 2) Tc-99m DTPA, 3) Tc-99m citrate, 4) Tc-99m bleomycin in four series of 10 patients who had known metastatic brain tumors.

The number and density of abnormal uptake areas observed on delayed brain scans performed 2-6 hr after injection of 15-20 mCi of each agent were compared in each series.

Tc-99m gluconate was found to offer the same ability to detect brain metastases than Tc-99m DTPA. It gave much more satisfactory tumor images than pertechnetate in 9 of 10 patients. The results of the scans using Tc-99m gluconate were generally better than those obtained with Tc-99m citrate and Tc-99m bleomycin.

This comparative study shows that Tc-99m gluconate and Tc-99m DTPA seem to be the best brain-scanning agents in the diagnosis of metastatic brain tumors.

SENSITIVITY OF RADIONUCLIDE ANGIOGRAPHY. Frank H. DeLand. University of Kentucky and VA Hospital, Lexington, Ky.

The purpose of this study was to evaluate the sensitivity of radionuclide cerebral angiography for the detection of abnormal blood flow. 100 consecutive patients who had had radionuclide dynamic studies (vertex projection) with N-Max and T-Max computer analysis and contrast cerebral angiography were analyzed. The clinical diagnosis of these patients were transient ischemic attacks (72), strokes (10), headaches (8), seizures (8), abscess (1), pseudotumor cerebri (1). 57% of the patients had abnormal sequential analogue cerebral blood flow studies; 64% had abnormal computer studies; and 43% had abnormal arteriograms. Of those patients who had abnormal analogue nuclide studies, half had abnormal contrast angiograms, and half of those patients with abnormal computer studies had abnormal contrast angiograms. Of 36 normal nuclide studies, 11 demonstrated abnormal angiograms. The angiographic abnormalities were characterized as small arteriosclerotic plaques of the carotid vessels without change in the cerebral blood flow or narrowing of the vertebral arteries. In all patients with abnormal analogue or digital nuclide studies, clinical evidence of abnormal flow was present. Abnormal static radionuclide images were found in only eight patients. This analysis indicates that: 1) cerebral radionuclide angiography is more sensitive than contrast angiography for demonstrating abnormalities of carotid blood flow, 2) is less sensitive for abnormalities of vertebral flow, 3) is nearly twice as sensitive as contrast angiography for the detection of changes in cerebral blood flow in patients with TIA's, and 4) computer analysis is 20% more sensitive than nuclide analogue information and is an important reinforcement of questionable abnormal studies.

USE OF THE RADIONUCLIDE BRAIN SCAN AND COMPUTERIZED TOMOGRAPHY FOR INTRACRANIAL INFECTIONS. Steven Pinsky, Ha Yong Yum, Dushyant Patel, Carlos Bekerman, and U. Yun Ryo. Michael Reese Medical Center, Chicago, IL

There are many areas where computerized tomography (CT) scanning has been shown to be superior to radionuclide scanning. It has been our experience that this is not true in infectious disease of the brain. This would apply to both intracranial abscesses as well as diffuse inflammatory processes. Of 15 patients studied by both techniques and with surgical or angiographic follow-up, the radionuclide scan was positive in 12 of 15 and the CT scan was positive in only 7 of 15 cases.

Of 5 intracranial abscesses, 3 were detected by both techniques and the other 2 were detected only by radionuclide brain scan. There were no cases of intracranial abscesses detected by CT scan not detected by radionuclide scan. Of 10 cases of diffuse inflammatory disease, 6 were detected only by radionuclide brain scan, while 3 were detected only by CT scan. There was only one case of diffuse inflammatory disease seen with both radionuclide scan and CT scan. Of the 15 cases of inflammatory disease there were only 4 detected by both techniques, 3 of these were abscesses. The 3 cases of diffuse inflammatory disease detected by CT scan and not by nuclear medicine, were

2 cases of encephalitis and one case of ventriculitis.

It would appear that the radionuclide scan is more sensitive than the CT scan for the detection of intracranial infection, but that both techniques used in conjunction will give the best diagnostic results.

A METHOD FOR EVALUATING INTRACRANIAL TUMOR REMOVAL IMMEDIATELY FOLLOWING CRANIOTOMY. Alan D. Waxman, Michael J. Apuzzo, and Jan K. Siemsen. LAC-USC Medical Center, Cedars-Sinai Medical Center, Los Angeles, Calif.

The extent of tumor removal following central nervous system surgery is difficult to evaluate using current brain scanning techniques. This is due to the effects of the surgery itself on surrounding brain tissue, as well as bone and scalp changes. The current technique makes use of the high Gallium affinity for central nervous system tumors as well as a relatively long physical and biological $T_{1/2}$.

14 patients with known central nervous system tumors were included in this study. All patients were injected with 5 mCi of Gallium 67 citrate prior to craniotomy. Tumor uptake was allowed to occur and the patients were scanned prior to surgery. Following the surgical procedure a repeat scan was done without reinjection.

The optimum time interval from Gallium injection to surgery was found to be 5 - 9 days. Intervals less than 5 days resulted in a significant accumulation in calvarial activity at the craniotomy site. Good correlation of residual activity and the extent of tumor removed was obtained in 10 of the 14 cases. Of the 4 cases in which the correlation was considered as poor, 3 were secondary to a short interval between injection and craniotomy of from 24 - 60 hours. One case showed extensive residual by scan, although surgically tumor removal was felt to be complete. This case was serially scanned for six months, showing a progressive increase in tumor size.

We conclude that the proper sequencing of Gallium scanning pre and postoperatively when done without reinjection allows for a rapid and accurate assessment of tumor removal following craniotomy.

BEDSIDE DETERMINATION OF CEREBRAL BRAIN DEATH. Larry L. Heck, Julius M. Goodman, Eugene D. Van Hove. Methodist Hospital of Indiana, Indianapolis, Indiana.

Objective confirmation of brain death is desirable even though the clinical diagnosis by an experienced physician is usually reliable. This is particularly necessary when the etiology is unknown and there are legal and transplant considerations involved. In brain death, the cerebral circulation is essentially halted. An intravenous radioactive bolus will pass to the base of the skull but it will not enter the intracranial circulation. The radionuclide technique has been criticized because of the need to transport a potentially salvageable patient attached to many life support mechanisms to the nuclear medicine department. A mobile gamma camera has been employed since late in 1975 to allow the study to be performed at the bedside.

A bolus of 20mCi of Tc-99m albumin is injected in a subclavian or antecubital vein and followed with a 20cc flush of normal saline. Serial 3 second images are obtained on 70mm film for a duration of one minute. A scalp tourniquet is used to decrease interference from extracranial blood flow. Anterior and lateral 400,000 count static post dynamic views are immediately performed to evaluate filling of the intracranial dural sinuses.

We have successfully employed radionuclide angiography in the determination of cerebral brain death in over 90 patients since 1969. Sixteen of the last 17 cases of clinically suspected brain death were confirmed with radionuclide angiography at the bedside. The other patient proved to have intracranial blood flow and subsequently recovered from a metabolic encephalopathy. This method has been more reliable than EEG.

THURSDAY, 4:00 p.m.-5:30 p.m.

LINDHEIMER ROOM

Minneapolis, MN and Bristol Laboratories, Syracuse, NY.

IN VITRO AND RADIOASSAY 3

*Chairman: Lawrence Demers
Co-Chairman: W. Newlon Tauxe*

SERUM DNA LEVELS IN PATIENTS WITH CANCER OR BENIGN LESIONS OF THE G.I. TRACT. S. A. Leon, B. Shapiro, E. Cohn, and M. Desai. Albert Einstein Medical Center, Philadelphia, PA.

Previous work had shown that cancer patients have elevated serum DNA concentration, compared to healthy controls. The purpose of this study was to compare the DNA levels in patients with malignant lesions with those of patients with benign or inflammatory disease. The DNA concentration in serum was measured by radioimmunoassay, capable of detecting as low as 25 ng/ml.

Normal levels of DNA, measured in 62 healthy individuals had a range of 0-100 ng/ml, with a mean of 13 ± 3 (SE). The DNA levels in 35 patients with colon or rectum carcinoma had a range of 0-700 ng/ml, with a mean of 124 ± 26 . This value is significantly different from that of the normal controls ($p < 0.001$) or patients with benign disease (see below) ($p < 0.005$). The range found in 12 patients with pancreas carcinoma was 30-2500 ng/ml, with a mean of 494 ± 188 (p normals < 0.02 , or p benign = 0.02). In a group of 15 patients with various G.I. cancers (esophagus, stomach, duodenum, liver, gallbladder, Hodgkin's stomach ulcer) the range was 0-410 ng/ml, with a mean of 124 ± 31 (p normals < 0.001 , or p benign = 0.005). In comparison, 12 patients with benign disease (gastritis, pancreatitis, colitis, duodenal ulcer) had a range of 0-85 ng/ml and a mean of 27 ± 9 ($p < 0.01$, not significant relative to controls).

We conclude that in most patients with malignant disease, the serum DNA levels are higher than those with benign disease or controls. The most striking results were obtained in pancreas carcinoma: 10 out of 12 cases (83%) had very high levels (200-2500 ng/ml). In comparison, patients with pancreatitis had undetectable levels of DNA. These results may have significant diagnostic value.

BETA-2 MICROGLOBULIN FOR DIAGNOSIS OF RENAL INSUFFICIENCY IN UROLOGICAL PATIENTS. Juan J. Touya, Victor Braren, Paul Versage, John Goddard and A. Bertrand Brill. Nuclear Medicine Division, Vanderbilt University Hospital, Nashville, Tenn.

Assay of Beta-2 microglobulin by radioimmunoassay (B-2 RIA) was evaluated as a diagnostic procedure for renal function impairment in 250 patients with varying disease of the urinary tract. Patients were classified as normal or abnormal based on BUN, serum creatinine, creatinine clearance, glomerular filtration rate measured with a radioactive chelate (GFR) and final clinical diagnosis. The normal value of B-2 RIA determined in 75 different blood samples from 5 normal volunteers was 0.5-1.85 ug/ml ($\pm 2SD$). The decision matrix and the receiver operating characteristic (ROC) curve methods were used to evaluate the results. A cut-off value of 3.0 ug/ml was selected experimentally for both methods to separate patients with impaired renal function from those with normal function in this representative sample of the population of a urological clinic. At this cut-off value, B-2 RIA had a sensitivity of 0.986, a specificity of 0.973 and an accuracy of 0.988. GFR at a cut-off value of 80 ml/min/1.73m² had a sensitivity = 1.000, specificity = 0.973 and accuracy of 0.988. The cost/effectiveness of the procedure was analyzed using a decision-flow diagram, and we concluded that B-2 RIA provides the same diagnostic accuracy as the GFR, but decreases the decision cost by 3 fold. BUN and serum creatinine were less sensitive and less specific than the B-2 RIA.

CLINICAL APPLICATIONS OF A RADIOIMMUNOASSAY FOR BLEOMYCIN. Michael K. Elson, Martin M. Oken, Stanley T. Crooke, and Rex B. Shafer. Nuclear Medicine Svc., V.A. Hospital,

Bleomycin levels were measured in serum and urine of patients receiving bleomycin by intramuscular injection. Serum levels peaked in 1 to 1½ hours. The half-life of circulating bleomycin in serum varied 2 to 4½ hours with a mean half-life of 3½ hours. Urinary excretion was quite variable. Forty-eight to 90% of the dose could be found in the urine within 24 hours of injection. The mean 24 hour urinary excretion was 67%.

The bleomycin levels in serum and urine were measured by radioimmunoassay. The assay, utilizing a Co-57 labeled bleomycin as the tracer, was described previously by this laboratory. By making appropriate dilutions of the antiserum and labeled bleomycin, the sensitivity of the assay was improved to detect as little as 1 picogram per ml. This increased sensitivity permits the measurement of bleomycin for longer times after injection and the determination of small quantities of bleomycin that may be found in tissue.

The radioimmunoassay for bleomycin, using a Co-57 labeled bleomycin tracer, is now available for clinical investigations of bleomycin toxicity.

MEASUREMENT OF SERUM PHENYTOIN (DPH) BY RIA. Bryan P. Shepherd, Geoffrey F. W. Smith, Toni Rowe and Keith Lloyd* The Radiochemical Centre, Amersham and Greenbanks Hospital*, Plymouth, U. K.

For optimum control of phenytoin therapy it is important to monitor serum levels: the method of choice has been Gas-Liquid Chromatography which has limited throughput. A radioimmunoassay for Phenytoin has been developed which directly measures a 20µl sample and uses a gamma label (¹²⁵I) with preprecipitated antibody. The immunogen employed to raise the antiserum is DPH-3-valerate-BSA whilst the label is an iodinated derivative of the tyrosine ester of DPH-3-acetic acid. There are only three pipetting steps in the assay which makes use of a centrifuge based separation. The assay range is 0-75µg/ml with optimum precision over the therapeutic range (10-20µg/ml). A hospital laboratory trial using eight separate reagent batches gave a between assay coefficient of variation of 2.9%. The correlation equation against the GLC method was Phenytoin by RIA = $0.67 + 0.888$ (Phenytoin by GLC), $r = 0.991$. No interference by other antiepileptic drugs is observed. Cross reactivity with the major metabolite 5-(p-hydroxyphenyl)-5-phenylhydantoin is <10%. The assay permits reliable and precise estimation of serum phenytoin levels. It can be conveniently fitted into any RIA laboratory routine with rapid sample turnover and minimal hands-on time. 60 samples in duplicate can be measured in two hours including one hour hands-on time.

A SENSITIVE RADIOENZYME-IMMUNOASSAY FOR THE MEASUREMENT OF DOPAMINE. Bahjat A. Faraj, Vernon M. Camp, and Farouk Ali. Department of Radiology (Division of Nuclear Medicine), Emory University School of Medicine, Atlanta, Ga.

Abnormalities in the biosynthesis and metabolism of catecholamines [epinephrine, norepinephrine and dopamine (D)] are associated with many pathological conditions such as hypertension, Parkinsonism and neurocrest tumors (Axelrod and Weinschilboum. *New Engl. J. Med.* 287: 237, 1972). We have recently been engaged in a program designed to measure D based on (a) the conversion of D to its respective 3-O-methyl dopamine (MD) metabolite by the enzyme catechol-O-methyltransferase (COMT) and (b) the simultaneous determination of the formed MD by radioimmunoassay (RIA) (Faraj et al., *J. Nucl. Med.* 17: 549, 1976; *Clin. Res.* 25: 35A, 1977). A hepatic (rat) COMT was partially purified by differential centrifugation and ammonium sulfate fraction according to a modified procedure of Cuello et al. (*J. Neurochem.* 21: 1337, 1973). Reaction mixtures are prepared by incubation of 1M-tris buffer (pH 9), 0.1M MgCl₂, 0.5mM S-adenosyl-1-methionine, enzyme (0.4 mg/ml) and D solutions containing 1-10 ng in 0.01 N HCl at 37°C for 15 min. The reaction is stopped by the addition of borate buffer (0.5M). The MD formed is extracted with ethylacetate and evaluated

by RIA in the presence of MD-antiserum (1:1000 dilution) and MD-³H (8000 cpm; sp. act. 9 Ci/mole) at 4°C overnight. The results indicated an 80-90% conversion of D to MD and that the assay is linear up to 7 ng. As low as 1 ng of D can be detected by this procedure. The diagnostic applicability of this radioenzyme-immunoassay is being tested by determining urinary and plasma levels of D in patients with different diseases. (Supported in part by a grant from NIH # GM-1-RO1-GM22472).

CLINICAL EXPERIENCES WITH SERUM FERRITIN DETERMINATIONS IN PATIENTS WITH ANEMIA. Jorge A. Franco, Klitia Vanags, Bernadine Kovaleski, Monika Schreyer, Joseph Homesley. Department of Nuclear Medicine, O'Connor Hospital, San Jose, California.

Several years ago in anticipation of the availability of serum Ferritin determinations, we stored frozen sera from patients referred for laboratory evaluation of anemia. Currently, we have determined Ferritin levels in the sera of 104 patients on whom we have a 2 year follow up. The purpose of the study was to retrospectively evaluate the impact of serum Ferritin determinations in the classification of our patients' anemia. The test is a solid phase double antibody radioassay. At the completion of the test, the residual radioactivity represents the bound antigen. Values lower than 12 ng/ml were considered diagnostic of iron deficiency. Levels between 12-25 ng, possible iron deficiency; values over 25 ng exclude iron deficiency. The final classification of the anemias was as follows: Iron deficiency 47, possible iron deficiency 4, secondary anemia 31, miscellaneous anemias including hemoglobinopathies 22. Abnormal Ferritin values, diagnostic of iron deficiency were found in 45 of 47 patients with iron deficiency, borderline low levels in 2 patients with proven iron deficiency and in 3 with possible iron deficiency. Much higher values were noted in the secondary and miscellaneous anemia groups. In our experience, serum Ferritin determinations are most valuable for the exclusion of iron deficiency in the differential diagnosis of anemia and the identification of cases of secondary anemia.

THURSDAY, 4:00 p.m.-5:30 p.m.

JANE ADDAMS ROOM

**RADIOPHARMACEUTICAL 5:
BIOKINETICS AND DOSIMETRY**

Chairman: Monte Blau
Co-Chairman: Manuel Tubis

RADIATION DOSE TO THYROID TISSUE IN I-131 THERAPY OF THYROID ADENOMA. Colum A. Gorman and James S. Robertson. Mayo Clinic/Foundation, Rochester, MN.

The radiation dose to suppressed thyroid tissue incident to I-131 treatment of solitary toxic adenomas was calculated in detail to provide a basis for evaluating the carcinogenic potential of this therapeutic modality. The MIRD method of dose calculation was used in a two-step procedure. First the activity needed to achieve a central dose of 30000 rad was calculated as a function of nodule diameter. Then the surrounding doses out to a distance of 6 cm from the nodule center were calculated and related to the suppressed thyroid tissue. The results indicate that absorbed doses of 15 to 2300 rads are incurred. Although these doses are in the range in which x-rays have produced thyroid cancer there have been few reported cases of thyroid cancer after iodine-131 treatment of hot nodules. Possible reasons include the patients age when irradiated, the lesser carcinogenic potential of iodine-131 as compared with x-rays, the relative metabolic inactivity of the suppressed tissue, and inadequate follow-up of treated patients.

A COMPARISON OF THE DOSIMETRY OF THE POSITRON EMITTER TO THE MORE CONVENTIONAL GAMMA-EMITTING RADIOPHARMACEUTICAL. Paul A. Feller, Vincent J. Sodd, and Hiroshi Nishiyama. Nuclear Medicine Laboratory, BRH, FDA, Cincinnati, Ohio.

Closer relationships between the accelerator scientists and the clinical physicians, and the installation of some small accelerators in nuclear medicine laboratories, have placed much emphasis on the use of the ultra-short half-lived positron emitters, C-11, N-13, and O-15. While the short physical half-lives of these radionuclides favor lower radiation dose to the patient, the positron emitted contributes heavily to the dose.

This paper compares the radiation doses from radio-pharmaceuticals labeled with C-11, N-13, or O-15 to those from some non-positron-emitting radioactive agents. Some of the comparisons made are: Myocardial agent N-13-ammonium chloride to Tl-201; pancreas agents C-11-carboxyl-labeled DL-valine and -DL-tryptophan, and N-13-valine to Se-75-L-selenomethionine; tumor agents C-11-ACPC and N-13-ammonia and -L-glutamine to Ga-67.

Conclusions drawn are that the doses from injected compounds of C-11, N-13, and O-15 are not negligible, but on a per-millicurie basis are comparable to doses received from Tc-99m compounds. However, reductions in total body patient doses of 10 to 1000 times per millicurie are achieved when compared to Ga-67, Tl-201, and Se-75. When replacing Se-75, the reduction of patient dose is a large factor to consider. However, when replacing Ga-67 or Tc-99m compounds, the reduction in dose becomes of secondary importance to factors such as comparable organ or tumor specificity, relative image quality, ease of handling and personnel exposure.

USE OF A PHARMACOKINETIC MODEL TO DETERMINE REGIONAL CUMULATIVE CONCENTRATIONS OF Tc-99m HIDA IN HUMANS. M. Loberg, S. Sikorski, E. Harvey, J. Ryan and M. Cooper. University of Maryland Hospital, Baltimore, Md.

Dosimetry calculations based on biodistribution data from lower animal species often inadequately approximate the true dosimetry in humans and seldom apply to the diseased state. Tc-99m HIDA illustrates this premise. To obtain its true dosimetry in humans, a pharmacokinetic model of Tc-99m HIDA was developed in dogs using data from tissue distribution studies, computer image analysis, and blood, urine, and bile sampling. The model consisted of 4 compartments: a central compartment including plasma and extravascular spaces in dynamic equilibrium with the liver compartment and excretory pathways through the biliary and renal systems. From knowledge of the normalized blood time-activity curve and cumulative urinary excretion the model accurately predicted the normalized time activity curves for each compartment in both normal and hyperbilirubinemic dogs. The model-dependent normalized liver curve agreed within 17% of the true curve as determined by serial sacrifice. Rate constants describing the model were determined for 14 normal and 5 jaundiced patients. Comparisons revealed no significant change in renal clearance rate while cumulative urinary excretion increased from an average of 15.7 to 55.9% in the presence of jaundice. The rate of biliary excretion decreased 5 fold but the cumulative concentration of Tc-99m-HIDA in the liver also increased from 0.30 to 0.90 µCi hrs/g-mCi; in humans even though a greater percentage of Tc-99m-HIDA is cleared through the kidneys in diseased states, the actual liver dose is greater. Model dependent calculations significantly modified conventional dosimetric estimates.

BIOKINETICS OF ²⁰¹Tl IN MICE AFTER ORAL AND INTRAVENOUS ADMINISTRATION OF TlCl. B.M.W. Tsui, I.V. Gloria, and K.A. Lathrop. University of Chicago, Chicago, IL.

Comparison between the biokinetics of ²⁰¹Tl administered p.o. and i.v. would provide information for possible oral usage, compartmental modeling, and a guide to the collection of human data for radiation absorbed dose calculation. Biologic distribution of ²⁰¹Tl was determined in mice between 0.5m and 7d after i.v. or p.o. administration. The data were approximated by a sum of exponentials using the

least-squares method. After i.v. injection the half-times in the blood are < 1m for ~ 98%, 12m for 1.4%, and 2d for 0.2%. Uptake in all tissues is ~ 90% of maximum within 1m. Myocardial concentration is maximal (~30%/g) at ~10m; ratios for heart/blood, -/lung, and -/liver at ~ 1h, and are 60, 2, and 6 respectively. Concentration in the kidney (~70%/g) exceeds all other tissues as does the ratio to blood (350). After oral administration blood concentration increases to ~ 0.4%/g between 1 and 5h, then decreases the same as after i.v. administration. A maximal myocardial concentration of ~10%/g is maintained between 1 and 5h, and highest heart/blood, -/lung, and -/liver ratios are 25, 1.6, and 1.2 at ~1.5h. Kidney concentration is equal to the i.v. injection, but the ratio to blood is lower (200). At 5h after either i.v. or p.o. administration of ²⁰¹Tl concentrations are about equal in all other tissues, with small intestine wall>muscle>spleen ≈ lung>colon wall>heart>liver>stomach>ovary>skin; tissue/blood ratios range between 10 and 50. These data suggest that adequate myocardial images might be produced after oral administration of ²⁰¹Tl, but that the counting interval and data accumulation times should be increased. A preliminary compartmental model has been constructed which may indicate other imaging uses and other areas for investigation in the human.

HIGHLY IODINATED ¹²³I-FIBRINOGEN AS AN ONCOPHILIC RADIO-PHARMACEUTICAL. Kenneth Krohn, Sally DeNardo, Gerald DeNardo, David Vera and David Wheeler. Radiology Department, University of California, Davis, CA.

I-Fibrinogen has a higher tumor concentration than either ⁶⁷Ga-Cit, ¹¹¹In-Bleo or I-Bleo in a murine tumor, and the maximum tumor concentration occurs earlier for I-Fib than for ⁶⁷Ga-Cit. The potential this finding suggests for imaging neoplasms with ¹²³I-fibrinogen is, however, diminished by the slow blood clearance of I-Fib. Excessive iodination of fibrinogen greatly increases its rate of blood clearance, and we therefore labeled human fibrinogen with large amounts of iodine by the iodine monochloride (ICl) and electrolytic methods and tested the in vitro and in vivo properties of these products.

Our electrolytic procedure was similar to one described previously; however, our ICl technique involved addition of a few microliters of concentrated ICl in 0.1 N HCl to a milliliter or more of buffered fibrinogen already containing ¹²³I-iodide. This was technically easier than "jet" iodination, and it was faster and easier than electrolytic iodination. It also eliminated the problem of fibrinogen precipitation with ICl overiodination (J Nucl Med 16:756, 1975).

I-Fibrinogen (50I/fib) deiodinated in vitro (37°C neutral citrate buffer) at 2.8 and 4.2%/d when prepared by the ICl and electrolytic methods, respectively. When injected into rabbits, the protein bound activity (TCA precipitability) after 24 hours was 95.5% for the ICl product versus only 32% for the electrolytic. The electrolytic product cleared from the blood slightly faster for any given level of I/fib.

We prefer extensive iodination by ICl to increase ¹²³I-fibrinogen clearance, and have achieved ten-fold higher tumor: blood ratios at 4 hrs after injection with 50I/fib. (Supported in part by American Cancer Society grant #DT-45.)

ESTROGEN DERIVATIVES. Toru Komai, Roger Johnsonbaugh, J. Krijn Mazaitis, Victor W. Jiang, Raymond E. Gibson, William C. Eckelman and Richard C. Reba. George Washington University Medical Center, Washington, D. C.

The recent literature has shown a correlation between the presence of the estrogen receptor proteins (ERP) in malignancy and the remission of the tumor after endocrine ablation. H-3 labeled estrogens concentrate in those human breast tumors that contain ERP. A gamma-emitting estrogen derivative would be useful to determine the presence of ERP in metastatic tumors by external imaging. To this end five compounds were obtained: estradiol (E), hexestrol (HEX), estradiol 17β succinyl tyrosine methylester (EST), estradiol 6-(O-carboxymethyl oxime tyrosine methyl ester and 17α ethynyl estradiol (EE). The compounds were iodinated and then analyzed by various chromatographic systems. The in vitro ERP binding affinity of the five compounds before and after iodination was determined by a competitive binding study using H-3 E. E and EE displaced H-3 E equally well

(50% inhibition at 2.9 x H-3 E) followed by HEX (50% inhibition at 6.4 x) and EST (50% inhibition at 200 x). In contrast, iodinated E could not displace H-3 E. Iodinated HEX could displace 50% of H-3 E at 100 fold excess but iodinated EE displaced H-3 E with an affinity equal to E and the parent compound EE. In this respect iodinated EE is the superior derivative. Iodinated HEX showed specific binding to ERP by sucrose gradient centrifugation but all iodinated compounds showed nonspecific binding. This nonspecific binding could be decreased for iodinated HEX and EE by thyroxine and iodoethynyl cyclohexanol. In agreement with these data iodinated HEX and EE showed high uterine uptake in immature rats. We suggest that the target to non target ratio in vivo can be anticipated by the extent of specific and non specific binding in vitro.

PREPARATION AND BIOLOGICAL KINETICS OF LIPOSOMES LABELED WITH RENAL AGENTS. Gerald D. Robinson, Alice W. Lee, and George V. Taplin. University of California, Los Angeles, California.

Lipid vesicles and liposomes have been shown to be potentially useful carriers for directing radiopharmaceuticals to target organs. We have prepared liposomes containing renal agents and have measured uptake and release of the label by the liver and its subsequent clearance through the kidneys of experimental animals.

Liposomes were prepared from 150 mg of a 15:5:1 ratio (by weight) of lecithin, cholesterol and stearylamine which was coated onto the inner surface of a 50 ml serum vial. Tc-99m-DTPA or labeled o-iodohippuric acid in 2.5 ml aqueous solution was added to the vial and the resulting suspension was shaken at 37°C for 15 min to achieve good dispersion. The liposomes were washed three times and redispersed in 2.5 ml of physiologic saline. Approximately a 5% labeling yield was usually achieved.

After intravenous injection in the rat, rapid uptake of activity by the RES was observed. At 5 min post injection 50 and 6% of the activity was found in the liver and spleen, respectively, with 15% in the kidneys. Within 60 min, over 70% of the activity was cleared through the kidneys into the bladder, with only 10% remaining in the liver. The biological kinetics were similar when either Tc-99m-DTPA or o-iodohippuric acid labeled liposomes were used. Using scintillation camera imaging after IV administration of liposomes in the dog, complementary uptake and turnover patterns were observed when the liver and bladder were chosen as areas of interest. Preliminary studies in rats given oral carbon tetrachloride suggest that reduced rates of uptake and turnover in the liver are observed, with resulting delay of clearance of the label.

HUMAN METABOLISM OF ALBUMIN CONJUGATES LABELED WITH In-111 USING VARIOUS BIFUNCTIONAL CHELATES. *David A. Goodwin, #Claude F. Meares, *Carol I. Diamanti, #Charles S-H Leung, #Jerrold T. Bushberg, and *Richard L. Goode, *Veterans Administration Hospital, Stanford University School of Medicine, Palo Alto, CA, and #Dept. of Chemistry University of California at Davis.

The biological properties of various conjugates of albumin (0.3 to 1.5 EDTA/molecule) were studied in nine cancer patients. Diazotization as well as alkylation was used to couple the bifunctional chelate to the protein. In-111 ions were added specifically to the chelating groups at the time the patient was available for study. The biological half life and whole body scans were obtained following injection of 1.7 mCi (average) intravenously. The plasma disappearance half time from day 6 through day 24 averaged 8.43 days with the azo-albumin (5 subjects), and 13.75 days (two observations in one subject) with the alkyl albumin. Approximately twice as much of the lightly labeled (0.3 EDTA/molecule) alkyl-albumin remained circulating with a disappearance equal to RISA (13.3 D) as did the heavily labeled (1.5 EDTA/molecule). An average of 50% of the injected activity was excreted in the urine in one week as the simple chelate (øEDTA) or a derivative thereof. With the alkyl-albumin excellent visualization of the vascular structures was seen up to day 3.

Alkylation provides a conjugate of albumin that has properties most closely approaching those of RISA in

humans, provided approximately 0.3 EDTA groups are added per molecule of albumin. The properties of human fibrinogen and bleomycin labeled with the alkylating agent are currently under investigation.

TECHNETIUM α -MPG: CHEMISTRY, STABILITY AND BIODISTRIBUTION. Garo P. Basmadjian, Michael Fitzgerald and Kenneth R. Hetzel. College of Pharmacy, The University of Oklahoma, Oklahoma City, OK., Abbott Laboratories, North Chicago, Ill., and Nuclear Medicine Section, Northwestern University, Chicago, Ill.

Alpha mercaptopropionyl glycine (α -MPG), an antidote for heavy metal intoxication was labeled with Technetium-99 and 99m. Studies of the chemistry of this complex showed it to be a green colored complex with a visible spectrum maxima at 400 and 650 m μ when the technetium-99 was reduced either by Sn⁺⁺ ions or by the -SH group of the α -MPG in an acid medium (oxidation state = +4). The Tc- α -MPG complex was stable in-vitro (in air and under N₂) and in-vivo. Using electrophoresis and ion-exchange chromatography, this complex was shown to have two negatively charged components. The quantities of each component could be varied by controlling the pH of the reaction medium. Using Sn-113 on a solid support indicated that the complex is a mixed-metal complex.

Formulation studies showed that a freeze-dried preparation of α -MPG and SnCl₂ at pH 7.5 had a shelf life of about 3 months at 4°C while a solution of these two ingredients even under N₂ and at 4°C, decomposed within 24 hours.

Biodistribution in rats, rabbits and dogs demonstrated rapid blood clearance with maximum biliary concentration at 45-90 min. Gamma camera scintiphotos in rabbits and dogs revealed immediate appearance of the Tc-99m complex in the liver, with subsequent visualization of the gallbladder and small intestine by 1 hour and 3 hours respectively.

Efforts to increase the lipid solubility of the complex by the use of the ethyl ester of the α -MPG are in progress.

The LD₅₀ of the formulation in rats is 1760mg/Kg. Human studies are in progress.

areas suggestive of intrahepatic biliary dilatation in all of them. The sequential scintiphotographic findings were as follows: (A) pooling of the complex in the dilated intrahepatic ductal system; (B) partial biliary stasis with delayed but progressive visualization of bowel activity; (C) non-visualization of the gallbladder and/or common bile duct. The diagnosis of intrahepatic calculi in all patients was confirmed by percutaneous transhepatic cholangiography, laparotomy and operative cholangiography.

Ongoing study continues. Initial results suggest that the Tc-99m-PG liver sequential study can serve as a useful screening technique for detecting intrahepatic stones.

EVALUATION OF Tc-99m PYRIDOXYLIDENEGlutamate (PG) CHOLESCINTIGRAPHY AS A DIAGNOSTIC TEST FOR CHOLECYSTITIS.

Robert C. Stadalnik*, Jess F. Kraus, Nathaniel M. Matolo, and Kenneth A. Krohn. Sacramento Medical Center of the University of California, Davis, School of Medicine, Sacramento, Calif.

More than 15 million people in the United States have gallstones, with about 300,000 operations being performed annually for this disease, and at least 6,000 deaths resulting from its complications. The purpose of this investigation was to determine the diagnostic value, sensitivity, specificity and accuracy of Tc-99m pyridoxylidene-glutamate cholescintigraphy (Tc-99m PGC) in patients with cholecystitis. In addition, we compared the diagnostic value of this screening test to that of oral cholecystography (OC) and ultrasonography (US). This test was given to 50 patients with acute, subacute, and/or chronic cholecystitis with cystic duct obstruction proven histologically and operatively, and also to 27 normal volunteers and 43 patients who subsequently were proven free of gallbladder disease. The screening test Tc-99m PGC was applied to all 120 subjects. In addition, 33 had OC, and 31 US.

The results show that the sensitivity, specificity and accuracy of Tc-99m PGC is 100%. Whereas for OC the sensitivity is 89%, specificity is 100%, and the accuracy is 94%. For US the sensitivity is 59%, specificity is 93%, and the accuracy is 74%.

These data show that this new screening test is a very accurate, safe, simple and meaningful diagnostic tool in the evaluation of patients with cholecystitis.

(* Picker Scholar, James Picker Foundation)

THURSDAY, 4:00 p.m.-5:30 p.m.

CHICAGO ROOM

GASTROINTESTINAL 2

Chairman: Samuel E. Halpern
Co-Chairman: G. T. Krishnamurthy

TECHNETIUM-99m-PYRIDOXYLIDENEGlutamate (Tc-99m-PG) SEQUENTIAL SCINTIPHOTOGRAPHY IN THE DETECTION OF INTRAHEPATIC STONES. Shin-Hwa Yeh, On-Kee Liu, and Miau-Ju Huang. Veterans General Hospital, Taipei, Taiwan.

It was reported that plain x-ray examination of the abdomen was not helpful in the detection of intrahepatic calculi. Both oral and intravenous cholangiography failed to yield useful information during the acute attack. Even during remission, 70% of conventional cholangiographic studies showed non-visualization of the biliary tree. This led us to perform Tc-99m-PG sequential scintiphotography as a screening technique in clinical situations strongly suspicious of intrahepatic stones.

Forty-eight hr after Tc-99m-sulfur colloid liver scintiphotography, sequential liver scintiphotos were recorded after I.V. injection of Tc-99m-PG on Polaroid films at 3- or 5-min intervals for the first 30-60 min, and at hourly intervals from 1-8 hr. Additional films were obtained at 12 hr and 24 hr after injection.

Four patients strongly suspicious of intrahepatic stones were studied. The colloid scan showed intrahepatic cold

GASTRIC EMPTYING TIME: A STANDARDIZED APPROACH VERIFIED IN NORMALS AND APPLIED IN STUDIES OF DIABETIC GASTROPARESIS. Karim Rezaei-Zadeh, Richard Byyny, and Malcolm Cooper. University of Chicago Hospitals, Chicago, Ill.

A standard oatmeal and milk Tc-99m sulfur colloid labeled meal has produced consistent results in the measurement of gastric emptying time in normal subjects. When applied clinically, it proved superior to saline loading and aspiration. In a double-blind study it clearly distinguished between placebo and drug response in diabetics with gastroparesis.

Fourteen patients and 9 normals were studied on 33 occasions. The test meal, 2 oz oatmeal, 8 oz milk, and 0.5 mCi Tc-99m sulfur colloid was given after overnight fast. Gamma camera images, recorded sequentially on tape for two hours, were analyzed using a region of interest over the stomach and a data analysis system [Ohio-Nuclear Series 150]. Four diabetic patients with gastroparesis confirmed by UGI series, cine fluoroscopy, and gastroscopy were studied using injections of placebo and metoclopramide double blindly by both the colloid and saline methods.

Clearance curves were fitted monoexponentially by least square technique [$r = > .90$]. Thirteen measurements in 9 normal volunteers gave a normal T-1/2 = 72 min \pm 13 min [1 SD]. In the 11 diabetic studies all patients were outside the normal range [$\alpha 0.05$] and showed a positive response to drug therapy. Saline loading produced inconsistent results, was abnormal in two patients, normal in one, and paradoxical in the fourth. Gastric emptying measured using a standard radiocolloid test meal is sensitive, reproducible, does not require intubation, is easily applicable, and appears clinically useful.

RADIOISOTOPIC LOCALIZATION OF ACUTE GASTROINTESTINAL BLEEDING SITE DURING EXPLORATORY LAPAROTOMY. Abass Alavi, Robert W. Dann and Stanley Baum, Hospital of The University of Pennsylvania, Phila. Penna.

Localization of a bleeding site may pose a difficult task during exploratory laparotomy. Not infrequently a patient may be operated on several times without successful localization of the bleeding site. The design of this project is based on the following considerations. A radioactive agent which is cleared very rapidly by a target organ, is injected intravenously. At the bleeding site a fraction of the injected activity extravasates and is eliminated from the circulation. In each recirculation another small fraction is added to the trapped activity in the bleeding site. After several recirculations a contrast is reached between the bleeding site and the surrounding background activity. We have used technetium sulfur colloid as an ideal radiopharmaceutical for this project. In four dogs a bleeding site was created by connecting the femoral artery to a loop of small bowel. A stopcock was used to regulate the bleeding rate. In one dog the bleeding site was initiated by lacerating the mucosa by a biopsy instrument. After the bleeding was initiated, 10 mCi of technetium sulfur colloid was injected intravenously. A long segment of the bowel including the bleeding site was monitored by a portable, well-collimated, one-inch NaI detector. The bleeding site was detected by observing a rise in the count rate while screening the loop of the bowel. We have been able to detect a bleeding rate as low as .17 ml/min. This procedure appears to be a simple and sensitive means for solving a rather difficult clinical problem.

ALTERED BODY DISTRIBUTION OF Tc-99m PERTECHNETATE IN HYPERTHYROID ALUMINEMIA. Theodore S.T. Wang, Rashid A. Fawwaz, Peter D. Esser and Philip M. Johnson, College of Physicians and Surgeons, Columbia University, New York City.

Failure of intravenous Tc-99m pertechnetate to leave the vascular space was observed in a woman referred for diagnosis of gastrointestinal bleeding. Since other studies with the same preparation showed normal localization, the cause of the abnormality was sought. Because the patient's medication included an antacid containing 7.2 g Al(OH)₃ per day and in view of reports that high plasma Al levels alter body distribution of sulfur colloid and diphosphonate, the possibility of a similar mechanism was investigated.

The patient's red cells, plasma and a sample of pooled plasma were mixed with Tc-99m pertechnetate and incubated at 37°C for 30 min. Each sample was subjected to instant thin layer chromatography (ITLC) in both 85% methanol and saline systems. Rf values with the 85% methanol system were: patient's plasma =0.90; pooled plasma =1.00. Both were 1.00 with the saline system. The patient's plasma Al level was 65µg/l (atomic-flame absorption spectrophotometry) the level in pooled plasma 5.8µg/l. Pooled plasma was then mixed with known quantities of Al(OH)₃ and subjected to the above procedure. At levels of 50µg/l and above in 85% methanol system the Rf values were 0.90; below that level, Rf =1.00. Three months later, with antacid therapy discontinued, the pertechnetate scan was repeated with normal results: patient's plasma Al level was 15µg/l, a normal value; the level in pooled plasma was again 5.8µg/l. ITLC of patient's and pooled plasma gave Rfs of 1.00.

It is concluded that elevated plasma Al levels may alter body distribution of Tc-99m pertechnetate, that such elevation can occur rapidly during antacid therapy, and that the ITLC can detect Al levels \approx 50µg/l.

DETECTION OF BACTERIAL DECONJUGATION OF BILE SALTS USING C-13 BREATH TEST. Y. Sasaki, H. Oh-hara, S. Takahashi, T. Maeda and K. Someya. St. Marianna University School of Medicine, Kawasaki, Japan

Increased bacterial deconjugation of bile salts has been detected by a simple breath analysis technique which consists of serial collection of CO₂ following the oral administration of glycine-1-C-14-cholate. Purpose of the present study is to replace C-14 glycine cholate(GC) by stable C-13-labelling in order to expand the applicability of the test to a larger population such as infants, pregnant women, young adults and healthy subjects.

Rats were preoperated to form jejunocolostomy. C-13-GC (50 mg/kg) and/or C-14-GC(0.2 µCi) were given into the duodenum through gastric fistula. Carbon dioxide in the expired breath was collected by neutralization of alkaline solution as reported previously. Isotope ratio of ¹³C/¹²C was measured by mass spectrometry. Radioactivity of C-14-CO₂ was measured in a liquid scintillation counter. Rats with jejunocolostomy gave CO₂ curves with significant peak at 1-3 hours after GC ingestion, which suggests C-14-glycine was freed from GC. In contrast CO₂ curves were flat without appreciable peak in control animals. C-13-CO₂ and C-14-CO₂ curves showed similar pattern. Carbon dioxide curves after i.v. administration of C-14 and C-13-glycine(loading dose) revealed delayed higher peak than the curves after i.v. administration of C-14-glycine alone(trace dose).

Our results suggest C-13-breath test after oral administration of C-13-GC can be used for the detection of bacterial deconjugation of bile salts which causes malabsorption. Data obtained by trace dose of C-14-GC may not be comparable with those obtained by loading dose of C-13-GC.

THE COMPLEMENTARY ROLE OF 67 GA AND CT SCANS FOR DETECTION OF ABDOMINAL INFLAMMATION. Robert Shimshak, Melvyn Korobkin, Paul Hoffer, Thomas Hill, Robert Schor and Herbert Kressel. University of California San Francisco, Ca

A retrospective study of all cases examined by both 67-Ga and CT scan for suspected intrabdominal inflammation over a six month period was performed.

15 of the 17 identified cases had adequate followup. All 8 cases of surgically proven inflammation were detected by 67-Ga scan and 7/8 by CT scan. CT missed one case of pericecal phlegmon. CT correctly identified all cases without inflammation but two falsely positive 67 Ga scans were noted. One was due to intrahepatic tumor and the other to colonic and pulmonary uptake. CT demonstrated a non-inflammatory abnormality as the probable cause of symptoms in 2/7 cases without inflammation.

Results with both modalities were not significantly different. However, when the two studies were used in a complementary manner the accuracy of diagnosis improved. 67-Ga scan is felt to be the screening procedure of choice for abdominal inflammation if the patient can tolerate the delay required. Abdominal CT screening is impractical due to the large number of slices needed for an adequate examination. This number is significantly reduced when the CT scan is directed by an abnormal 67-Ga scan. A normal CT scan does not rule out inflammatory disease especially of phlegmonous nature. However, CT scan may not be necessary if a 67-Ga scan is normal. The principle advantages of CT are greater anatomic detail obtainable prior to surgery, the detection of non-inflammatory disease and the demonstration of fistulous communications using contrast agents.

67-Ga screening with subsequent directed CT scanning is recommended in most cases of possible intrabdominal inflammation.